THE DESIGN OF DISCRETE GABOR EXPANSION ALGORITHMS AND AN EFFICIENT REALIZATION OF THE GERCHBERG-PAPOULIS ALGORITHM IN THE ZAK SPACE

by

Andrzej K. Brodzik

A dissertation submitted to the Graduate Faculty in Engineering in partial fulfillment of the requirements for the degree of Doctor of Philosophy.

The City University of New York

1995

This manuscript has been read and accepted for the Graduate Faculty in Engineering in satisfaction of the dissertation requirement for the degree of Doctor of Philosophy.

Sept 27, 1995
Date

Richard Palmer
Chair of Examining Committee

9/27/95
Date

Executive Officer

Supervisory Committee

The City University of New York

Contents

1 Introduction **1**

1.1 Problem Statement 1

1.2 Dissertation Outline 3

2 The Zak Transform **5**

2.1 Notation 5

2.2 Zak Transform 10

2.2.1 The Continuous Zak Transform 11

2.2.2 The Finite Zak Transform 19

3 The Gabor Expansion - A Brief Overview **26**

3.1 Introduction 27

3.2 Survey of Algorithms 29

3.2.1 The Biorthogonal Method 30

3.2.2 The Zak Transform Method 32

3.2.3 The Convolution Method 34

3.2.4 The Discrete Case 36

3.2.5 Weyl-Heisenberg Systems and Frames 40

3.2.6 Computational Efficiency 43

3.3 Applications 48

3.4 Relation to Other Time-Frequency Representations 57

3.4.1 Short Time Fourier Transform 58

3.4.2 Wigner Distribution 60

3.4.3 Ambiguity Function 62

3.4.4 Wavelet Transform 65

4 Weyl-Heisenberg Systems: Computing Oversampled Discrete Gabor Expansions **69**
4.1 Introduction 70
4.2 Weyl-Heisenberg Systems 72
4.3 Finite Zak Transform (FZT) 73
4.4 Application of FZT to W-H systems. 75
4.4.1 Critical Sampling. 76
4.4.2 Integer Oversampling 79
4.4.3 Fractional Oversampling 82
4.5 Examples and Implementation Remarks 87

5 Extrapolation of Band-Limited Signals and the Finite Zak Transform **106**
5.1 Introduction 107
5.2 Gerchberg-Papoulis Algorithm 108
5.3 The Finite Zak Transform 111
5.4 Gerchberg-Papoulis-Zak Algorithm 116

6 Conclusions **125**
6.1 Role of Time-Frequency Analysis 125

Bibliography **129**

List of Figures

2.1 The first four Hermite functions (clockwise from top-left). 24
2.2 Zak transform magnitude of the first four Hermite functions (clockwise from top-left). 25

4.1 Zak transform partition of the Gaussian window for R=2: Z_{g_0} (top), Z_{g_1} (bottom). 93
4.2 Factorization of F for Case 1.A.: F_0 (top), F_1 (bottom). 94
4.3 Gabor coefficients corresponding to the factor F_0 in Case 1.A. . 95
4.4 Factorization of F for Case 1.B.: F_0 (top), F_1 (bottom). 96
4.5 Gabor coefficients corresponding to factorization in Case 1.B. . . 97
4.6 Factorization of F for Case 1.C.: F_0 (top), F_1 (bottom). 98
4.7 Gabor coefficients corresponding to factorization in Case 1.C. . . 99
4.8 Factorization of F for Case 1.D.: F_0 (top), F_1 (bottom). 100
4.9 Gabor coefficients corresponding to factorization in Case 1.D. . 101
4.10 Zak transform partition of a composite window for $R = 3$ (Case 2.): (a) Z_{g_0}, (b) Z_{g_1}, (c) Z_{g_2}. 102
4.11 Partition of F for $S' = 3$, $S = 2$ (Case 3.): F_0 (top), F_1 (bottom). 103
4.12 Partition of G for $S' = 3$, $S = 2$ (Case 3.): (a) $G_{1,1}$, (b) $G_{2,1}$, (c) $G_{3,1}$, (d) $G_{1,2}$, (e) $G_{2,2}$, (f) $G_{3,2}$. 104
4.13 Gabor coefficients (Case 3.): (a) $s' = 0$, (b) $s' = 1$, (c) $s' = 2$ . . 105

5.1 The signal g: a), its Fourier transform G: b), the segment f: c) and its Fourier transform F: d). 118
5.2 F_N, the truncation of F: a), its inverse Fourier transform $\check{F}_N$: b), truncation of $\check{F}_N$: c) and result of the last step of the iteration: d). 119
5.3 Restored signal f_r at r-th iteration: a) $r = 1$, b) $r = 10$, c) $r = 100$. 120

5.4 Zak transform magnitudes of g (top) and its Fourier transform G (bottom). 121
5.5 Zak transform magnitudes of segment f (top) and its Fourier transform F (bottom). 122
5.6 Truncation in the Zak space Z_{F_N} (top) and its inverse Fourier transform $\check{Z}_{F_N}$ (bottom). 123
5.7 Truncation in the Zak space of $\check{Z}_{F_N}$ (top) and the result of addition (step 6 of the algorithm, bottom). 124

Chapter 1

Introduction

1.1 Problem Statement

The advantage of the Fourier transform is that it allows the decomposition of a signal into individual frequency components, providing an alternative way of looking at a signal. Such decomposition, however, does not yield an easily interpretable information about the time localization of spectral components. For non-stationary signals in particular application of Fourier methods leads to physically meaningless descriptions. A typical example of such a signal is human speech, but non-stationarity is present in numerous different situations including seismology, radar and sonar, image processing, communications, etc.. In these situations successful signal processing requires operating in a joint time-frequency domain.

One of the methods that addresses these need is Gabor expansion. It possesses a number of desirable properties - linearity, best possible time-frequency localization according to the uncertainty principle and admissibility of the Gaussian

function as a window. One particular disadvantage of the Gabor expansion is that the Gabor functions do not constitute orthonormal basis, a fact that led many to believe that stable, efficient and fast algorithms are not attainable, or at least, difficult to built.

This work demonstrates that these believes are not justified. Stable and efficient algorithms for computing Gabor expansions can be easily constructed while retaining all of the method's desirable properties. Ease of computation, excellent time-frequency localization and availability of physical interpretation establish Gabor expansion as a highly useful tool for analyzing many types of non-stationary signals.

The language of the Zak transform is at the center stage of both: the theory of Gabor expansion and its application towards construction of successful algorithms. First, the Zak transform helps to clarify the stability issues and to formulate simple and easily computable criteria for existence of legal Gabor expansions. Secondly, application of the Zak transform simplifies the structure of algorithms and improves efficiency of computations, reducing them to the 2-D finite Fourier transform calculations.

Another example of successful application of time-frequency methods to signal processing problems presented in this work is the Zak space formulation of the Gerchberg-Papoulis algorithm. The iterative procedure of Gerchberg-Papoulis for restoration of a band-limited signal from partial data involves transition between time domain and frequency domain at each iteration, rendering the algorithm computationally expensive.

This work shows that the computational cost of the algorithm can be significantly reduced by performing the computation in a joined time-frequency space, using the finite Zak transform calculus as the main tool. The intimate relationship between the Fourier transform and the Zak transform is exploited to replace the Fourier transform computations by pointwise multiplications. The new approach accomplishes reduction in multiplicative complexity from $2Plog_2P$ to $2P$ per iteration, while preserving the structure of the algorithm.

1.2 Dissertation Outline

The objective of this work has been stated. Chapter two begins with some mathematical preliminaries that will be needed throughout. This is followed by a review of the Zak transform fundamental properties. Examples of common signals in the Zak space is given. In chapter three the basic issues of the theory of Gabor expansion are described and a survey of existing computational algorithms is presented. A summery of applications of Gabor expansion is given and the Gabor method is compared to the Short Time Fourier Transform, Wavelet Transform, Wigner Distribution and Ambiguity Function.
In chapter four numerical algorithms for computing Gabor expansions are presented for critical sampling and integer and rational oversampling. Clear and easily computable conditions are established for existence of Gabor expansions and for stability of computations. Algorithm selection criteria are given in terms of the Zak transform properties of a signal. The main computational task in the resulting algorithms is shown to be a 2-D finite Fourier transform.

In chapter five the problem of signal extrapolation from partial data is stated and a joined time-frequency solution is given. The solution is compared to the Gerchberg-Papoulis algorithm. Concluding remarks and directions for future research are offered in chapter six.

Chapter 2

The Zak Transform

In this chapter we establish notation, define terminology and introduce the Zak transform, which will be used throughout this work as a tool in both: explaining the theoretical issues relevant in Gabor expansion and construction of new algorithms presented in chapters four and five. The main references are Tolimieri *et al* [8] and Janssen [53].

2.1 Notation

C is the set of complex numbers. The modulus of a complex number $z \in C$ is denoted by $|z|$, the complex conjugate by z^*. R is the set of real numbers. Z is the set of integers. I is identified with the interval $[0, 1)$.
Sequences and series with undefined limits are taken over Z, and integrals with undefined limits are taken over R. All functions are defined on the real line and are complex-valued, unless otherwise indicated.

Lebesgue space $L^p(R)$ is defined as

$$L^p(R) = \{f : \|f\|_p = (\int |f(t)|^p dt)^{1/p} < \infty\}, \quad 1 \leq p < \infty. \tag{2.1}$$

For $1 \leq p \leq \infty$, $L^p(R)$ is a *Banach space* with norm $\|\cdot\|_p$, and $L^2(R)$ is a *Hilbert space* with inner product

$$< f, g >= \int f(t)g^*(t)dt. \tag{2.2}$$

Given a Hilbert space H with norm $\|\cdot\|$, inner product $< \cdot, \cdot >$ and a sequence $\{x_n\}$ of elements in H, we have:

1. If $y = \sum_n \alpha_n x_n$ (where the range of n is finite), then y is a *linear combination* of x_n, or y is linearly dependent on x_n.

2. A sequence $\{x_n\}$ is linearly dependent if there is $\sum_n \alpha_n x_n = 0$ with not all $\alpha_n = 0$. Otherwise the sequence is *linearly independent.*

3. The *span* of $\{x_n\}$ is the set of all finite linear combinations of x_n.

4. The sequence $\{x_n\}$ is a *basis* for H if for every $y \in H$ there exists a unique sequence of scalars $\{\alpha_n\}$ such that $y = \sum_n \alpha_n x_n$.

5. A sequence $\{x_n\}$ is *orthogonal* if $m \neq n$ implies $< x_m, x_n >= 0$.

6. A sequence $\{x_n\}$ is *orthonormal* if it is orthogonal and $\|x_n\| = 1$ for all n.

7. A sequence $\{x_n\}$ is *complete* if span of $\{x_n\}$ is dense in $L^2(R)$, or equivalently if the only element $x \in L^2(R)$ which is orthogonal to every x_n is $x = 0$.

8. An orthonormal sequence $\{e_n\}$ satisfying the following equivalent conditions:

   (a) $\{e_n\}$ is complete,

   (b) $\sum_n | < x, e_n > |^2 = \|x\|^2$ for all $x \in H$,

   (c) $x = \sum_n < x, e_n > e_n$ for all $x \in H$,

   is called an *orthonormal basis.*

9. A sequence $\{e_n\}$ is called the *standard basis* for H if

$$< e_m, e_n >= \delta_{mn} \tag{2.3}$$

   where

$$\delta_{mn} = \begin{cases} 1, & m = n, \\ 0, & m \neq n, \end{cases} \tag{2.4}$$

   is the *Kronecker delta.*

Operators

Assume G and H are Hilbert spaces with norms $\|\cdot\|_G$, $\|\cdot\|_H$ and inner products $< \cdot, \cdot >_G$, $< \cdot, \cdot >_H$, respectively and that $f : G \to H$.

1. The *range* of f is $range(f) = \{f(x) : x \in G\}$.

2. f is *linear* if $f(ax + by) = af(x) + bf(y)$ for all $x, y \in G$ and $a, b \in C$.

3. f is *one-to-one* if $x \neq y$ implies $f(x) \neq f(y)$.

4. f is *onto* if $range(f) = H$.

5. f is *bijective* if it is one-to-one and onto.

6. The *norm* of f is $\|f\| = sup\{\|f(x)\|_H : x \in G \text{ and } \|x\|_G = 1\}$.

7. f is an *isometry* if it is on-to-one and norm preserving i.e. $\|f(x)\|_H = \|x\|_G$ for all $x \in G$.

8. If f is one-to-one, linear and onto, than it is called a *linear isomorphism.*

9. A *unitary* f is a linear bijective isometry.

Translation, modulation and dilation.

Define the following operators:

translation

$$(T_a)f(t) = f(t+a), \quad a \in R, \tag{2.5}$$

modulation

$$(R_b)f(t) = f(t)e^{2\pi ibt}, \quad b \in R, \tag{2.6}$$

dilation

$$(D_c)f(t) = c^{1/2}f(ct), \quad c \in R^+. \tag{2.7}$$

The operators T_a, R_b and D_c are norm preserving i.e.

$$\|f\| = \|T_a f\| = \|R_b f\| = \|D_c f\|, \tag{2.8}$$

and we have

$$(T_a R_b)f(t) \;=\; e^{2\pi ib(t+a)}f(t+a), \tag{2.9}$$

$$(R_b T_a) f(t) = e^{2\pi i b t} f(t+a), \tag{2.10}$$

$$(T_a D_c) f(t) = c^{1/2} f(ct+a), \tag{2.11}$$

$$(D_c T_a) f(t) = c^{1/2} f(ct+ca), \tag{2.12}$$

$$(R_b D_c) f(t) = c^{1/2} e^{2\pi i b t} f(ct), \tag{2.13}$$

$$(D_c R_b) f(t) = c^{1/2} e^{2\pi i b c t} f(ct). \tag{2.14}$$

Moreover, we will use $f_{mn}(t) = R_b T_{-a} f(t) = f(t-a) e^{2\pi i b t}$.

Fourier transform.

The *Fourier transform* $\hat{f}$ of f and the inverse transform $\check{f}$ are defined by

$$\hat{f}(\nu) = \int f(t) e^{-2\pi i \nu t} dt, \quad \check{f}(\nu) = \hat{f}(-\nu), \quad \nu \in R. \tag{2.15}$$

We have $\check{\hat{f}} = \hat{\check{f}} = f$, and

$$\widehat{(T_a f)} = R_a \hat{f}, \tag{2.16}$$

$$\widehat{(R_a f)} = T_{-a} \hat{f}, \tag{2.17}$$

$$\widehat{(D_a f)} = D_{1/a} \hat{f}. \tag{2.18}$$

For $f, g \in L^2(R)$ we have the *Plancherel formula*

$$\|f\|_2 = \|\hat{f}\|_2 = \|\check{f}\|_2 \tag{2.19}$$

and the *Parseval formula*

$$< f, g > = < \hat{f}, \hat{g} > = < \check{f}, \check{g} > . \tag{2.20}$$

The *convolution* operator $f(x) \circ g(x)$ is defined by

$$f(t) \circ g(t) = \int f(\tau) g(t-\tau) d\tau. \tag{2.21}$$

2.2 Zak Transform

The Zak Transform (also termed Weil-Brezin mapping or kq representation) was known already by Gauss, but it was not until Zak rediscovered it and studied systematically that it came to attention of the signal processing community. Since than it became an important mathematical tool for signal analysis applications, especially for constructing algorithms in Gaborian analysis. The two main features that Zak Transform brings to the computation of the discrete Gabor expansions are: a well-defined criterium for selecting legal Gabor expansions and simplification of the overall algorithmic structure. In chapter four we will apply the finite Zak transform to design efficient and flexible algorithms for computing discrete Gabor expansions at integer and fractional oversampling rates. A crucial feature of the Zak transform is its intimate relationship with the Fourier transform. Indeed, the Zak transform can be interpreted as a generalization of the Fourier transform with the function $f(t)$ sampled at integer points r with the time offset τ. This relationship will be exploited in chapter five to replace the Fourier transform computations by operations performed in the Zak domain in the Gerchberg-Papoulis signal extrapolation procedure, to obtain an efficient joint time-frequency domain algorithm.
While these two examples provide convincing arguments for bringing the Zak transform to the center stage of signal processing, a number of issues still remain to be explored. The relationship between signal properties in the time domain and in the Zak space should be investigated in more detail, especially with regard to Zak transform zeros and surface curvature. Application of

the finite (and multiplicative) Zak transform to multirate filtering is another promising area of research. Finally, the use of Zak transform as a representational tool in signal processing should be farther investigated.

In the following we will review some of the more important properties of the continuous Zak transform, give simple examples of signals in the Zak space and provide a formulation of the discrete Zak transform. Most of the properties reviewed in the section will be given without proofs, which can be found in Janssen's paper [53] or in [8].

2.2.1 The Continuous Zak Transform

The Zak Transform of a continuous signal $f(t)$ can be defined by

$$Z_f(\nu,\tau) = \sum_r f(\tau + r)e^{2\pi i r\nu}, \quad r \in Z, \quad -\infty < \tau, \nu < \infty, \tag{2.22}$$

where ν and τ can be interpreted as time and frequency variables.

The main properties of the continuous Zak transform are:

1. Energy preservation.

   ZT is an isometry from Hilbert space $L^2(R)$ onto $L^2(I^2)$ with the inner products

$$< f, g >= \int_{-\infty}^{\infty} f(t)g^*(t)dt$$

and

$$< Z_f, Z_g >= \int_0^1 \int_0^1 Z_f(\nu,\tau) Z_g^*(\nu,\tau) d\nu d\tau.$$

We have

$$< f, g >=< Z_f, Z_g > . \tag{2.23}$$

In particular

$$\|f(t)\|_2^2 = \|Z_f(\nu,\tau)\|_2^2. \tag{2.24}$$

2. Inversion formula.

The function f can be recovered from Z_f by the inversion formula

$$f(\tau + r) = \int_0^1 Z_f(\nu,\tau) e^{-2\pi i r\nu} d\nu. \tag{2.25}$$

3. Periodicity.

ZT is periodic in frequency variable and quasiperiodic in time variable:

$$Z_f(\nu+1,\tau) = Z_f(\nu,\tau), \tag{2.26}$$

$$Z_f(\nu,\tau+1) = Z_f(\nu,\tau) e^{-2\pi i\nu}. \tag{2.27}$$

Hence, Z_f is completely determined by its values on the unit square I^2.

4. Time and frequency shifts.

$$(ZT_a)_f(\nu,\tau) = Z_f(\nu,\tau+a), \tag{2.28}$$

$$(ZR_b)_f(\nu,\tau) = Z_f(\nu+b,\tau)e^{2\pi ib\tau}; \tag{2.29}$$

so the time shift in the signal is reflected in time shift in the Zak transform.

5. Dilations.

$$(ZD_c)_f(\nu,\tau) = c^{-1/2}\sum_{r=0}^{c-1} Z_f(\frac{\nu+r}{c}, c\tau) \tag{2.30}$$

and

$$(ZD_{1/c})_f(\nu,\tau) = c^{-1/2}\sum_{r=0}^{c-1} Z_f(c\nu, \frac{\tau+r}{c})e^{2\pi ir\nu}. \tag{2.31}$$

6. Fourier transform.

We have the following relations

$$Z_{\hat{f}}(\nu,\tau) = Z_f(-\tau,\nu)e^{-2\pi i\nu\tau} \tag{2.32}$$

and

$$Z_{\hat{f}}(\nu,\tau) = Z_f(\tau,-\nu)e^{-2\pi i\nu\tau}, \tag{2.33}$$

so, up to a phase factor $e^{-2\pi i\nu\tau}$, 90 degrees rotation of the Zak transform of f produces the Zak transform of $\hat{f}$.

7. Time-limited and band-limited signals.

Let $0 \le a, b \le 1/2$. We have the formulas

$$Z_f(\nu,\tau) = f(\tau), \quad |\tau| \le 1/2, \quad -\infty < \nu < \infty, \tag{2.34}$$

$$Z_f(\nu,\tau) = \hat{f}(-\nu)e^{-2\pi i\nu\tau}, \quad -\infty < \tau < \infty, \quad |\nu| \leq 1/2, \tag{2.35}$$

when f is time-limited to [-a, a] and band-limited to [-b, b], respectively. Hence, when f is time-limited to [-a, a], then $Z_f(\nu,\tau) = 0$ for $a \leq |\nu| \leq 1/2$, and when f is band-limited to [-b, b], then $Z_f(\nu,\tau) = 0$ for $b \leq |\tau| \leq 1/2$.

8. Time reversal and complex conjugation.

$$Z_{f_-}(\nu,\tau) = Z_f(-\nu,-\tau), \tag{2.36}$$

$$Z_{f^*}(\nu,\tau) = Z_f^*(-\nu,\tau). \tag{2.37}$$

9. Convolution.

$$Z(f \circ g)(\nu,\eta) = \int_0^1 Z_f(\nu,\tau)Z_g(\nu,\eta-\tau)d\tau, \quad -\infty < \nu,\eta < \infty. \tag{2.38}$$

$$Z(fg)(\xi,\tau) = \int_0^1 Z_f(\nu,\tau)Z_g(\xi-\nu,\tau)d\nu, \quad -\infty < \xi,\tau < \infty. \tag{2.39}$$

so the effect of convolution and multiplication of functions f and g in time domain is reflected by convolution of the Zak transforms Z_f and Z_g in the time and frequency domain, respectively.

10. Combined time-frequency shifts.

$$Z_{R_mT_{-n}f}(\nu,\tau) = Z_{f_{mn}}(\nu,\tau) = Z_f(\nu,\tau)e^{2\pi i(n\nu+m\tau)}. \tag{2.40}$$

11. Fourier transform of the product $Z_f(\nu,\tau)Z_g^*(\nu,\tau)$.

$$< f, g_{mn} >= \sum_{\nu}\sum_{\tau} Z_f(\nu,\tau)Z_g^*(\nu,\tau)e^{-2\pi i(n\nu+m\tau)}. \tag{2.41}$$

The double summation can also be interpreted as a cross-ambiguity function of signals f and g expressed in terms of their Zak transforms.

12. Zeros of ZT.

If Z_f is a continuous function of the two variables ν and τ, then $Z_f(\nu_0, \tau_0) = 0$ for some ν_0, τ_0 with $0 \leq \nu_0, \tau_0 < 1$. This is known as the Zero theorem. The proof can be constructed as follows.

Suppose Z_f is continuous and has no zeros. Take

$$Z_f(\nu, \tau) = |Z_f(\nu, \tau)| e^{2\pi i \varphi(\nu, \tau)}, \quad -\infty < \nu, \tau < \infty,$$

where φ is a continuous function in both variables. From (2.26) and (2.27) we have the following periodicity relations

$$\begin{aligned} Z_f(\nu, 1) &= Z_f(\nu, 0) e^{-2\pi i \nu}, \\ Z_f(1, \tau) &= Z_f(0, \tau), \end{aligned}$$

which lead to

$$\begin{aligned} \varphi(\nu, 1) &= \varphi(\nu, 0) - \nu + p, \\ \varphi(1, \tau) &= \varphi(0, \tau) + q, \end{aligned}$$

where p and q are integers independent of ν and τ, respectively, by continuity of φ. Calculating $\varphi(1, 1)$ in two different ways, we have:

$$\begin{aligned} \varphi(1, 1) &= \varphi(1, 0) - 1 + p = \varphi(0, 0) + q - 1 + p \\ \varphi(1, 1) &= \varphi(0, 1) + q = \varphi(0, 0) + p + q. \end{aligned}$$

Since this a contradiction, Z_f must have a zero.

The following result gives some indications where one might expect zeros in the Zak transform.

If Z_f is continuous and

- f is even then $Z_f(1/2, 1/2) = 0$,
- f is odd then $Z_f(0,0) = 0$, $Z_f(0,1/2) = 0$ and $Z_f(1/2,0) = 0$.

The first four Hermite functions have the following zero patterns:

$h_0 : (1/2, 1/2)$,
$h_1 : (0,0), (0,1/2), (1/2,0)$,
$h_2 : (0,0), (1/2,1/2)$,
$h_3 : (0,0), (0,1/2), (1/2,0), (1/2,1/2)$.

Examples of time-signals and their Zak transforms

1. Rectangular window function.

Let

$$f(t) = \begin{cases} 1, & 0 \le t < 1, \\ 0, & t < 0 \ \ or \ \ t \ge 1. \end{cases}$$

We have

$$Z_f(\nu, \tau) = e^{-2\pi i[\tau]\nu}, \quad -\infty < \nu, \tau < \infty,$$

where $[\tau]$ denotes the largest integer $\le \tau$. Z_f has a unit modulus everywhere and is discontinuous at all integer τ.

2. Sync function.

$$f(t) = \frac{sin(\pi t)}{\pi t}.$$

Similarly as in the previous case, Z_f has a unit modulus everywhere.

3. Gaussian window function.

Let

$$f(t) = 2^{1/4} e^{-\pi t^2}, \quad -\infty < t < \infty.$$

We have

$$Z_f(\nu, \tau) = 2^{1/4} e^{-\pi \tau^2} \theta_3(\pi(\nu - i\tau); e^{-\pi}), \quad -\infty < \nu, \tau < \infty,$$

where θ_3 is the third theta function, given by

$$\theta_3(z; q) = 1 + 2 \sum_n q^{n^2} cos(2\pi n z), \quad z \ \ complex.$$

Z_f has a single zero on the unit square at (1/2,1/2).

4. Two-sided exponential window function.

Let

$$f(t) = e^{-2\pi\alpha|t|}, \quad -\infty < t < \infty, \quad \alpha > 0.$$

We have

$$Z_f(\nu, \tau) = \frac{zr^\tau}{z - r} + \frac{zr^{1-\tau}}{1 - rz}, \quad -\infty < \nu, \tau < \infty,$$

where

$$z = e^{2\pi i\nu}, \quad r = e^{-2\pi\alpha}, \quad 0 \le \nu \le 1.$$

Z_f has a single zero on the unit square at (1/2,1/2).

5. One-sided exponential window function.

Let

$$f(t) = \begin{cases} e^{-2\pi\alpha t}, & t \ge 0, \\ 0, & t < 0. \end{cases}$$

We have

$$Z_f(\nu,\tau) = \frac{zr^\tau}{z-r}, \quad -\infty < \nu, \tau < \infty,$$

where z and r are defined in the previous example. Z_f has no zeros on the unit square.

6. Chirp.

Consider

$$f(t) = e^{\pi i t^2}, \quad -\infty < t < \infty.$$

We have

$$\begin{aligned} Z_f(\nu,\tau) &= \sum_r e^{\pi i(\tau+r)^2} e^{2\pi i r\nu} \\ &= e^{\pi i\tau^2} \sum_r e^{2\pi i r(\tau+\nu+1/2)} \\ &= e^{\pi i\tau^2} \sum_r \delta(\tau+\nu+1/2-r), \end{aligned}$$

which shows that Z_f is concentrated on lines $\tau = -\nu + r - 1/2$.

2.2.2 The Finite Zak Transform

Sample the continuous signal $f(t)$ at $t_k = k\Delta = \frac{kT}{M}$ and define

$$f(k) = f(t_k),$$

such that

$$f(k) = f(k+P), \quad k \in Z, \tag{2.42}$$

where P is a product of integers M and N. A P-periodic function f is determined by its values

$$f(0), f(1), ..., f(P-1). \tag{2.43}$$

Alternatively, we can represent f as a two-dimensional $M \times N$ array

$$f(k,r) = f(k+rM), \quad 0 \leq k < M, \quad 0 \leq r < N, \tag{2.44}$$

so the P-point data in (2.43) can be remapped as

$$\begin{bmatrix} f(0,0), & f(1,0), & \ldots & , f(M-1,0) \\ f(0,1), & f(1,1), & \ldots & , f(M-1,1) \\ . & & & \\ . & & & \\ . & & & \\ f(0,N-1), & f(1,N-1), & \ldots & , f(M-1,N-1) \end{bmatrix} \tag{2.45}$$

The discrete Zak transform $Z_f(l,k), \quad l,k \in Z$ of a periodic signal $f(k)$ with period P is expressed by the formula

$$Z_f(l,k) = \sum_{r=0}^{N-1} f(k+rM) e^{2\pi i \frac{rl}{N}}. \tag{2.46}$$

$Z_f(l,k)$ is M-quasiperiodic in k variable

$$Z_f(l,k+M) = e^{-2\pi il/N} Z_f(l,k) \tag{2.47}$$

and N-periodic in l variable

$$Z_f(l+N,k) = Z_f(l,k). \tag{2.48}$$

Proof.

$$\begin{aligned} Z_f(l,k+M) &= \sum_{r=0}^{N-1} f(k+rM+M)e^{2\pi irl/N} \\ &= \sum_{r=0}^{N-1} f(k+rM)e^{2\pi i(r-1)l/N} \\ &= e^{-2\pi il/N} Z_f(l,k) \end{aligned}$$

The second relation follows from N-periodicity of $e^{2\pi irl/N}$ in l. □

It follows that $Z_f(l,k)$ is completely determined by its values

$$Z_f(l,k), \quad 0 \le l < N, \quad 0 \le k < M. \tag{2.49}$$

To obtain (2.49), we compute the N-point Fourier transform of each column of (2.45). Overall, computing Z_f requires M N-point Fourier transforms.

The finite Zak transform preserves information. The function $f(k)$ can be recovered from its Zak transform by the formula

$$f(k) = \frac{1}{N} \sum_{l=0}^{N-1} Z_f(l,k), \quad 0 \le k < P-1, \tag{2.50}$$

or

$$f(k+rM) = \frac{1}{N}\sum_{l=0}^{N-1} Z_f(l,k)e^{-2\pi\frac{rl}{N}}, \quad 0 \le k < M, \quad 0 \le r < N, \tag{2.51}$$

which follows directly from substituting (2.44) for (2.42).

All properties of the continuous Zak transform described in Section 2.2.1. have discrete counterparts. We will conclude with the discrete form of two important formulas: the combined time-frequency shifts and the Zak space relation between a function and its Fourier transform.

Define

$$g_{mN,nM}(k) = g(k-nM)e^{2\pi i\frac{mNk}{P}}. \tag{2.52}$$

Then

$$Z_{g_{mN,nM}}(l,k) = e^{2\pi i(\frac{mk}{M}+\frac{nl}{N})}Z_g(l,k). \tag{2.53}$$

Proof.

$$\begin{aligned} Z_{g_{mN,nM}}(l,k) &= \sum_{r=0}^{N-1} f(k+rM-nM)e^{2\pi i\frac{rl}{N}}e^{2\pi i\frac{m}{M}(k+rM)} \\ &= e^{2\pi i\frac{mk}{M}}Z_f(l+mN,k-nM) \\ &= e^{2\pi i\frac{mk}{M}}Z_g(l,k-nM) \\ &= e^{2\pi i(\frac{mk}{M}+\frac{nl}{N})}Z_g(l,k) \quad \square. \end{aligned}$$

We have the following relation between the Zak transforms of a function f and its Fourier transform $\hat{f}$

$$M^{-1} Z_{\hat{f}}(l,k) = Z_f(-k,l) e^{-2\pi i k l/P} \tag{2.54}$$

and Zak transforms of a function f and its inverse Fourier transform $\check{f}$

$$M^{-1} Z_{\check{f}}(l,k) = Z_f(k,-l) e^{-2\pi i k l/P}. \tag{2.55}$$

Proof. Set

$$G(l,k) = Z_f(-k,l) e^{-2\pi i k l/P}.$$

Since

$$\begin{aligned} G(l+N,k) &= G(l,k), \\ G(l,k+M) &= G(l,k) e^{-2\pi i l/N}, \end{aligned}$$

then

$$G(l,k) = Z_g(l,k)$$

where

$$g(l) = M^{-1} \sum_{k=0}^{M-1} G(l,k).$$

Expanding

$$g(l) = M^{-1} \sum_{l=0}^{M-1} \sum_{r=0}^{N-1} e^{-2\pi i k l/P} f(l+rM) e^{-2\pi i r k/N}$$

$$
\begin{aligned}
&= M^{-1} \sum_{l=0}^{M-1} \sum_{r=0}^{N-1} f(l+rM) e^{-2\pi i \frac{k}{P}(l+rM)} \\
&= M^{-1} \sum_{p=0}^{P-1} f(p) e^{-2\pi i \frac{pk}{P}}) \\
&= M^{-1} \hat{f}(p).
\end{aligned}
$$

The second relation follows from the first one. □

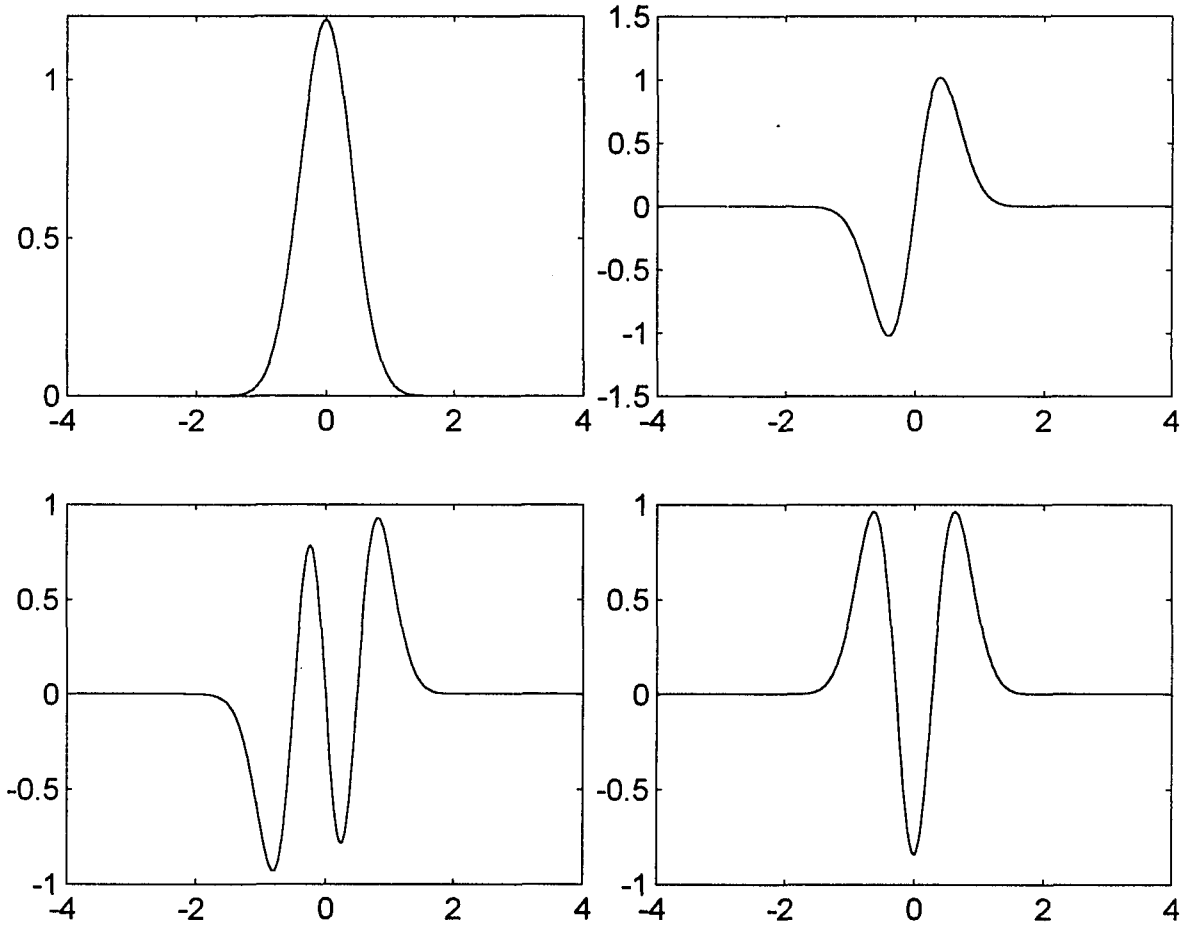

Figure 2.1: The first four Hermite functions (clockwise from top-left).

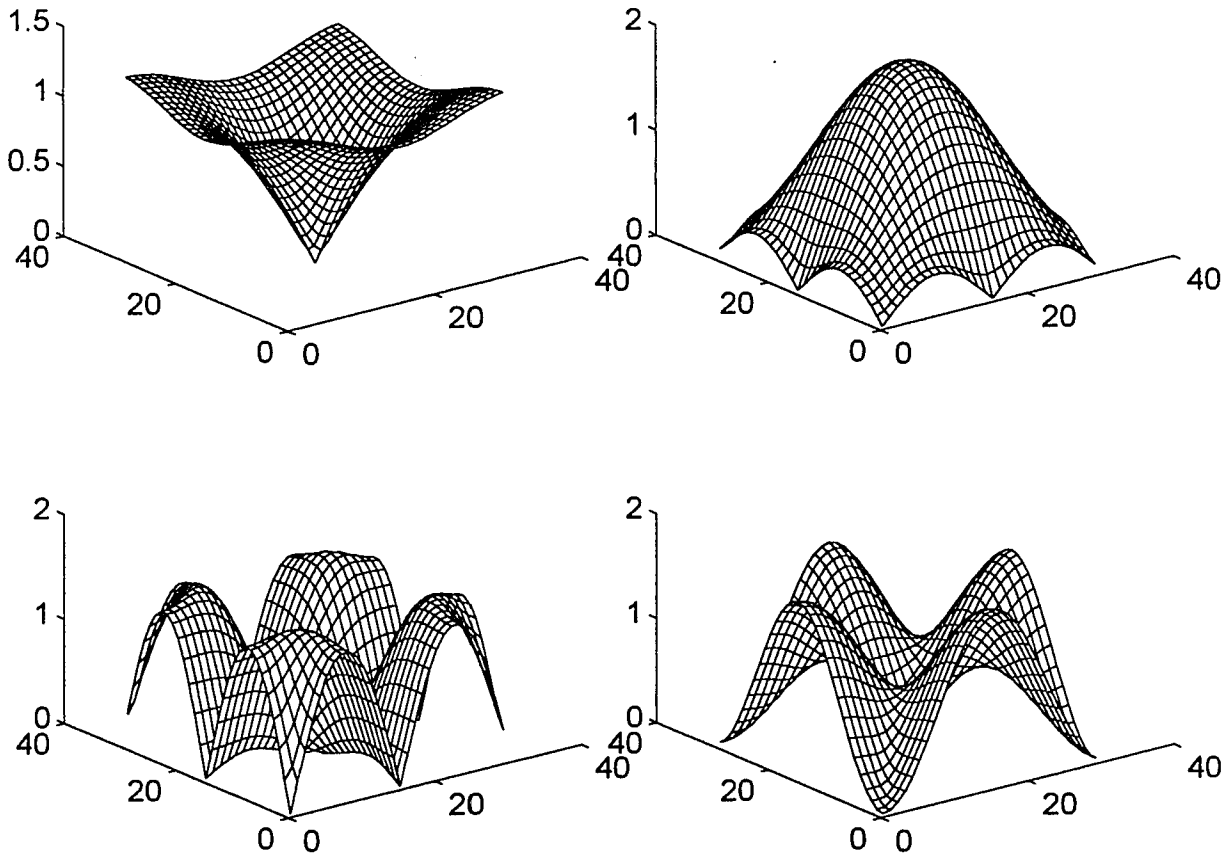

Figure 2.2: Zak transform magnitude of the first four Hermite functions (clockwise from top-left).

Chapter 3

The Gabor Expansion - A Brief Overview

This chapter is intended as a concise introduction to the field. It exposes the Gabor expansion as a valuable time-frequency tool for a signal analyst and reviews some of the concepts that are central to the theory of Gabor representation, such as the joint time-frequency localization and the invertibility of the discrete Gabor transform. Understanding of these concepts is essential in construction of efficient and flexible algorithms for digital signal processing.

This chapter has been organized into four sections. The first section addresses the basic concepts of Gabor expansion theory. The second section presents a survey of Gabor expansion algorithms. Section three discusses the many applications of Gabor expansion, especially image processing. Finally, section four establishes the relation of Gabor expansion to other time-frequency methods.

The material presented here spans fife decades of research done by engineers and mathematicians. Articles by Tolimieri *et al* [8,9] and Orr [62] provide an excellent introduction to the field. More advanced readers will appreciate an

early text by Tolimieri *et al* [6] and a more recent paper by Janssen [51]. Much of the material covered in section two can be found in Orr [61,62]. In section three numerous references are given but perhaps the most important ones are Porat and Zeevi [65] and Porat and Friedlander [40]. For section four see Cohen [27] and Hlawatsch and Boudreaux-Bartels [47].

3.1 Introduction

A Gabor representation [41] of a function $f(t)$ is a series expansion of the form

$$f(t) = \sum_m \sum_n a_{mn} g_{mn}(t), \tag{3.1}$$

where $g_{mn}(t)$ are the time and frequency shifted versions of the synthesis window function $g(t)$

$$g_{mn}(t) = g(t - nT)e^{2\pi i m\Omega t}, \tag{3.2}$$

$g(t)$ is a finite energy window function normalized according to

$$\int_{-\infty}^{\infty} |g(t)|^2 dt = 1, \tag{3.3}$$

and a_{mn}, $m, n \in Z$ are the Gabor coefficients. Thus Gabor expansion represents a signal $f(t)$ as a superposition of shifted (over discrete times nT) and modulated (with discrete frequencies $m\Omega$) versions of the elementary signal $g(t)$. Each shifted and modulated window $g(t)$ is assigned a weight a_{mn}, square magnitude of which provides a measure of energy of the signal $f(t)$ at the (m, n)-th logon.

The time shift T and the frequency shift Ω satisfy the relationship $\Omega T = 1$

which defines the critical sampling. Gabor expansion constitutes a special case of more general structures called Weyl-Heisenberg systems which are not restricted to the above condition. We will return to the concept of Weyl-Heisenberg systems later in the chapter.

The classical choice for the window function is the Gaussian signal

$$g(t) = 2^{1/4} e^{-\pi t^2} \tag{3.4}$$

distinguished by the product of its effective widths on the time and frequency axes, being the minimal possible according to the uncertainty principle. Indeed, using the second moments of g as a measure of duration of $g(t)$ and $\hat{g}(\nu)$

$$(\Delta t)^2 = \frac{\int t^2 |g(t)|^2 dt}{\int |g(t)|^2 dt},$$

$$(\Delta \nu)^2 = \frac{\int \nu^2 |\hat{g}(\nu)|^2 d\nu}{\int |\hat{g}(\nu)|^2 d\nu}$$

it can be shown [63] that the product of the time spread Δt and the bandwidth $\Delta \nu$ is limited by the inequality

$$\Delta t \Delta \nu \geq 1/4\pi \tag{3.5}$$

and achieves the minimum when g is a Gaussian signal.

Besides having the best joined time-frequency resolution the Gaussian function has a number of other desirable properties: it is an eigenfunction of the Fourier transform, has the 'proper' smoothness, fast decay and lack of ringing, and can describe the receptive field of a visual cortical neuron [32], which has significant

advantages in such applications as image coding and computer vision.

There are other choices possible for the window function, two of which are especially interesting: the rectangular function

$$g(t) = \begin{cases} 1, & 0 \leq t \leq 1, \\ 0, & otherwise, \end{cases}$$

and the sinc function $g(t) = \frac{sin\pi t}{\pi t}$. In the first case the Gabor expansion has an especially easy interpretation: the signal $f(t)$ is 'split' into a discrete set $\{f_i\}$ defined on successive time intervals $[nT, (n+1)T]$, with a Fourier transform being taken of each f_i. Since the rectangular function and the sinc function form a Fourier transform pair, the later window provides a signal description at successive frequency intervals. Incidentally, the shifted and modulated sets of both the rectangular window and the sinc window form orthonormal basis. In general however this does not need to be the case. For a Gaussian window in particular the inner product

$$< g, g_{mn} >= exp[-\frac{\pi}{2}(m^2 + n^2)],$$

which implies that the set (3.2) for g in (3.4) is not orthogonal.

3.2 Survey of Algorithms

Since the set $\{g_{mn}\}$ does not constitute an orthonormal basis, the standard inner product rule can not be used for computing the expansion coefficients and alternative techniques have to be developed. In this section we will describe three methods for computing Gabor coefficients: the biorthogonal method, the

Zak transform method and the deconvolution method.

In 1980 Bastiaans proposed a solution to the Gabor expansion inverse problem utilizing the concept of biorthogonal window. As it became evident that a stable and unique solution cannot be expected for windows with desirable localization properties, Bastiaans theory was later extended to oversampling situations via theory of frames. A radically different approach was taken by Auslander and Tolimieri, who used the calculus of the Zak transform to develop an efficient method for computing Gabor coefficients and specified conditions for stability of the computation. Later, again using the Zak transform theory, Auslander and Tolimieri formulated the deconvolution algorithm, relating Gabor representation to the ambiguity function and the short-time Fourier transform. In this section we will discuss the ideas that led to formulation of the three methods, explain the transition from infinite and continuous to finite and discrete case and compare the algorithms computational efficiency.

3.2.1 The Biorthogonal Method

In [12] Bastiaans have shown that if f can be expressed as

$$f(t) = \sum_m \sum_n a_{mn} g_{mn}(t)$$

and simultaneously in the form

$$f(t) = \sum_m \sum_n b_{mn} h_{mn}(t),$$

then the Gabor coefficients can be synthesized as follows

$$a_{mn} = \int f(t)h^*_{mn}(t)dt =< f, h_{mn} > . \tag{3.6}$$

Substituting (3.6) into (3.1) leads to the completeness relation

$$\sum_{t_1}\sum_{t_2} g^*_{mn}(t_1)h_{mn}(t_2) = \delta(t_1 - t_2), \tag{3.7}$$

from which we conclude that the expansions do exist. Applying the Poisson formula to (3.7) yields the biorthogonal relation [85]

$$\int g^*_{mn}(t)h_{kl}(t)dt = \delta_{m-k}\delta_{n-l}, \tag{3.8}$$

which for $k = l = 0$ takes form

$$\int g^*_{mn}(t)h(t)dt = \delta_m\delta_n, \tag{3.9}$$

or equivalently

$$Z^*_g(\nu,\tau)Z_h(\nu,\tau) = 1, \tag{3.10}$$

from which h can be computed through the inverse Zak transform

$$h(\tau) = ZT^{-1}\{\frac{1}{Z^*_g(\nu,\tau)}\}. \tag{3.11}$$

Application of (3.6) is obstructed by several problems. First, it is not trivial to determine a function that is biorthogonal to an arbitrary given function. Except for a few signals such as the Gaussian and the exponential, biorthogonal functions are not known analytically. Second, since continuous functions lead to zeros in Z_g the equation (3.8) has a homogenous solution. The analysis

function h in that case is not unique: if $h(t)$ is a window function then $x(t)$ can be constructed such that the $Z_g^* Z_x$ product vanishes on the same set as does the product $Z_g^* Z_h$, so the sum $h(t) + x(t)$ constitutes a proper window too. Third, it is very difficult to have the window function and the biorthogonal function both having a good time-frequency localization. As can be seen from (3.10) the Zero theorem intervenes and a continuous, well localized g inevitably leads to an infinite energy, discontinuous window h. As a result the coefficients have bad convergence properties and a stable signal reconstruction is not possible. One can attempt to find a stable solution in the oversampled situation, where numerical methods exist [85] for determining the biorthogonal function through solving an underdetermined linear system. The procedure however is cumbersome and the solution is non-unique. In [69] Qian used the window's non-uniqueness by imposing additional constrains on biorthogonal function and constructed an algorithm which produces a biorthogonal function that is closest to a given window.

3.2.2 The Zak Transform Method

The second method of computing Gabor coefficients is based on Zak transform introduced in chapter two. Taking the Zak transform of both sides of (3.1) yields

$$Z_f(\nu, \tau) = \sum_m \sum_n a_{mn} Z_{g_{mn}}(\nu, \tau). \tag{3.12}$$

Using (2.40), we have the following relation among the Zak transforms of f and g, and the Gabor coefficients

$$Z_f(\nu,\tau) = Z_g(\nu,\tau)\sum_m\sum_n a_{mn}e^{2\pi i(nT\nu+m\Omega\tau)}. \tag{3.13}$$

Dividing by Z_g and taking the inverse Fourier transform of both sides yields the inverse formula

$$a_{mn} = \int_T\int_\Omega \frac{Z_f(\nu,\tau)}{Z_g(\nu,\tau)}e^{-2\pi i(nT\nu+m\Omega\tau)}d\nu d\tau. \tag{3.14}$$

Due to the Zero theorem the Zak transform of a smooth window has zeros in the unit square. Unless Z_f has matching zeros, the ratio Z_f/Z_g is not square integrable and the formula (3.14) does not produce finite Gabor coefficients. For a Gaussian window in particular Z_g has a zero at (1/2,1/2) and the energy of expansion coefficients

$$\sum_m\sum_n |a_{mn}|^2 = \infty. \tag{3.15}$$

A relation between zero sets of the window g, the signal f, completeness of the Gabor expansion and stability of the computation will be discussed in detail in chapter four. It is worth mentioning however, that unlike in the case of the biorthogonal method, the Zak transform algorithm provides simple and easily computable criteria for determining stability of the Gabor expansion and, as will be seen later in the chapter, constitutes the most efficient and flexible technique for computing Gabor coefficients.

3.2.3 The Convolution Method

We start with the equation (3.13) from Section 3.2.2. and multiply both sides by Z_g^*

$$Z_f(\nu,\tau)Z_g^*(\nu,\tau) = |Z_g(\nu,\tau)|^2 \sum_m \sum_n a_{mn} e^{-2\pi i(nT\nu + m\Omega\tau)}. \tag{3.16}$$

The left-hand side of (3.16) is a doubly periodic function. We can write

$$Z_f(\nu,\tau)Z_g^*(\nu,\tau) = \sum_m \sum_n b_{mn} e^{-2\pi i(nT\nu + m\Omega\tau)}. \tag{3.17}$$

Providing that f and g are smooth, the Fourier series in (3.17) converges absolutely and its coefficients are given by

$$b_{mn} = \int\int Z_f(\nu,\tau)Z_g^*(\nu,\tau)e^{2\pi i(nT\nu + m\Omega\tau)}d\nu d\tau. \tag{3.18}$$

Using (2.40) we have

$$b_{mn} = \int\int Z_f(\nu,\tau)Z_{g_{mn}}^*(\nu,\tau)d\nu d\tau \tag{3.19}$$

and by (2.41) becomes

$$b_{mn} = \int f(t)g_{mn}^*(t)dt, \tag{3.20}$$

or

$$b_{mn} =< f, g_{mn} > . \tag{3.2i}$$

Similarly, since $|Z_g|^2$ is doubly periodic, we can write

$$|Z_g(\nu,\tau)|^2 = \sum_m \sum_n c_{mn} e^{-2\pi i(nT\nu + m\Omega\tau)}, \tag{3.22}$$

where

$$c_{mn} =< g, g_{mn} > . \tag{3.23}$$

We can write (3.16) as

$$\sum_m \sum_n b_{mn} e^{-2\pi i(nT\nu+m\Omega\tau)} = \sum_m \sum_n c_{mn} e^{-2\pi i(nT\nu+m\Omega\tau)} \times \sum_m \sum_n a_{mn} e^{-2\pi i(nT\nu+m\Omega\tau)} \tag{3.24}$$

or as

$$b_{mn} = \sum_p \sum_q c_{m-p,n-q} a_{pq}, \tag{3.25}$$

which constitutes a double convolution

$$b = c \circ a. \tag{3.26}$$

To compute Gabor coefficients we have to deconvolve (3.26). Combining (3.16), (3.17) and (3.21) and making the finite approximation we can write

$$\sum_{m=0}^{M-1} \sum_{n=0}^{N-1} < f, g_{mn} > e^{-2\pi i(nT\nu+m\Omega\tau)} = |Z_g(\nu,\tau)|^2 \sum_{m=0}^{M-1} \sum_{n=0}^{N-1} a_{mn} e^{-2\pi i(nT\nu+m\Omega\tau)}. \tag{3.27}$$

We compute Gabor coefficients via inverse Fourier transform:

$$a_{pq} = \int_T \int_\Omega \{\frac{1}{|Z_g(\nu,\tau)|^2}\} \sum_{m=0}^{M-1} \sum_{n=0}^{N-1} < f, g_{mn} > e^{-2\pi i[(n-q)T\nu+(m-p)\Omega\tau]} d\nu d\tau. \tag{3.28}$$

As in the Zak transform method care must be taken to avoid zeros of Z_g in the sampling process. If Z_g vanishes at some point, the division step in the deconvolution algorithm becomes numerically unstable.

The importance of the deconvolution formula lies in providing comparison

between Gabor representation and a sampled short-time Fourier transform, which leads to interpretation of the sampled short-time Fourier transform as a two-dimensional convolution of Gabor coefficients with a sampled autoambiguity function of the window. We will return to this relationship in section four.

3.2.4 The Discrete Case

Numerical implementation of (3.1) and (3.14) requires discretization and finitization, which necessitates taking periodic extensions of the time functions. Periodization and sampling of $f(t)$ reduces the continuous Gabor expansion to a discrete linear mapping that relates the samples of the periodized f with period P to a doubly periodic $M \times N$ array of Gabor coefficients, where M is the number of frequency cells, N is the number of time cells and $MN = P$. We will derive the discrete version of (3.1) in the context of W-H expansion (with $\Omega T \leq 1$), obtaining the discrete Gabor sum formulation as a special case. Set $MN = M'N' = P,\ \Omega T = 1/R,\ M = RM',\ N' = RN.$

Take the periodic extension $f^{N'T}(t)$ of $f(t)$ such that

$$f^{N'T}(t) = \sum_{\alpha} f(t + \alpha N'T), \quad \alpha \in Z, \tag{3.29}$$

and write the W-H expansion of $f^{N'T}(t)$ as

$$\begin{aligned} f^{N'T}(t) &= \sum_{\alpha}\sum_{m}\sum_{n} a_{mn'} g(t - n'T + \alpha N'T) e^{2\pi i (t+\alpha N'T) m\Omega} \\ &= \sum_{m}\sum_{n} a_{mn'} g^{N'T}(t - n'T) e^{2\pi i t m\Omega}, \end{aligned} \tag{3.30}$$

where

$$g^{N'T}(t) = \sum_{\alpha} g(t + \alpha N'T). \tag{3.31}$$

Observe that Gabor coefficients a_{mn} are invariant to joint periodization of the signal and the window. Set $m = p + rM, \quad n' = q' + sN', \quad 0 \leq p < M, \quad 0 \leq q' < N', \quad r, s \in Z$, which yields

$$\begin{aligned} f^{N'T}(t) &= \sum_{r} \sum_{s} \sum_{p=0}^{M-1} \sum_{q'=0}^{N'-1} a_{p+rM,q'+sN'} g^{N'T}(t - (q' + sN')T) e^{2\pi i t(p+rM)\Omega} \\ &= \sum_{r} \sum_{s} \sum_{p=0}^{M-1} \sum_{q'=0}^{N'-1} a_{p+rM,q'+sN'} g^{N'T}(t - q'T) e^{2\pi i t(p+rM)\Omega}. \end{aligned} \tag{3.32}$$

Sample the continuous signal $f^{N'T}(t)$ at $\mathrm{t}_k = \frac{kT}{M'}$ and introduce a shorthand notation

$$\tilde{f}(k) = f^{N'T}(\frac{kT}{M'}) \tag{3.33}$$

$$\tilde{g}(k) = g^{N'T}(\frac{kT}{M'}). \tag{3.34}$$

The expression (3.32) reduces to

$$\begin{aligned} \tilde{f}(k) &= \sum_{r} \sum_{s} \sum_{p=0}^{M-1} \sum_{q'=0}^{N'-1} a_{p+rM,q'+sN'} \tilde{g}(k - q'M') e^{2\pi i \frac{k(p+rM)}{RM'}} \\ &= \sum_{p=0}^{M-1} \sum_{q'=0}^{N'-1} \{ \sum_{r} \sum_{s} a_{p+rM,q'+sN'} \} \tilde{g}(k - q'M') e^{2\pi i \frac{kp}{M}}. \end{aligned} \tag{3.35}$$

Define a doubly periodized array

$$\tilde{a}_{pq'} = \sum_{r} \sum_{s} a_{p+rM,q'+sN'}, \tag{3.36}$$

which in effect yields the formula

$$\tilde{f}(k) = \sum_{p=0}^{M-1} \sum_{q'=0}^{N'-1} \tilde{a}_{p,q'} \tilde{g}(k - q'M') e^{2\pi i \frac{kp}{M}}. \tag{3.37}$$

The array $\tilde{a}_{p,q'}$ is periodic in time and frequency with periods M and N' and it forms a two-dimensional discrete Fourier transform pair with the array $a_{p,q'}$. For $\Omega T = 1$ (or, equivalently, for $M = M'$, $N = N'$) the formula (3.37) reduces to

$$\tilde{f}(k) = \sum_{p=0}^{M-1} \sum_{q=0}^{N-1} \tilde{a}_{p,q} \tilde{g}(k - qM) e^{2\pi i \frac{kp}{M}}. \tag{3.38}$$

To obtain the finite and discrete equivalent of (3.14) we start with (3.13), writing it in a periodized and sampled version. Sampling the continuous variables ν and τ at $\nu_l = \frac{l\Omega}{N}, \tau_k = \frac{kT}{M}$ and setting

$$Z_f(l,k) = Z_f(\frac{l\Omega}{N}, \frac{kT}{M}), \tag{3.39}$$

$$Z_g(l,k) = Z_g(\frac{l\Omega}{N}, \frac{kT}{M}), \tag{3.40}$$

we have

$$\begin{aligned} Z_f(l,k) &= Z_g(l,k) \sum_r \sum_s \sum_{p=0}^{M-1} \sum_{q=0}^{N-1} a_{p+rM,q+sN} e^{2\pi i \Omega T (\frac{(p+rM)k}{M} + \frac{(q+sN)l}{N})} \\ &= Z_g(l,k) \sum_{p=0}^{M-1} \sum_{q=0}^{N-1} \tilde{a}_{p,q} e^{2\pi i (\frac{pk}{M} + \frac{ql}{N})}. \end{aligned} \tag{3.41}$$

After dividing both sides of (3.41) by Z_g and taking the inverse DFT we obtain the discrete counterpart of (3.14)

$$\tilde{a}_{p,q} = \frac{1}{MN} \sum_{k=0}^{M-1} \sum_{l=0}^{N-1} \frac{Z_f(l,k)}{Z_g(l,k)} e^{-2\pi i (\frac{pk}{M} + \frac{ql}{N})}. \tag{3.42}$$

Similarly, we can obtain ([62]) the discrete counterparts of the deconvolution formula (3.28)

$$\tilde{a}_{pq} = \frac{1}{MN} \sum_{l=0}^{N-1} \sum_{k=0}^{M-1} \{ \frac{1}{|Z_g(l,k)|^2} \} \sum_{r=0}^{M-1} \sum_{s=0}^{N-1} < \tilde{f}, \tilde{g}_{rs} > e^{-2\pi i[(s-q)Tl/N + (r-p)\Omega k/M]}, \tag{3.43}$$

and the biorthogonal formula (3.6):

$$\tilde{a}_{p,q} = \frac{1}{M} \sum_{k=0}^{MN-1} \tilde{f}(k) \tilde{h}(k - qM) e^{-2\pi i \frac{kq}{M}}. \tag{3.44}$$

Equation (3.42) is the exact finite discrete version of the continuous representation (3.14), providing a care is taken to avoid aliasing in time and frequency produced in the process of discretization. To limit time aliasing, the period MN of the signal and window must be taken sufficiently long with respect to their lengths, so no overlap occurs in the periodized f and g. To guarantee good frequency resolution the sampling rate M/T must exceed the bandwidth of f. If those conditions are met, then the array a_{pq} can be identified with one period of the array $\tilde{a}_{pq}$ and the formula

$$f(k) \approx \sum_{p=0}^{M-1} \sum_{q=0}^{N-1} a_{p,q} g(k - qM) e^{2\pi i \frac{kp}{M}} \tag{3.45}$$

provides a good approximation of the signal f. We will assume the approximation (3.45) holds throughout the remainder of the chapter.

The discrete formula (3.42) suffers from convergence problems similar to the ones encountered in the continuous situation. If the zero set of Z_f does not contain the zero set of Z_g, then (3.42) does not lead to a stable reconstruction

of Gabor coefficients. Various attempts were made to alleviate this problem. In [4] a subinteger shift of the sampling grid was suggested. Others proposed a decomposition of the signal into two parts: one with a zero matching the zero of the window and the other with a zero matching the shifted version of the window [2], [9], [21]. Still another way to avoid the zero problem arises from the observation that the Zak transform of the signal equals the Zak transform of the window times trigonometric polynomial whose coefficients are Gabor coefficients (3.41). If the ranges of the indices m and n are finite, one recovers the polynomial from samples located far away from the zeros of Z_g.

All of the proposed solutions have a limited application: they either assume computations are performed at a fixed sampling rate, or constrain the choice of the window. In chapter four a new method is introduced that provides a general solution to the zero problem.

3.2.5 Weyl-Heisenberg Systems and Frames

The Gabor expansion is a special case of Weyl-Heisenberg systems

$$f(t) = \sum_m \sum_n a_{mn} g(t - nT) e^{2\pi i m \Omega t},$$

which is defined by the choice of the tessellation parameters $\Omega = T = 1$. In the context of Weyl-Heisenberg systems selection of the window g and the parameters Ω and T determines completeness, uniqueness and convergence of the representation. For $\Omega T > 1$ the representation is incomplete. For $\Omega T = 1$ (the critical sampling case) the representation is in general unstable. As a consequence of the Balian-Low theorem the set $\{ g_{m\Omega, nT} : m, n \in Z \}$ does not

constitute an orthogonal basis and the standard Hilbert space inner product methods do not apply, if the window function is smooth and has fast decay (which is the case when g is Gaussian). An oversampling ($\Omega T < 1$) alleviates the stability problem, the representation in that case however is not unique, i.e. there is more than one set $\{a_{m,n}\}$ that satisfies (3.1) for a given f.

The Weyl-Heisenberg systems are often described in the language of frames, which provides a convenient overview of the computational issues.

The set of functions

$$\{g_{m\Omega,nT} : m, n \in Z\} \tag{3.46}$$

constitutes a frame if there exist positive numbers A, B, independent of f, called frame bounds, $0 < A \leq B < \infty$, such that for all $f \in L^2(R)$

$$A\|f\|_2^2 \leq \sum_m \sum_n | < f, g_{m\Omega,nT} > |^2 \leq B\|f\|_2^2. \tag{3.47}$$

The frame condition (3.47) guarantees that a numerically stable algorithm can be found to compute f from $< f, g_{m\Omega,nT} >$.

Several special cases are important to highlight. If the set (3.46) is orthonormal then the upper frame bound $B = 1$ and

$$\sum_m \sum_n | < f, g_{m\Omega,nT} > |^2 \leq \|f\|_2^2. \tag{3.48}$$

The function f will not in general be determined by the coefficients (which are not unique). However, if (3.46) is an orthonormal basis then $A = B = 1$ (an exact frame) and

$$\sum_m \sum_n | < f, g_{m\Omega,nT} > |^2 = \|f\|_2^2, \tag{3.49}$$

so f can be recovered from

$$f = \sum_m \sum_n < f, g_{m\Omega,nT} > g_{m\Omega,nT}. \tag{3.50}$$

For $A = B$ the set (3.46) constitutes a tight frame

$$\|f\|_2^2 = A^{-1} \sum_m \sum_n | < f, g_{m\Omega,nT} > |^2, \tag{3.51}$$

and we have

$$f = A^{-1} \sum_m \sum_n < f, g_{m\Omega,nT} > g_{m\Omega,nT}, \tag{3.52}$$

where the frame constant A indicates the rate of redundancy of the frame. Close to tight frames are snug frames, for which the ratio A/B is close to 1. They do not constitute basis but lead to inversion formulas with rapid convergence properties.

In case of any frame, a 'dual' frame can be constructed such that the set

$$\{\overline{g}_{m\Omega,nT} : m, n \in Z\} \tag{3.53}$$

is a frame with bounds A^{-1} and B^{-1}, so

$$B^{-1}\|f\|_2^2 \leq \sum_m \sum_n | < f, \overline{g}_{m\Omega,nT} > |^2 \leq A^{-1}\|f\|_2^2, \tag{3.54}$$

and

$$f = \sum_m \sum_n < f, g_{m\Omega,nT} > \overline{g}_{m\Omega,nT}. \tag{3.55}$$

Theory of frames was utilized by several researchers [59,94] to compute constrained biorthogonal windows in oversampling situations.

3.2.6 Computational Efficiency

In this section we focus on computational complexity of the discrete Gabor expansion algorithms [61]. The three main methods are evaluated: the Zak transform based, the deconvolution method and the biorthogonal method. Only the critical sampling case is considered. The evaluation of complexity of various algorithms is done by counting the number of multiplications required. The difference in number of machine cycles needed to perform real or complex multiplication and multiplication or division is ignored. The focus of the evaluation is the analysis relation for each method, as the synthesis in general performs identical operations in reverse. The investigation of computational complexity of the Gabor expansion presented here follows by and large the evaluation performed by Orr [61]. It includes evaluation of a variation on the biorthogonal method (not considered in [61]), where the inner product computation is performed in the Zak space.

Let us first identify and evaluate the component calculations that in various order occur in all of the three algorithms. They are: the Zak transform, 1-D or 2-D DFT, the inner product of integer-shifted windows and simple multiplications.

1. A P-point 1D or 2D DFT, where P is a power of 2, requires $P \log_2 P$ multiplications.

2. Since Zak transform can be treated as a DFT with the time offset as a parameter, we can compute $Z_f(l,k)$ as M N-point FFT's, each FFT

corresponding to:

$$Z_f(l,\cdot) = \sum_{r=0}^{N-1} f(\cdot,r)e^{2\pi i r\frac{l}{N}}, \tag{3.56}$$

where $f(k,r) = f(k+rM),\ 0 \le k \le M-1,\ 0 \le r \le N-1.$

The number of multiplications needed is $P\log_2 N,\ P = MN.$

3. An inner product $< f, g_n >= \sum_{k=0}^{M-1}\sum_{r=0}^{N-1} f(k,r)g^*(k,r-n)$ requires NP multiplications.

4. $Z_g,\ |Z_g|^2,\ h$ and Z_h are produced in the precomputational step and are not included in the total count of operations.

We now proceed with evaluation of the algorithms.

Zak transform method

The analysis formula is given by:

$$a_{mn} = \frac{1}{MN}\sum_{k=0}^{M-1}\sum_{l=0}^{N-1}\frac{Z_f(l,k)}{Z_g(l,k)}e^{-2\pi i(n\frac{l}{N}+m\frac{k}{M})}. \tag{3.57}$$

The operations needed are: the Zak transform of f ($P\log_2 N$), the ratio Z_f/Z_g (P) and the 2-D DFT on the ratio array ($P\log_2 P$). The total count is:

$$P(\log_2 P + \log_2 N + 1). \tag{3.58}$$

The deconvolution method

The analysis formula is given by:

$$a_{mn} = DFT^{-1}\{\frac{\sum_{r=0}^{M-1}\sum_{s=0}^{N-1} < f, g_{rs} > e^{-2\pi i[(s-n)l/N+(r-m)k/M]}}{|Z_g(l,k)|^2}\}, \tag{3.59}$$

where $< f, g_{rs} >$ can be expressed as

$$\sum_{k=0}^{M-1} \sum_{p=0}^{N-1} f(k,p) g^*(k, p-s) e^{2\pi i r k/N}. \tag{3.60}$$

The operations needed are: computation of the inner product $< f, g_s >$ (PN), 1-D DFT on $< f, g_s >$ yielding $< f, g_{rs} >$ $(P \log_2 M)$, 2-D DFT on the product $< f, g_{rs} >$ $(P \log_2 P)$, division by $|Z_g|^2$ (P) and the final inverse 2-D DFT $(P \log_2 P)$. The total count is:

$$P[2 \log_2 P + \log_2 M + N + 1]. \tag{3.61}$$

An alternative (and faster) way to proceed is to compute the inner product in the Zak space. From (2.41) we have

$$< f, g_{rs} >= \sum_{l=0}^{N-1} \sum_{k=0}^{M-1} Z_f(l,k) Z_g^*(l,k) e^{2\pi i (sl/N + rk/M)}. \tag{3.62}$$

The first two steps in the proceeding computation are replaced by calculation of Z_f $(P \log_2 N)$, the product $Z_f Z_g^*$ (P) and 2-D DFT of the product $(P \log_2 P)$. In effect we have:

$$P[3 \log_2 P + \log_2 N + 2]. \tag{3.63}$$

The biorthogonal method

The analysis formula is given by:

$$a_{mn} = \sum_{k=0}^{M-1} \sum_{r=0}^{N-1} f(k,r) h_{mn}^*(k,r). \tag{3.64}$$

Table 3.1: Complexity results for Gabor expansion algorithms

Computational method	Complexity
Zak transform	$P(\log_2 P + \log_2 N + 1)$
Biorthogonal-Zak	$P(\log_2 P + \log_2 N + 1)$
Biorthogonal	$P(\log_2 M + N)$
Deconvolution-Zak	$P[3\log_2 P + \log_2 N + 2]$
Deconvolution	$P[2\log_2 P + \log_2 M + N + 1]$

The operations needed are: computation of the inner product $< f, h_n >$ (PN multiplications) and N M-point 1-D DFT's ($P\log_2 M$). The total count is:

$$P(\log_2 M + N). \tag{3.65}$$

In an alternative scenario one takes advantage of the Zak transform in computing the inner product (in a similar fashion as in the case of the deconvolution method) which yields $P\log_2 N$ multiplications for calculation of Z_f, P multiplications for computing of $Z_f Z_h^*$ and $P\log_2 P$ computations for 2-D DFT. The total count in this case is

$$P(\log_2 P + \log_2 N + 1). \tag{3.66}$$

Table 1. summarizes the complexity results.

Summary

The results of this section demonstrate that the computational cost of the biorthogonal method is identical to the Zak transform based, providing the

inner product is computed in the Zak domain. The number of operations required in both cases is of the order of $P \log_2 P$. The deconvolution method comes as the least efficient, even though the use of the Zak transform helps again to reduce the total number of multiplications to the order of $3P \log_2 P$.

3.3 Applications

Literature detailing applications of Gabor expansion spans numerous different fields. Teti and Kritikos used successfully Gabor expansion for SAR ocean image analysis [78], Womack and Cruz have shown its advantages in seismic data filtering [87], Farkash *et al* introduced a Gabor-based scheme for analog speech scrambling [36], Qian *et al* applied Gabor expansion to speech processing [71] and Anderson *et al* used it for medical image compression [3].

Perhaps the most complete body of work exists for implementation of Gabor transform to image representation. It has been the topic of several papers by Porat, Zeevi and Gertner [65,66,88,91,92] and was researched independently, from the neural networks perspective, by Dougman [32-34].

Dougman recognized in 1980 [32] that receptive field profiles encountered in cortical cells can be modeled by a family of **2-D Gabor filters**

$$G(x,y) = e^{-\pi[(x-x_0)^2\alpha^2+(y-y_0)^2\beta^2]}e^{-2\pi i[u_0(x-x_0)+v_0(y-y_0)]} \tag{3.67}$$

which constitute a generalization of the 1-D Gabor Elementary Functions. He computed the theoretical lower bound of joined uncertainty of the 2-D Gabor filters in the time-frequency domain. Defining uncertainty in each of the four variables x, y, u and v by the normalized second moments $(\Delta x), (\Delta y), (\Delta u), (\Delta v)$, being the effective widths and lengths of the 2-D filter in time and frequency, respectively, he has shown that a 2-D uncertainty principle exists:

$$(\Delta x)(\Delta y)(\Delta u)(\Delta v) \geq 1/16\pi^2 \tag{3.68}$$

and that the 2-D Gabor filters achieve the maximal possible joint resolution in the conjoint 4-D time-frequency space.

Dougman also demonstrated decorrelating consequences of expanding an image into 2-D Gabor elementary functions, achieving reduction in entropy for the Lena portrait from 7.57 in the pixel representation to 2.55 in the Gabor transform.

In [33] Dougman proposed a neural network to find the coefficients in the Gabor decomposition, but because of the iterative nature of this method the speed of the convergence at which usable results can be obtained is unknown, his approach does not seem to be suitable for real-time applications.

A more conventional implementation technique was given in [65] where **Porat and Zeevi** developed a **generalized Gabor scheme for image representation** which includes implementation of position-dependent sampling rate (which is related to inhomogeneity of cell density in human vision), octave relations between central frequencies and phase quantization.

Compactness of finite Gabor representation is studied computationally, using two types of one-dimensional signals. The first is periodic, sine-wave signal; the other is an aperiodic signal, synthesized by modulating a sine-wave in both amplitude and frequency. A set of coefficients is computed via the biorthogonal method with a Gaussian window and the signals are reconstructed from a finite subset of Gabor elementary functions. It is concluded that periodic images have no advantage over aperiodic ones when signal representation is accomplished by the Gabor scheme (in fact the aperiodic signal has a more

compact coefficient set). The result is compared with the global Fourier transform in which periodic signals have simpler representation.

To study the effects of **phase quantization** the authors proposed a formulation of the expansion

$$f(t) = \sum_m \sum_n |a_{mn}| e^{i\alpha_{mn}} g_{mn}(t) \tag{3.69}$$

where $|a_{mn}|$ is the magnitude of a_{mn} and α_{mn} is its phase. It is shown that for N quantization levels the signal reconstructed from a quantized-phase set $\{a_{mn}\}$ can be expressed by

$$f(t) = \sum_m \sum_n |a_{mn}| g_{mn}(t) \{ \sum_p sinc(p + \frac{1}{N}) e^{i(pN+1)\alpha_{mn}} \} \tag{3.70}$$

where $sinc(x) = \frac{sin(\pi x)}{\pi x}$, and α_{mn} is the quantified phase. The expression shows that for $p \neq 0$ 'false' images are added with wrong phase information; these false images however become weaker as N increases ($sinc(x)$ approaches zero for arguments close to integers). The analytical results were computationally tested for 5 and 24 quantization levels. The tests have shown a good approximation for 24 levels and a fair one (the signal was still easily recognizable) for 5 levels. These results were related to calculations of the attenuation factor $B(N) = sinc(\frac{1}{N})$ for $N = 5$ and 24 where $B(5) = 0.935$ and $B(24) = 0.997$, which indicates that the original images remain dominant in both cases.

The Porat-Zeevi generalized Gabor scheme incorporates two essential features in human vision: the **position-dependant sampling rate** , which combines nonuniform spatial sampling and logarithmic scaling along the frequency axes,

and **oversampling** which is defined in terms of an overlapping window function. The rationale behind incorporating position-dependant sampling is reduction of the dimensionality of the representation. In implementation of the Gabor image representation scheme as a visual data acquisition system the highest sampling is performed on the area of interest, selected by directing the 'visual axes' of the system toward it, whereas the background of this area of interest is sampled at a lower rate. Illustrations of several time-frequency lattice tessellations are given, no procedure however is developed to provide specific implementation guidelines or to evaluate the inherently involved in such a scheme trade-offs.

As a related concept, a **pyramidal scheme** of multiresolution (Gaborian Pyramid) is considered, where the effective spatial widths of the Gabor elementary functions become narrower as the frequency number increases. Analytical formulation of the Gaborian Pyramid is given and it is shown that the coefficient sets derived from the Gaborian Pyramid and from the standard Gabor expansion are equivalent.

The authors extend the Gabor scheme farther by proposing a **two-dimensional generalization** . The 2-D signal $f(x,y)$ is expressed by

$$f(x,y) = \sum_{m_x n_x m_y n_y} a_{m_x n_x m_y n_y} g_{m_x n_x m_y n_y}(x,y) \tag{3.71}$$

where $g_{m_x n_x m_y n_y}(x,y)$ is a time-frequency shifted 2-D window function

$$g_{m_x n_x m_y n_y}(x,y) = g(x - m_x D_x, y - n_y D_y) e^{i(n_x W_x x + n_y W_y y)} \tag{3.72}$$

D_x, D_y being the effective window widths in x and y direction respectively and W_x, W_y being the corresponding frequency widths. The window $g(x, y)$ is separable

$$g(x, y) = g_x(x)g_y(y), \tag{3.73}$$

$g_x(x)$ and $g_y(y)$ however do not need to be of the same type. The 2-D generalization is also given in polar coordinates.

In [91] **Zeevi and Gertner** proposed a similar formalism which accomplishes the 2-D signal representation by means of the **Zak transform** .

Since physiological experiments reveal that the visual system is sensitive to spatial phase and similar results were obtained in experiments carried out with speech, the phase-only reconstruction of signal is sufficient under variety of conditions. Porat and Zeevi investigated **image representation by localized phase** using both Gabor scheme and STFT [92]. In both cases it was shown that image represented by localized phase-only information reproduce adequately the edge relationship while compressing the gray level information, unlike the localized magnitude-only representation that distorts the edge information. The authors compared image reconstruction from localized phase (Gabor/STFT) versus from global Fourier phase for 1-D and 2-D signals. In all cases the localized phase reconstruction scheme yielded superior results, both in terms of rms error and computational efficiency.

The authors also demonstrated that the magnitude information can be efficiently recovered from the phase-only information by an iterative technique

which involves repeated transformation between the frequency and spatial domains, applied along with the proper constraint on structure of the localized components of the image. Again, it was shown that the localized phase scheme has a far better rate of convergence and the number of computer operations per iteration is reduced, which in effect saves $\log_2 N/\log_2(N/M)$ operations for an image of N pixels and M segments.

One of the main tasks of a visual system is to separate the image into discrete entities or segments in order to understand the scene. This segmentation is based mainly on the detection of differences between the regions, defining the edges between them. Texture (or pattern) discrimination (which includes color and/or intensity of the surface) is one of the most important aspects of image segmentation. Global approaches to texture discrimination however are unable to give reasonable results when the image consists of more than one type of texture. Furthermore, contrast changes due to conditions of nonuniform illumination may hinder classification when global features are used, even in the case of one-texture image.

In [66] Porat and Zeevi presented an approach to generalized **texture analysis and synthesis** based on local feature extractors with the image represented by a set of two-dimensional Gabor elementary functions. Assuming that the primitives of natural textures are localized frequency components in the form of GEF, the authors based their analysis on computing correlations of such primitives with textured images. Six localized features derived from the first

and second order moments of the three primary features - spatial frequency along the preferred orientation, orientation of the spatial frequency and intensity information - were defined and computed in the experiments. They were: the dominant localized frequency F, variance of the dominant localized frequency VF, dominant orientation T, variance of the dominant orientation VT, mean of the localized intensity level L and variance of the localized intensity level VL. For each localized area m_x, m_y the six-dimensional feature space is specified, for which a classification scheme can be applied.

The resultant feature-vector was tested on eight textures. The most informative features proved to be VF and VL. In another experiment discrimination by the pair (VF, VL) was tested on rotated and translated versions of the original textures (in 49 different orientations). Texture discrimination using a simple classifier of minimum distance was found to be stable in the presence of additive noise, and degradation in performance occurred only at high noise levels. For classification accuracy of about 90 percent, use of two features (VF, VL) were found to be sufficient. Addition of a third feature (T) yielded an improved results in cases where use of two-feature vector proved insufficient (especially when testing rotated images).

In [35] **Ebrahimi and Kunt** developed an **image compression** technique based on Gabor expansion (pyramidal Gabor decomposition) and have shown that it leads to a significant reduction in the blocking effects dominant in the image, if compressed via the widely used Discrete Cosine Transform.

Another field where Gabor expansion has been recognized to be extremely useful is **signal detection** . In [40] **Friedlander and Porat** developed the basic theory and algorithms for a detection scheme for partially overlapped transient signals of unknown shapes and arrival times, using the Gabor representation with one-sided exponential window. In the numerical experiments they tested sensitivity of the Gabor detector to mismatch in the damping coefficient, the effect of noninteger arrival time and noninteger frequency. It was found that the Gabor transform based detector is reasonably tolerant to variations in the window width (mismatch by a factor of 4 in either direction still yields a single dominant Gabor coefficient with relatively small sidelobs) and in the arrival time, but is less tolerant to frequency variations. It is shown that the scheme is capable of separating transients having different arrival times with their waveforms partially overlapping, even in the case when the Gaussian white noise having standard deviation equal to the amplitude of the signal is added.

To gain a better understanding of Gabor representation of random signals, the effect of additive white noise was studied and standard properties of the Gabor coefficients of white noise were computed. The second order moments of the Gabor coefficients were shown to be chi-square for the 'noise-only' situation and non-central chi-square for 'signal+noise' situation. They were then used to introduce a detection statistic based on the Gabor coefficients.

The test platform of Friedlander and Porat was adapted by **Tolimieri** *et al* [5] who made a comparison of the Gabor expansion and the Short-Time Fourier

Transform for signal detection in a noisy environment. The numerical experiments confirmed the theoretical predictions that the STFT method with the one-sided exponential window outperforms the Gabor expansion with respect to signal to noise ratio by 2.6dB to 3.7dB depending on the choice of the time grid. While the result gives STFT an advantage when signal detection in absence of coefficient thresholding is applied, this does not constitute a real-life situation. In practice some thresholding is always used and since the STFT based detection suffers from the blurring effect which in turn compromises its resolution, a significant loss of information in the reconstructed signal can occur if thresholding levels comparable to the noise amplitude is applied. This trade-off between noise reduction and distortion is much less severe in the Gabor scheme due to its excellent localization properties. Another advantage of the Gabor expansion lies in its computational efficiency for both: the forward and reverse transform, while STFT inversion formula requires in general up to $O(P^2 \log_2 P)$ operations.

3.4 Relation to Other Time-Frequency Representations

The preceding sections of this chapter have primarily dealt with the description of Gabor expansion, its properties, applications and computational methods. The aim of this section is to discuss the connection of the Gabor expansion with other time-frequency signal representations.

We consider four well known time-frequency methods: Short-Time Fourier Transform (STFT), Wigner Distribution (WD), Ambiguity Function (AF) and Wavelet Transform (WT). It is shown that the five representations are closely interrelated. Samples of STFT spectrum can be expressed as a convolution of Gabor coefficients and samples of auto AF of the window g. STFT can also be seen as a Gabor expansion computed on an infinitely dense lattice. STFT is related to the WD: the squared magnitude of STFT is a weighted version in time and frequency of the WD and constitutes a special case of the smoothed WD. Ambiguity Function is a correlative dual of WD and the two representations are related by a Fourier transform pair. Cross AF of signals f and g can be interpreted as a STFT of f with window g. The representation that appears to be the most distinct from the group is WT. Still, despite the different approach to frequency discrimination, WT is related to STFT, since both wavelets and time-frequency shifts of the STFT window are special cases of coherent states associated with a Lie-group. Again, the relation with the cross AF is stressed, STFT being interpreted as a narrow-band cross AF and WT as a wide-band cross AF.

The most comprehensive review of time-frequency methods was done by Cohen [27]. A more compact characterization was given by Hlawatsch and Boudreaux-Bartels [47] and some of the relations were also stressed by Claasen and Mecklenbrauker [26]. Daubechies has studied localization and invertibility of STFT and WT [29-30]. A comprehensive survey of results on Gabor expansion and wavelets in terms of coherent states was given by Heil and Walnut [44]. Tolimieri and Orr [5] have given the relationship between STFT and Gabor expansion a precise formulation and demonstrated that the Gabor expansion has advantages in transient signal detection in certain situations. Kadambe and Boudreaux-Bartels compared existence of cross-terms in WD, WT and STFT in analysis of multicomponents signals [56]. Jones and Parks have made a similar comparison of several versions of WD with STFT [54]. Flandrin detailed relationships between Gabor expansion, WT and AF by considering signal decomposition as a detection-estimation problem [38]. A group-theoretic approach to Gabor expansion and STFT was presented by Feichtinger and Grochenig [37].

3.4.1 Short Time Fourier Transform

The Short Time Fourier Transform [1,5,15,16,27,29,37,47,54,55,60] pair is defined as

$$STFT_f(\tau,\nu) = \int f(t)g^*(t-\tau)e^{-2\pi i\nu t}dt \tag{3.74}$$

$$f(t) = \frac{1}{\int |g(\tau)|^2 d\tau} \int\int STFT_f(\tau,\nu)g(t-\tau)e^{2\pi i\nu t}d\tau d\nu. \tag{3.75}$$

The above formulas show a striking resemblance to the Gabor transform pair

$$a_{mn} = \int f(t)h^*(t - nT)e^{-2\pi imn\Omega t}dt, \tag{3.76}$$

$$f(t) = \sum_m \sum_n a_{mn}g(t - nT)e^{2\pi imn\Omega t}, \tag{3.77}$$

which sometimes leads to interpretation of the Gabor transform as a special case of STFT, in which the continuous variables τ and ν are taken on the discrete grid $(nT, m\Omega)$. In fact, sampling the STFT spectrum on the Gabor lattice yields an inner product formulation, similar to (2.125)

$$STFT_f(nT, m\Omega) = \int f(t)g^*(t - nT)e^{-2\pi imn\Omega t}dt. \tag{3.78}$$

A careful inspection of (3.74-3.78) shows however, that there is a fundamental difference between the two representations: while STFT uses the same window for synthesis and analysis, the Gabor expansion utilizes two distinct windows g and h, related via the biorthogonality condition (3.8). As a result the simplistic interpretation of Gabor expansion as a sampled version of STFT does not hold. Instead, the true relationship between the two representations is revealed in (3.25):

$$< f, g_{mn} >= \sum_r \sum_s a_{rs} < g, g_{m-r,n-s} > . \tag{3.79}$$

The above relation defines the sampled STFT spectrum as a double convolution of Gabor coefficients with the sampled auto AF of the window g. The STFT spectrum is thus a smeared replica of the Gabor coefficient array. It can be shown that the Gabor spectrum will in fact become identical with STFT in the limiting case, if we let the Gabor lattice to become infinitely dense, so $\Omega T \rightarrow 0$ which will constrain the biorthogonal window h to approach g.

3.4.2 Wigner Distribution

Most of the well-known time-frequency signal representations (TFR's) can be categorized as either linear or quadratic (some of them, like signal-adaptive radially-Gaussian kernel distribution are neither linear nor quadratic). STFT, Gabor expansion and wavelet transform belong to the first group. Ambiguity function, spectrogram, Rihaczek distribution, Wigner distribution and its generalizations belong to the second one. Wigner distribution [24-26,27,46,47,52, 54,56,68,72,86]

$$WD_f(t,\xi) = \int f(t+\frac{\tau}{2}) f^*(t-\frac{\tau}{2}) e^{-2\pi i \xi \tau} d\tau \tag{3.80}$$

is considered one of the most important quadratic TFR's due to a large number of desirable properties it possesses [24-26]. For example, it satisfies time-frequency shift invariance, preserves time and frequency support and the auto-WD is real valued. The WD also satisfies the marginal properties, that is the time and frequency integrals of the WD correspond to the signal instantaneous power and its spectral energy density, respectively. Hence, the WD can be loosely interpreted as a two-dimensional distribution of signal energy over the time-frequency plane (the WD may assume negative values, which together with the uncertainty principle prohibits an interpretation as a pointwise energy density distribution).

The main drawback of the WD is existence of cross terms. The WD of the sum of two signals $f(t) + g(t)$ is

$$WD_{f,g}(t,\xi) = WD_f(t,\xi) + WD_g(t,\xi) + 2Re\{WD_{f,g}(t,\xi)\} \tag{3.81}$$

where the first two terms WD_f and WD_g are autocomponents and the last term $WD_{f,g}$ is the cross term defined as

$$WD_{f,g}(t,\xi) = \int f(t+\frac{\tau}{2})g^*(t-\frac{\tau}{2})e^{-2\pi i\xi\tau}d\tau. \tag{3.82}$$

Cross terms are inherent in all quadratic time-frequency representations and can never be completely eliminated (if unitarity of the representation is to be preserved). However, since cross terms have oscillations at high frequencies, they can often be reduced by low-pass filtering (smoothing) the Wigner distribution. The price one has to pay is a loss of some of the desirable WD properties and a loss of time-frequency concentration, since smoothing generally causes broadening of the WD's signal terms. Among the attempts to obtain a cross term suppressed WD, the better known constructs are the pseudo-Wigner distribution (PWD), the smoothed Wigner distribution (SWD) and the Choi-Williams distribution (CWD). The PWD is defined as

$$PWD_f(t,\xi) = \int f(t+\frac{\tau}{2})f^*(t-\frac{\tau}{2})h(\tau)e^{-2\pi i\xi\tau}d\tau. \tag{3.83}$$

and involves frequency-direction convolution. The SWD reduces the cross terms in both: time and frequency by two-dimensional convolution

$$SWD_f(t,\xi) = \int f(t+\frac{\tau}{2})f^*(t-\frac{\tau}{2})h(t,\tau)e^{-2\pi i\xi\tau}d\tau. \tag{3.84}$$

If we rewrite (3.74) as

$$STFT_f(t,\nu) \;\; = \int f(\tau)g^*(\tau-t)e^{-2\pi i\nu\tau}d\tau, \tag{3.85}$$

then the complex spectrogram, which is the squared magnitude of STFT, can be interpreted as a two-dimensional convolution of Wigner distributions of the

signal and the window:

$$|STFT(t,\xi)|^2 = WD_f(t,\xi) \circ WD_g(-t,\xi). \tag{3.86}$$

The spectrogram is thus a special case of SWD where the smoothing kernel is the inverse Fourier transform of the WD of the time-reversed window function

$$h(t,\tau) = F^{-1}\{WD_g(-t,\xi)\}. \tag{3.87}$$

Choi and Williams have recently developed a shift-scale invariant distribution

$$CWD_f(t,\xi) = \int\int f(\mu + \frac{\tau}{2}) f^*(\mu - \frac{\tau}{2}) h(t;\mu,\tau) e^{-2\pi i \xi \tau} d\mu d\tau. \tag{3.88}$$

with the smoothing kernel

$$h(t;\mu,\tau) = \sqrt{\frac{\sigma}{4\pi\tau^2}} e^{-\frac{\sigma(\mu-t)^2}{4\tau^2}} \tag{3.89}$$

which preserves the signal energy marginals and proves useful for signals having cross terms equally pronounced in both time and frequency direction.
Finally, Morris and Qian [68] proposed a cross term deleted WD representation (CDR) computed via Gabor expansion, which retains the original time-frequency concentration at the cost of a loss of its unitary character.

3.4.3 Ambiguity Function

Ambiguity function is defined as [9,10,11,26,27,47,89]:

$$AF_{f,g}(\tau,\nu) = \int f(t + \frac{\tau}{2}) g^*(t - \frac{\tau}{2}) e^{-2\pi i \nu t} dt. \tag{3.90}$$

This general form of ambiguity function is also known as a cross-ambiguity function of signals f and g. For $f(t) = g(t)$ AF reduces to auto-ambiguity function of f:

$$AF_{f,f}(\tau,\nu) = \int f(t+\frac{\tau}{2})f^*(t-\frac{\tau}{2})e^{-2\pi i\nu t}dt. \tag{3.91}$$

Since AF satisfies the correlative marginal properties i.e. for $\nu = 0$ or $\tau = 0$ it simplifies to either the time-domain or the frequency-domain correlation function, it can be interpreted as a joint time-frequency correlation function. The maximum value of the auto AF occurs at the origin and equals the signals energy. In radar signal detection, when f and g are the transmitted and received signals, the maximum of the squared magnitude of the cross AF can be interpreted as the maximum likelihood estimator of the range τ and velocity ν of a moving target. The squared magnitude of the auto AF (the auto-ambiguity surface) provides a measure of effectiveness in radar signal design. The AF is related to the WD in the sense that they are a Fourier transform pair:

$$AF_{f,g}(\tau,\nu) = \int_t\int_\xi WD_{f,g}(t,\xi)e^{-2\pi i(\nu t-\tau\xi)}dtd\xi. \tag{3.92}$$

Hence, the properties of the WD such as time-frequency shifts and time-frequency moments have their equivalents for the AF and the differences in those properties determine the differences between the two signal representations. For example, the time-frequency shift of the signal leads to a corresponding shift in the WD, while the effect on the AF is a change in phase only. Moreover, the WD is always real while AF is in general complex. In a case when the signal is even or odd function of time, the WD and the AF are equal

up to a scale factor.

Both the WD and AF belong to the class of shift-invariant quadratic TFR's, known as the quadratic Cohen class. While the WD leads to a family of energetic time-frequency distributions C_E, in the sense that every member of C_E is a two-dimensional filtered version of WD with a characteristic kernel function, the AF, which is a correlative dual of WD, leads to the class of correlative time-frequency distributions C_C. In case of C_C, the members are derived by simple multiplication (rather than convolution) of AF and the Fourier transform of the characteristic kernel function. Hence, even if one's interest is to design a specific energetic time-frequency distribution, it is often more convenient to work with the dual C_C family of TFR's.

A different interpretation of AF can be obtained, if we write the cross AF as

$$AF_{f,g}(\tau,\nu) = \int f(t)g^*(t-\tau)e^{-2\pi i\nu t}dt, \tag{3.93}$$

or in the form of inner product

$$AF_{f,g}(nT,m\Omega) =< f(t), g_{m,n}(t) > . \tag{3.94}$$

By arguments of Section 3.2.3 this leads to a double convolution relation:

$$b_{m,n} = \sum_r \sum_s c_{m-r,n-s}a_{rs} \tag{3.95}$$

where $b_{m,n}$ is a sampled cross-ambiguity function of f and g, $a_{r,s}$ are Gabor coefficients of the signal f and $c_{m,n}$ are coefficients in the expansion of a doubly periodic function $|Zg|^2$ (see equation 3.24).

3.4.4 Wavelet Transform

There is a close similarity between wavelet transform and STFT. Recall the STFT formula in the continuous version

$$STFT_f(\tau,\nu) = \int f(t)g(t-\tau)e^{-2\pi i\nu t}dt, \tag{3.96}$$

and the discretized version, where $\tau = nT$ and $\nu = m\Omega$

$$STFT_f(n,m) = \int f(t)g(t-nT)e^{-2\pi imn\Omega t}dt, \tag{3.97}$$

The wavelet transform (WT) [27,28-30,38,44,47,54,56,58,73] provides a similar time-frequency description with analogous formulas:

$$WT_f(a,b) = |a|^{-1/2}\int f(t)h(\frac{t-b}{a})dt, \tag{3.98}$$

and

$$WT_f(m,n) = a_0^{-m/2}\int f(t)h(a_0^{-m}t - nb_0)dt, \tag{3.99}$$

where a and b are restricted to $a = a_0^m$, $b = nb_0a_0^m$, $m,n \in Z$, $a_0 > 1$, $b_0 > 0$ and the following admissibility condition is satisfied:

$$\int h(t)dt = 0. \tag{3.100}$$

The obvious similarity in the two transforms comes from the fact that both take inner products of f with a family of doubly indexed functions, $g_{mn}(t) = g(t-nT)e^{2\pi imn\Omega t}$ in (3.97) and $h_{ab}(t) = |a|^{-1/2}h(\frac{t-b}{a})$ in (3.98). The functions h_{ab} are called wavelets and the function $h_{00}(t)$ is a 'mother wavelet' which is equivalent to the window function g in STFT analysis. A popular choice for

h is the second derivative of the Gaussian $h(t) = (1 - t^2)e^{-t^2/2}$.

The inner product formulation contains a measure of correlation of signals f and g. In fact both STFT and WT can be related to the cross AF. The STFT, associated with Weyl-Heisenberg group can be interpreted as a narrow-band cross AF used in the radar situations, where Doppler shift is approximated by a frequency shift of the signal spectrum. The WT on the other hand, associated with the '$ax + b$' group can be interpreted as a wide-band cross AF used in sonar applications, where the Doppler effect varies in the signal's spectrum causing a stretching or a compression in the signal. The difference between the wide-band AF and WT lies in the range of the dilation parameter: in the case of AF the Doppler shift remains near unity, whereas WT is generally used to analyze signals over a large number of octaves.

The essential difference between WT and STFT lies in the shape of the analyzing functions g_{mn} and h_{ab}. While the set $\{g_{mn}\}$ consists of a fixed envelope and width functions g, uniformly shifted in time and frequency, the wavelets have a constant shape, their time-widths being functions of frequency: for high frequencies h_{ab} are narrow and for low frequencies h_{ab} are wide. This scaling effect can be related to frequency change $a = f_0/f$, where f_0 is the central frequency of h_{00}, which means that scaling by a factor of a induces a frequency change by the inverse factor $1/a$.

The difference in frequency discrimination in the two transforms can be illustrated in the context of a filter bank system. In the STFT case the bandpass filter's bandwidth is independent of the analysis frequency f. In contrast, the

bandwidth of the WT filter is proportional to f or, equivalently to the filter's relative bandwidth Q. As a result, the WT is better able than STFT to resolve short-duration high frequency phenomena.

A critical aspect of both transforms is their invertibility. In the continuous case a function can be reconstructed from its WT by use of the 'resolution of identity' formula

$$f(t) = \frac{c_h^{-1}}{a^2} \int \int WT_f(a,b) h_{ab}(t) da db, \tag{3.101}$$

where

$$c_h = 2\pi \int |\hat{h}(\xi)|^2 |\xi|^{-1} d\xi < \infty. \tag{3.102}$$

In the discrete case the reconstruction (in the critical sampling situation) depends on the existence of orthonormal basis. It was found that there are in fact some choices of h, a_0 and b_0 that make h_{mn} an orthonormal basis for $L^2(R)$. The earliest known example is the Haar basis, generated by

$$h(t) = \begin{cases} 1, & t \geq 0, \\ -1, & t < 0, \\ 0, & t < 0. \end{cases} \tag{3.103}$$

with $a_0 = 2, b_0 = 1$ and $h_{mn}(t) = 2^{-m/2} h(2^{-m}t - n)$, which however do not have good localization properties. A well localized orthonormal wavelet basis were discovered only fairly recently by Stromberg and independently by Meyer. A significant advances in the field were made by Daubechies who constructed orthonormal wavelet basis with compact support [28] and by Mallat and Meyer, who devised a multiresolution analysis [58] which was subsequently used as a vehicle in construction of new orthonormal basis.

While it was demonstrated that wavelet orthonormal basis are relatively easy to find and do not require restrictions on parameters a_0, b_0, for the STFT the Balian-Low theorem narrows the search for orthonormal basis to one special case: $\Omega T = 1$. In that case orthonormal basis can be found, but they can not have good localization properties in time and/or frequency domain. This is illustrated by two examples: the rectangular function and $g(t) = \frac{sin\pi t}{\pi t}$. Both functions generate an orthonormal basis. In the first case however $\int \xi^2 |\hat{g}(\xi)|^2 d\xi = \infty$ and in the second case $\int t^2 |g(t)|^2 dt = \infty$.

Chapter 4

Weyl-Heisenberg Systems: Computing Oversampled Discrete Gabor Expansions

Previously, a theoretical foundation for designing algorithms for computing Gabor coefficients at critical sampling was established applying the finite Zak transform. This theory established clear and easily computable conditions for existence of Gabor expansion and for stability of computations. The main computational task in the resulting algorithm was a 2-D finite Fourier transform.

In this chapter we extend the applicability of the approach to integer and rationally oversampled Gabor systems by developing a deeper understanding of the relationship established by the finite Zak transform between linear algebra properties of Gabor systems and function theory in Zak space. This relationship will impact on questions of existence, parameterization and computation of Gabor expansions.

4.1 Introduction

During the last four years powerful new methods have been introduced for analyzing Wigner transform of discrete and periodic signals [68,72,86] based on finite Gabor expansions [7,8,9,13,41,85]. A recent work [68] adapted these methods to gain control over the cross-term interference problem [46] by constructing signal systems in time frequency space for expanding Wigner transform from Gabor systems based on Gaussian-like signals.

The computational feasibility of the method in [68] depends strongly on the availability of efficient and stable algorithms for computing Gabor expansion coefficients. Since in general, Gabor systems are not orthogonal, standard Hilbert space inner product methods do not apply. Moreover since critically sampled Gabor systems may not form a basis, oversampling in time-frequency is necessary for the existence of arbitrary signal expansions. In fact this is usually the case for systems based on the Gaussian. In [68,72,85,86] the concept of biothogonals was applied to the problem of Gabor coefficient computation but many details as to existence and stability were left unresolved.

In [8,9,23] a theoretical foundation for designing algorithms for computing Gabor coefficients at critical sampling was established with the finite Zak transform at center stage. This theory established clear and easily computable conditions for existence of Gabor expansion and for stability of computations. The

main computational task in the resulting algorithm was a 2-D finite Fourier transform.

In this chapter the finite Zak transform will be established as a fundamental and powerful tool for studying critically sampled and rationally oversampled Gabor systems and for designing algorithms for computing Gabor coefficients for discrete and periodic signals, by developing a deeper understanding of the relationship between finite Zak transform zero sets and properties of Gabor systems. The role of the finite Zak transform is analogous to that played by the Fourier transform in replacing complex convolution computations by simple pointwise multiplication. In this new setting properties of Gabor systems such as their spanning space and dimension can be determined by simple operations on functions in Zak space. This relationship will impact on questions of existence, parameterization and computation of Gabor expansions and will lead to:

- simple criteria for completeness of a Gabor system based on an explicit description in Zak space of the linear span of a Gabor system. For a fixed window this criteria determines time-frequency sample rates necessary for completeness.

- explicit parameterization of the collection of all Gabor expansions of a signal over a specific Gabor system.

- the design of algorithms both at critical sampling and oversampling whose main computational task is implemented by 2-D finite Fourier transform offering the advantage of efficient, accurate and flexible code.

4.2 Weyl-Heisenberg Systems

Choose an integer $P > 0$. A discrete function $f(k), k \in Z$ is called P-periodic if

$$f(k+P) = f(k), \qquad k \in Z.$$

Denote by $L^2(P)$ the Hilbert space of all P-periodic functions with inner product

$$< f, g >= \sum_{k=0}^{P-1} f(k)g^*(k), \qquad f, g \in L^2(P).$$

For $0 \leq m, n < N$ and $g \in L^2(P)$ define $g_{m,n} \in L^2(P)$ by

$$g_{m,n}(k) = g(k-n)e^{2\pi imk/P}, \qquad k \in Z. \tag{4.1}$$

Suppose $P = NM = N'M'$. The *Weyl-Heisenberg* (W-H) *System* (g, M', N) is the set of functions

$$\{g_{mN,n'M'} : \quad 0 \leq m < M, \quad 0 \leq n' < N'\}. \tag{4.2}$$

We distinguish three cases

critically sampling $\quad N = N', \quad M = M'$

oversampling $\quad N' > N, \quad M' < M$

- *integer oversampling* $\quad M = RM', \quad R \in Z$

- *rational oversampling* $\quad M = RM', \quad R \in Q - Z$

undersampling $\quad N' < N, \quad M' > M$

We call g the *analysis signal* and (M', N) the *time-frequency sampling* rate

of the W-H system (g, M', N). Fixed time-frequency translates of W-H systems will also be called W-H systems. Fix $0 \leq n < N, \quad 0 \leq m' < M'$. The W-H system $(g, M', N)_{n,m'}$ is the set of functions

$$\{g_{n+mN,m'+n'M'} : \quad 0 \leq m < M, \quad 0 \leq n' < N'\}. \tag{4.3}$$

The two W-H systems are related by

$$g_{n+mN,m'+n'M'} = e^{2\pi i n n'/N'}(g_{n,m'})_{mN,n'M'}. \tag{4.4}$$

An expansion of an $f \in L^2(P)$ over a W-H system is called a *W-H expansion.* In this work we will develop efficient algorithms for describing linear span of a W-H system and for computing W-H expansions. This algorithms will provide simple conditions for completeness of a W-H system. For $g \in L^2(P)$, completeness conditions can be applied to produce algorithms which determine time-frequency sampling rates (M', N) such that (g, M', N) is a complete W-H system. The algorithm computing W-H expansions will parameterize the collection of all W-H expansions of a function over a given W-H system.

4.3 Finite Zak Transform (FZT)

Suppose $P = NM$. For $f \in L^2(P)$ define the *finite Zak Transform* (FZT) $Z_f(l, k), \quad k, l \in Z$ by

$$Z_f(l, k) = \sum_{r=0}^{N-1} f(k + rM)e^{2\pi i r l/N}, \quad k, l \in Z. \tag{4.5}$$

Elementary properties of FZT including FZT based algorithms for computing W-H expansions over complete critically sampled W-H systems can be found

in [8] and in Chapter 2. We will briefly discuss these results without proof and extend the role of the FZT to general W-H systems.

Theorem 1 *If* $f \in L^2(P)$ *then*

$$Z_f(l, k+M) = e^{-2\pi i l/N} Z_f(l,k), \quad k, l \in Z. \tag{4.6}$$

$$Z_f(l+N, k) = Z_f(l,k), \quad k, l \in Z. \tag{4.7}$$

Theorem 1 implies Z_f is P-periodic in each variable and is completely determined by its values

$$Z_f(l,k), \quad 0 \leq k < M, \quad 0 \leq l < N. \tag{4.8}$$

Denote by $L^2(N,M)$ the Hilbert space of all functions $F(l,k)$, $0 \leq k < M$, $0 \leq l < L$, with inner product

$$< F, G >= \sum_{k=0}^{M-1} \sum_{l=0}^{N-1} F(l,k) G^*(l,k), \quad F, G \in L^2(N,M). \tag{4.9}$$

Define $Z_f^0 \in L^2(N,M)$ by

$$Z_f^0(l,k) = Z_f(l,k), \quad 0 \leq k < M, \quad 0 \leq l < N. \tag{4.10}$$

In [8] we find the following theorem.

Theorem 2 *The mapping* $N^{-1/2} Z^0$ *is an isometry from* $L^2(P)$ *onto* $L^2(N,M)$. *If* $F \in L^2(N,M)$ *and* $f \in L(P)$ *is defined by*

$$f(k+rM) = N^{-1} \sum_{l=0}^{N-1} F(l,k) e^{-2\pi i r l/N}, \quad 0 \leq k < M, \quad 0 \leq l < N, \tag{4.11}$$

Then $F = Z_f^0$.

Theorem 2. permits free movement between operations in $L^2(P)$ and operations in $L^2(N, M)$. Algorithms for W-H systems and expansions are given in $L^2(N, M)$. The FZT translates between linear algebra properties of W-H systems in $L^2(P)$ and function theoretic properties in $L^2(N, M)$.

4.4 Application of FZT to W-H systems.

Application of the FZT to W-H systems is based on formulas contained in the following theorem [8]

Theorem 3 *If* $g \in L(P), \quad P = NM, \quad$ *and* $\quad 0 \leq m, n < P$, *then*

$$Z_{g_{mn}}(l, k) = e^{2\pi imk/P} Z_g(l + m, k - n), \quad k, l \in Z. \tag{4.12}$$

In particular, if $\quad 0 \leq m < M, \quad 0 \leq n < N$, *then*

$$Z_{g_{mN,nM}}(l, k) = Z_g(l, k) e^{2\pi i(mk/M + nl/N)}, \quad k, l \in Z. \tag{4.13}$$

By Theorem 1 the product function

$$Z_f(l, k) Z_g^*(l, k), \quad k, l \in Z \quad f, g \in L^2(P) \tag{4.14}$$

is M-periodic in the variable k and N-periodic in the variable l and can be viewed as a function in $L^2(N, M)$. The Fourier expansion of the product function is given in the following theorem

Theorem 4 *For* $f, g \in L(P), \quad P = NM,$

$$Z_f(l,k)Z_g^*(l,k) = \sum_{m=0}^{M-1}\sum_{n=0}^{N-1} < f, g_{mN,nM} > e^{2\pi i(mk/M+nl/N)}. \tag{4.15}$$

4.4.1 Critical Sampling.

Theorem 2 is a powerful tool for analyzing W-H systems. We first consider critically sampled W-H systems by extending the following result.

Theorem 5 *The critically sampled W-H system*

$$(g, M, N) = \{g_{mN,nM} \quad 0 \le m < M, \quad 0 \le n < N\} \tag{4.16}$$

is a basis of $L^2(P)$ *if and only if* Z_g *never vanishes.*

Define

$$I_{N,M} = \{(l,k): \quad 0 \le k < M, \quad 0 \le l < N\}. \tag{4.17}$$

By Theorem 4 and Theorem 2 we can identify the space of all $f \in L^2(P)$ satisfying

$$< f, g_{mN,nM} >= 0, \qquad 0 \le m < M, \qquad 0 \le n < N, \tag{4.18}$$

with the space of all $F \in L^2(N, M)$ satisfying

$$F(l,k)Z_g(l,k) = 0, \quad k, l \in I_{N,M}. \tag{4.19}$$

The space of such $F \in L^2(N, M)$ can be identified with the orthogonal complement of the linear span of (g, M, N). If Z_g never vanishes, this complement

is $\{0\}$ and (g, M, N) is a basis of $L^2(P)$ which is the content of theorem 5. More generally, we have the following result.

Theorem 6 *If the zero set ζ of Z_g in $I_{N,M}$ has exactly K points then the dimension of the linear span of (g, M, L) is $P - K$. An $f \in L^2(P)$ is in the linear span of (g, M, N) if and only if Zf vanishes on ζ.*

By Theorem 3, an $f \in L^2(P)$ has an expansion over (g, M, N)

$$f = \sum_{m=0}^{M-1} \sum_{n=0}^{N-1} a_{mN,nM} g_{mN,nM} \tag{4.20}$$

if and only if

$$Z_f(l,k) = Z_g(l,k) \sum_{m=0}^{M-1} \sum_{n=0}^{N-1} a_{mN,nM} e^{2\pi i(mk/M + nl/N)}, \quad (l,k) \in I_{N,M}, \tag{4.21}$$

if and only if we can write

$$Z_f(l,k) = Z_g(l,k) P(l,k), \quad (l,k) \in I_{N,M}, \tag{4.22}$$

where $P \in L^2(N, M)$. The W-H expansion coefficients are given by the 2D $M \times N$ FT of $P(l,k)$, $(l,k) \in I_{N,M}$.

If Z_g never vanishes then (4.22) defines a linear isomorphism from $L^2(N, M)$ onto $L^2(P)$. In this case, W-H coefficients for the expansion of f over (g, M, N) are given by the 2-D $M \times N$ FT of the quotient

$$P(l,k) = \frac{Z_f(l,k)}{Z_g(l,k)}.$$

Suppose that the zero set ζ of Z_g in $I_{N,M}$ has exactly K points with $K > 0$. Then (g, M, N) is linearly dependent and does not span $L^2(P)$. In this case (4.22) defines a linear homomorphism from $L^2(N, M)$ onto the linear span of (g, M, N). Choose $f \in L^2(P)$ in the linear span of (g, M, N). Define $Q^\alpha(l, k), \quad (l, k) \in I_{N,M}$ by

$$Q^\alpha(l,k) = \begin{cases} \frac{Z_f(l,k)}{Z_g(l,k)}, & (l,k) \in \zeta^c, \\ \alpha(l,k), & (l,k) \in \zeta, \end{cases} \tag{4.23}$$

where ζ^c is a complement of ζ in $I_{N,M}$. The space of such Q^α is a K-dimensional subspace of $L^2(N, M)$. Since Z_f vanishes on ζ,

$$Z_f(l,k) = Z_g(l,k)Q^\alpha(l,k), \qquad (l,k) \in I_{N,M},$$

and a set of W-H coefficients for the expansion of f over (g, M, N) is given by the 2D $M \times N$ FT of $Q^\alpha(l, k), \quad (l, k) \in I_{N,M}$. Moreover every expansion of f over (g, M, N) is given in this way leading to the next result.

Theorem 7 *If the zero set ζ of Z_g in $I_{N,M}$ has exactly K points then every f in the linear span of (g, M, N) has a K-dimensional space of W-H expansions over (g, M, N). The coefficient space of W-H expansions of f over (g, M, N) is given by the set of all 2D $M \times N$ FT of the K-dimensional space of functions $Q^\alpha \in L^2(N, M)$ of the form (4.23).*

Based on Theorem 7. we have the following algorithm.

- Compute

$$Q^\alpha(l,k) = \begin{cases} \frac{F(l,k)}{G(l,k)}, & (l,k) \notin \zeta, \\ \alpha(l,k), & (l,k) \in \zeta. \end{cases} \tag{4.24}$$

- Compute the 2D $M \times N$ FT of Q^α

$$a_{mN,nM} = \sum_{l=0}^{N-1} \sum_{k=0}^{M-1} Q^\alpha(l,k) e^{2\pi i(\frac{mk}{M} + \frac{nl}{N})} \tag{4.25}$$

If the critically sampled W-H system (g, M, N) is a basis of $L^2(P)$, than $Q^\alpha = P = \frac{F}{G}$ for all (l,k) in $I_{N,M}$.

4.4.2 Integer Oversampling

The integer *oversampled* W-H system $\mathbf{g} = (g, M', N)$, $M = RM'$ is the disjoint union of critically sampled W-H systems.

$$\mathbf{g} = \bigcup_{r=0}^{R-1} \mathbf{g}_r, \quad \mathbf{g}_r = (g_r, M, N), \quad g_r = g_{0,rM'}, \quad 0 \le r < R. \tag{4.26}$$

By Theorem 3, $f \in L^2(P)$ is in the linear span of $\mathbf{g}$ if and only if $F = Z_f$ can be written in the form

$$F(l,k) = \sum_{r=0}^{R-1} Z_{g_r}(l,k) P_r(l,k), \quad (l,k) \in I_{N,M}, \quad P_r(l,k) \in L^2(N,M), \quad 0 \le r < R. \tag{4.27}$$

Denote the zero set of Z_{g_r} by ζ_r and set $\zeta = \bigcap_{r=0}^{K-1} \zeta_r$. Then $f \in L^2(P)$ is in the linear span of $\mathbf{g}$ if and only if we can write

$$F = \sum_{r=0}^{R-1} F_r, \quad F_r \in L^2(M,N) \tag{4.28}$$

where

$$F_r \quad \text{vanishes} \quad \text{on} \quad \zeta_r, \quad 0 \le r < R. \tag{4.29}$$

This leads to the following theorem which we state in a form slightly more general than necessary.

Theorem 8 *If* $\mathbf{g}$ *is the disjoint union of critically sampled W-H systems* $g_r = (\mathbf{g}_r, M, N)$, $0 \leq r < R$ *and* ζ *is the intersection of the zero sets of the collection of functions* Z_{g_r}, $0 \leq r < R$ *in* $I_{N,M}$ *then the dimension of the linear span of* $\mathbf{g}$ *is* $P - K$ *where* K *is the order of* ζ. *A function* $f \in L^2(P)$ *is in the linear span of* $\mathbf{g}$ *if and only if* Z_f *vanishes on* ζ.

The relationship between $L^2(N, M)$ and the linear span of $\mathbf{g}$ is more complicated then before. For $(l, k) \in I_{N,M}$, set

$$\mathbf{G}(l, k) = [Z_{g_0}(l, k), \cdots, Z_{g_{R-1}}(l, k)]. \tag{4.30}$$

Then we can write (4.27) in the form

$$F(l, k) = \mathbf{G}(l, k) \begin{bmatrix} P_0(l, k) \\ \cdot \\ \cdot \\ \cdot \\ P_{R-1}(l, k) \end{bmatrix} \tag{4.31}$$

which which defines a linear homomorphism of the RP-dimensional space of R-tuples of functions in $L^2(N, M)$ onto the linear span of $\mathbf{g}$. Choose $f \in L^2(P)$ in the linear span of $\mathbf{g}$. An algorithm for computing a W-H expansion of f over $\mathbf{g}$ is given as follows.

- Decompose $F = Z_f$

$$F = \sum_{r=0}^{R-1} F_r, \quad F_r \in L^2(N, M), \tag{4.32}$$

where F_r vanishes on the zero set ζ_r of Z_{g_r}, $0 \leq r < R$ in $I_{N,M}$,

- Compute

$$Q_r^\alpha = \begin{cases} \frac{F_r(l,k)}{Z_{g_r}(l,k)}, & (l,k) \notin \zeta_r, \\ \alpha_r(l,k), & (l,k) \in \zeta_r. \end{cases} \tag{4.33}$$

  This stage is understood to be taken as in the critically sampled case with arbitrary values assigned to the quotient at points where the functions Z_{g_r}, $0 \leq r < R$ vanish.

- Compute the 2D $M \times N$ FT of Q_r^α

$$a_{mN,nM}^r = \sum_{l=0}^{N-1} \sum_{k=0}^{M-1} Q_r^\alpha(l,k) e^{2\pi i(\frac{mk}{M} + \frac{nl}{N})}. \tag{4.34}$$

If we assume that $PlogP$ computations are needed for the P-point FT then the multiplicative complexity of one W-H expansion computation is

$$Plog_2 N + R(Plog_2 P) + RP, \tag{4.35}$$

but advantage can be taken of the large number of zero data values. For example, we can choose the decomposition $F = \sum_{r=0}^{R-1} F_r$ such that $F_1, ..., F_{R-1}$ each has only one non-zero point, so that the computation of the 2D FT of $Q_1, ..., Q_{R-1}$ is trivial. In that case the complexity of the computation is similar to the critically sampled situation.

Since F vanishes on the intersection $\bigcap_{r=0}^{R-1} \zeta_r$, a decomposition of F of the above form can always trivially be constructed. However in general it is not unique and two distinct decompositions lead to distinct W-H expansions.

The coefficient set of W-H expansions of $f \in L^2(P)$ over $\mathbf{g}$ is parameterized by the collection of decompositions of F and by the arbitrarily assigned values to the quotients at the points where Z_{g_r}, $0 \leq r < R$ vanish.

4.4.3 Fractional Oversampling

Denote by $\overline{M}$ the least common multiple (LCM) of M and M' and define S and S' by $\overline{M} = SM = S'M'$. Since $P = MN = M'N'$ is a common multiple of M and M', S divides N, S' divides N' and $N/S = N'/S' = P/\overline{M}$.

We can uniquely write $0 \leq n' < N'$ in the form

$$n' = s' + \overline{n}S', \quad 0 \leq s' < S', \quad 0 \leq \overline{n} < \frac{N'}{S'}.$$

Then

$$g_{mN,n'M'} = (g_{0,s'M'})_{mN,\overline{n}\overline{M}}, \quad 0 \leq \overline{n} < \frac{N}{S}, \quad 0 \leq m < M.$$

Set $g_{s'} = g_{0,s'M'}$. Then $\mathbf{g}$ is the disjoint union of undersampled W-H systems

$$\mathbf{g} = \sum_{s'=0}^{S'-1} \mathbf{g}_{s'},$$

where

$$\mathbf{g}_{s'} = (g_{s'}, \overline{M}, N) = \{(g_{s'})_{mN,\overline{n}\overline{M}} : \ 0 \leq \overline{n} < \frac{N}{S}, \ 0 \leq m < M\}.$$

Set $G_{s'} = Z_{g_{s'}}$ and $F = Z_f$. Since

$$Z((g_{s'})_{mN,\overline{n}\overline{M}})(l,k) = G_{s'}(l,k)e^{2\pi i(\frac{m}{M}k + \overline{n}\frac{S}{N}l)}, \tag{4.36}$$

$f \in L^2(P)$ has a W-H expansion over $\mathbf{g}_{s'}$ if and only if

$$F(l,k) = \sum_{s'=0}^{S'-1} G_{s'}(l,k)P_{s'}(l,k) \tag{4.37}$$

where $P_{s'}(l,k) \in L^2(N,M)$ satisfies

$$P_{s'}(l + \frac{N}{S}, k) = P_{s'}(l,k), \quad (l,k) \in I_{N,M},$$

leading to the following result.

Theorem 9. A function $f \in L^2(P)$ is in the linear span of $\mathbf{g}$ *if and only if* $F = Z_f$ *has the form*

$$F(l,k) = \sum_{s'=0}^{S'-1} G_{s'}(l,k) P_{s'}(l,k), \quad (l,k) \in I_{N,M}, \tag{4.38}$$

where

$$P_{s'}(l + \frac{N}{S}, k) = P_{s'}(l,k), \quad 0 \leq s' < S', \quad (l,k) \in I_{N,M}. \tag{4.39}$$

A collection of W-H expansion coefficients of f *over* $\mathbf{g}$ *is given by the collection of* $2D$ $\frac{N}{S} \times M$ *FT of* $P_{s'}(l,k) \in L^2(\frac{N}{S}, M)$, $0 \leq s' < S'$.

By Theorem 9., f is in the linear span of $\mathbf{g}$ if and only if there exists $P_{s'}(l,k) \in L^2(\frac{N}{S}, M)$, $0 \leq s' < S'$ such that

$$F(l + s\frac{N}{S}, k) = \sum_{s'=0}^{S'-1} G_{s'}(l + s\frac{N}{S}, k) P_{s'}(l,k), \quad 0 \leq s < S, \tag{4.40}$$

where $(l,k) \in I_{\frac{N}{S},M}$, or in matrix form as

$$\begin{bmatrix} F(l,k) \\ F(l+\frac{N}{S},k) \\ \cdot \\ \cdot \\ \cdot \\ F(l+(S-1)\frac{N}{S},k) \end{bmatrix} = \mathbf{G}(l,k) \begin{bmatrix} P_0(l,k) \\ P_1(l,k) \\ \cdot \\ \cdot \\ \cdot \\ P_{S'-1}(l,k) \end{bmatrix}, \quad (l,k) \in I_{\frac{N}{S},M}, \tag{4.41}$$

where $\mathbf{G}(l,k)$ is the $S \times S'$ matrix

$$\left[\; G_{s'}(l + s\frac{N}{S}, k) \; \right]_{\substack{0 \leq s < S, \\ 0 \leq s' < S',}} \quad (l,k) \in I_{\frac{N}{S},M}. \tag{4.42}$$

Denote by $r(l,k)$ the rank of $\mathbf{G}(l,k)$. The dimension of the linear span of $\mathbf{g}$ is

$$\sum_{(l,k)\in I(\frac{N}{S},M)} r(l,k). \tag{4.43}$$

In particular, if

$$r(l,k) = S, \quad (l,k) \in I_{\frac{N}{S},M} \tag{4.44}$$

then $\mathbf{g}$ is complete and every $f \in L^2(P)$ has a W-H expansion over $\mathbf{g}$.

There are several linear algebra techniques and programming packages that can be applied to characterize the linear span of $\mathbf{g}$ and to compute W-H expansion coefficients for $f \in L^2(P)$ in this linear span [39]. Gauss elimination is perhaps the most well known technique but QR-decomposition or singular value decomposition (SVD) of $\mathbf{G}(l,k)$ are more suited to applications which subject W-H expansion coefficients to least-square constraints. We will briefly review and introduce notation for SVD at this time.

For each $(l,k) \in I_{\frac{N}{S},M}$, the singular value decomposition of $\mathbf{G}(l,k)$ has the form

$$\mathbf{G}(l,k) = \mathbf{U}(l,k)\mathbf{\Sigma}(l,k)\mathbf{V}(l,k), \tag{4.45}$$

where $\mathbf{U}(l,k)$ is a unitary $S \times S$ matrix, $\mathbf{V}(l,k)$ is a unitary $S' \times S'$ matrix and $\mathbf{\Sigma}(l,k)$ is a 'diagonal' $S \times S'$ matrix

$$\mathbf{\Sigma} = diag(\sigma_0, \sigma_1, ..., \sigma_{S-1}).$$

Set

$$\mathbf{F}(l,k) = \begin{bmatrix} F(l,k) \\ F(l+\frac{N}{S},k) \\ \cdot \\ \cdot \\ \cdot \\ F(l+(S-1)\frac{N}{S},k) \end{bmatrix}, \quad (l,k) \in I_{\frac{N}{S},M}, \tag{4.46}$$

(4.47)

$$\mathbf{P}(l,k) = \begin{bmatrix} P_0(l,k) \\ P_1(l,k) \\ \cdot \\ \cdot \\ \cdot \\ P_{S'-1}(l,k) \end{bmatrix}, \quad (l,k) \in I_{\frac{N}{S},M}. \tag{4.48}$$

Theorem 10. A function $f \in L(P)$ is in the linear span of $\mathbf{g}$ *if and only if for every $(l,k) \in I_{\frac{N}{S},M}$, $\mathbf{F}(l,k)$ is in the linear span of the set of S-tuples*

$$\sigma_0(l,k)U_0(l,k), ..., \sigma_{S-1}(l,k)U_{S-1}(l,k).$$

For f in the linear span of $\mathbf{g}$ we can solve for $\mathbf{P}(l,k)$ by introducing the *pseudoinverse* of $\mathbf{G}(l,k)$

$$\mathbf{G}^+(l,k) = \mathbf{V}(l,k)\mathbf{\Sigma}^+(l,k)\mathbf{U}^{-1}(l,k), \tag{4.49}$$

where $\mathbf{\Sigma}^+(l,k)$ is the $S' \times S$ diagonal matrix

$$\mathbf{\Sigma}^+ = diag(\sigma_0^+, \sigma_1^+, ..., \sigma_{S-1}^+)$$

with

$$\sigma_s^+(l,k) = \begin{cases} \frac{1}{\sigma_s(l,k)}, & \sigma_s(l,k) \neq 0, \\ 0, & \sigma_s(l,k) = 0. \end{cases} \tag{4.50}$$

Then

$$\mathbf{P}(l,k) = \mathbf{G}^+(l,k)\mathbf{F}(l,k), \quad (l,k) \in I_{\frac{N}{S},M}. \tag{4.51}$$

The algorithm proceeds as follows.

Precomputation Stage

- compute

$$\mathbf{G}(l,k), \quad (l,k) \in I_{\frac{N}{S},M}.$$

- compute the Singular Value Decomposition

$$\mathbf{G}(l,k) = \mathbf{U}(l,k)\mathbf{\Sigma}(l,k)\mathbf{V}(l,k), \quad (l,k) \in I_{\frac{N}{S},M}.$$

- compute the *pseudoinverse*

$$\mathbf{G}^+(l,k) = \mathbf{V}^{-1}(l,k)\mathbf{\Sigma}^+(l,k)\mathbf{U}^{-1}(l,k), \quad (l,k) \in I_{\frac{N}{S},M}.$$

Computation Stage

- compute

$$\mathbf{P}(l,k) = \mathbf{G}^+(l,k)\mathbf{F}(l,k), \quad (l,k) \in I_{\frac{N}{S},M}.$$

- compute the 2D $\frac{N}{S} \times M$ FT of $P_{s'}$

$$a^{s'}_{mN,\overline{n},\overline{M}} = \sum_{l=0}^{\frac{N}{S}-1} \sum_{k=0}^{M-1} P_{s'}(l,k) e^{2\pi i(\frac{mk}{M} + \frac{\overline{n}Sl}{N})}.$$

- define

$$a_{mN,n'M'} = a^{s'}_{mN,\overline{n}\overline{M}}, \quad n' = s' + \overline{n}S', \quad 0 \leq n' < N', \quad 0 \leq m < M.$$

Then a W-H expansion of f is given by

$$f = \sum_{s'=0}^{S'-1} \sum_{m=0}^{M-1} \sum_{\overline{n}=0}^{N/S-1} a^{s'}_{mN,\overline{n}\overline{M}} g^{s'}_{mN,\overline{n}\overline{M}} \tag{4.52}$$

$$= \sum_{m=0}^{M-1} \sum_{n'=0}^{N'-1} a_{mN,n'M'} g_{mN,n'M'}. \tag{4.53}$$

The multiplicative complexity of the computation is

$$P(log_2 N + \frac{S'}{S}) + P\frac{S'}{S} log_2 \frac{P}{S}, \tag{4.54}$$

where $PlogP$ is the complexity of the P-point FT and S^2 is the complexity of the action of an $S \times S$ matrix on a vector.

4.5 Examples and Implementation Remarks

In this section we give implementation examples for the integer and fractionally oversampled Weyl-Heisenberg systems. The window is the Gaussian function (except for Case 2. where a composite window is employed) with a single zero at (1/2,1/2) and the signal is the second Hermite function with the zero set $\{(0,0),(0,1/2),(1/2,0)\}$.

Case 1: integer oversampling, single zero window.

Take $M = N = 32$ and $R = 2$. The partitions Z_{g_0} and Z_{g_1} have zeros at

(1/2,1/2) and (0,1/2), respectively (Fig. 4.1). Since the intersection ζ of the zero sets of Z_{g_0} and Z_{g_1} is empty, there are many possible factorizations of F, i.e.:

A. Assign $F(1/2, 1/2)$ to F_1 and all the other points of F to F_0 (Fig. 4.2.):

$$F_0 = \begin{cases} F, & (l,k) \neq (1/2,1/2), \\ 0, & (l,k) = (1/2,1/2), \end{cases}$$

$$F_1 = \begin{cases} 0, & (l,k) \neq (1/2,1/2), \\ F, & (l,k) = (1/2,1/2). \end{cases}$$

This is the most computationally efficient factorization, since the DFT corresponding to the second partition degenerates to a pointwise multiplication.

B. Assign an area (a $p \times p$ square or a disk of radius r, p and r being free parameters) surrounding point (1/2,1/2) to F_1 and all the other points to F_0 (Fig. 4.4., in this example $p = P/3$):

$$F_0 = \begin{cases} F, & k,l \leq P/3 \text{ or } k,l > 2P/3, \\ 0, & P/3 < k,l \leq 2P/3, \end{cases}$$

$$F_1 = \begin{cases} 0, & k,l \leq P/3 \text{ or } k,l > 2P/3, \\ F, & P/3 < k,l \leq 2P/3. \end{cases}$$

C. Half of F (for $k \leq P/2$) is assigned to F_0 and the other half to F_1 (Fig. 4.6.).

D. Assign a strip of F containing point (1/2,1/2) to F_1 and all the other points to F_0 (Fig. 4.8.):

$$F_0 = \begin{cases} F, & k \leq P/3 \text{ or } k > 2P/3, \\ 0, & P/3 < k \leq 2P/3, \end{cases}$$

$$F_1 = \begin{cases} 0, & k \leq P/3 \text{ or } k > 2P/3, \\ F, & P/3 < k \leq 2P/3. \end{cases}$$

This factorization provides the minimum energy solution (Fig. 4.9.).

Case 2: integer oversampling, complex zero window.

Take a composite window with zeros at (0,1/2) and (1/2,1/2) (Fig. 4.10.a). Since for $R = 2$ Z_{g_1} has zeros at (0,1/2) and (1/2,1/2), the intersection ζ is nonempty and oversampling by two does not produce a legal W-H expansion. Construction of a legal W-H expansion is still possible, however, for higher sampling rates. Taking $R = 3$, for example, produces Z_{g_1} with zeros at (1/3,1/2) and (5/6,1/2) (Fig. 4.10.b), and Z_{g_2} with zeros at (1/6,1/2) and (2/3,1/2) (Fig. 4.10.c), which together with Z_{g_0} have an empty intersection ζ.

Case 3: fractional oversampling.

Take $M = N = 30$, $S = 2$ and $S' = 3$. $\overline{M} = SM = 60$ and $M' = \frac{S}{S'}M = 20$. Set $g = h_0, f = h_1$. Figures 4.12. a-f, 4.11. and 4.13. a-c show partitions of $\mathbf{G}(l,k)$, $\mathbf{F}(l,k)$ and the Gabor coefficients $a^{s'}_{mN,\overline{n}\overline{M}}$, respectively.

The algorithms described in this chapter possess highly parallel structure, and are especially suitable for a distributed memory parallel processing en-

vironment. Assume that a distributed memory parallel computer has k ($< min(N, M)$) processors. Set

$$K = N/N_1 = M/N_2$$

In the critical sampling case the algorithm can be implemented as follows:

- Each processor receives N_1 N-point input data
- Compute N_1 N-point real FFT
- Point-wise multiplication of the precalculated Zak transform of the basis function $1/Z_g(a, b)$
- Compute N_1 N-point Hermitian FFT
- Data permutation between processors (matrix transpose)
- Compute N_2 M-point real FFT

Implementation of integer oversampled case has similar structure as the critically sampled case, and the fractionally oversampled case has a better parallel structure, since it has S' relatively small 2-dimensional $N/S \times M$ FFT's, and they might be carried out locally in each processor without interprocessor data permutation. In [22] implementation results on single RISC processor of i860 and the Paragon parallel multiprocessor system were given for sampling sizes both of powers of two and mixed sizes with factors 2, 3, 4, 5, 6, 7, 8, 9. The timing results on single i860 processor and on 4- and 8-node computing systems show that real-time computation of W-H expansions is realizable.

Multiplicative complexity of algorithms analyzed in this chapter is as follows:

- critical sampling

  $$Plog_2N + Plog_2P + P$$

- integer oversampling (trivial factorization)

  $$Plog_2N + Plog_2P + 2P$$

- integer oversampling (non-trivial factorization)

  $$Plog_2N + RPlog_2P + RP$$

- fractional oversampling

  $$P(log_2N + \frac{S'}{S}) + P\frac{S'}{S}log_2\frac{P}{S}$$

The computationally most expensive operation in both situations: the integer oversampling and the fractional oversampling is the calculation of the 2-D FT of polynomials Q_r ($RP\log_2 P$) and $P_{s'}$ ($S'\frac{P}{S}\log_2\frac{P}{S}$), respectively. Whenever the application allows the trivial factorization, the integer oversampling technique is more efficient. When the trivial factorization is not considered, the fractionally oversampled algorithm performs better, both: in a single processor environment and in a parallel system, providing $S'/S < 2$ or, more generally, for $R \geq S'/S$. A minor disadvantage of implementation of the integer oversampling algorithm on a parallel machine is a restriction on allowable sampling

rates: for complex zero pattern windows factorization of Z_g for some R leads to parameterization of the expansion.

Choice of factorization might be motivated by factors other then computational efficiency. Constrains can be imposed on the Gabor coefficients to yield minimum energy solution, i.e.:

$$\sum_{m,n,r} |a^r_{mN,nM}|^2 = min.$$

Another desirable goal is optimization of the factorization for best localization of the Gabor coefficients. Early investigations show that coefficients localization is related to the smoothness of partitions of F. A definite answer however has not yet been found, and farther work in this area is needed.

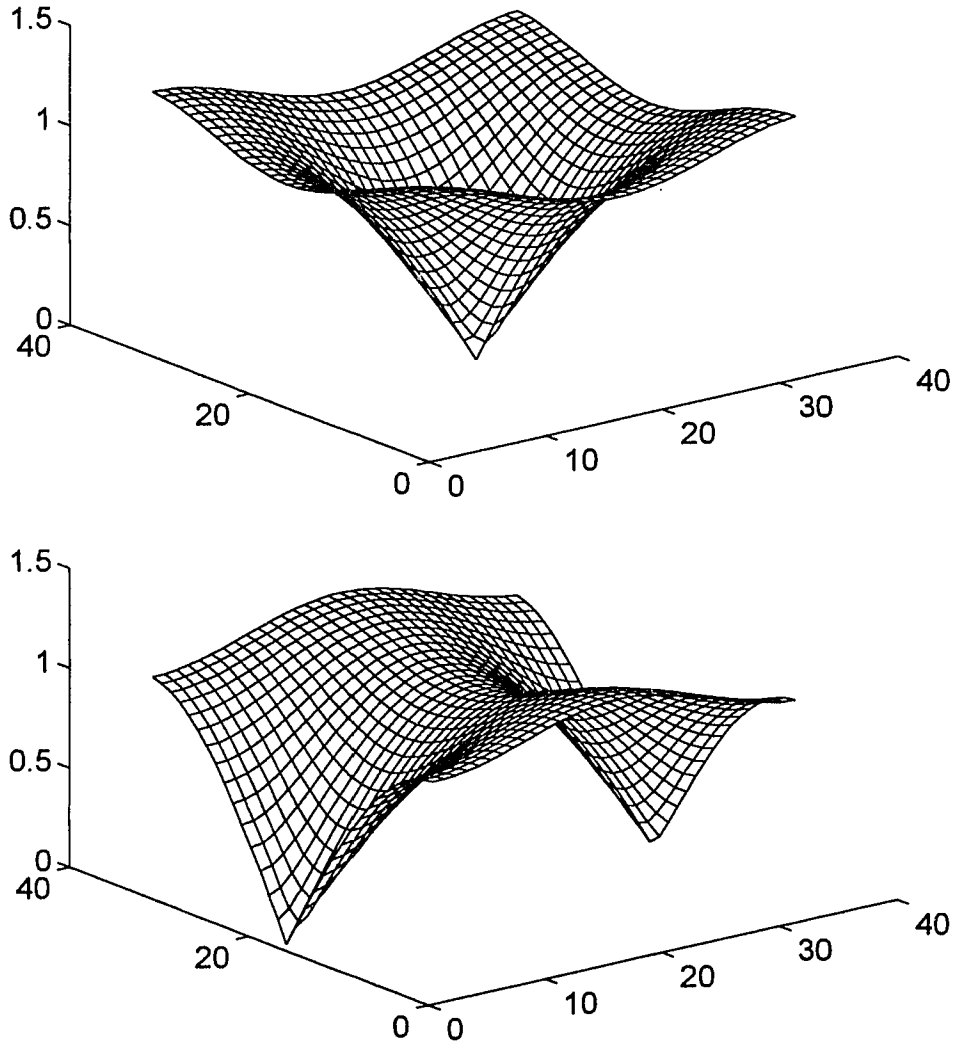

Figure 4.1: Zak transform partition of the Gaussian window for R=2: Z_{g_0} (top), Z_{g_1} (bottom).

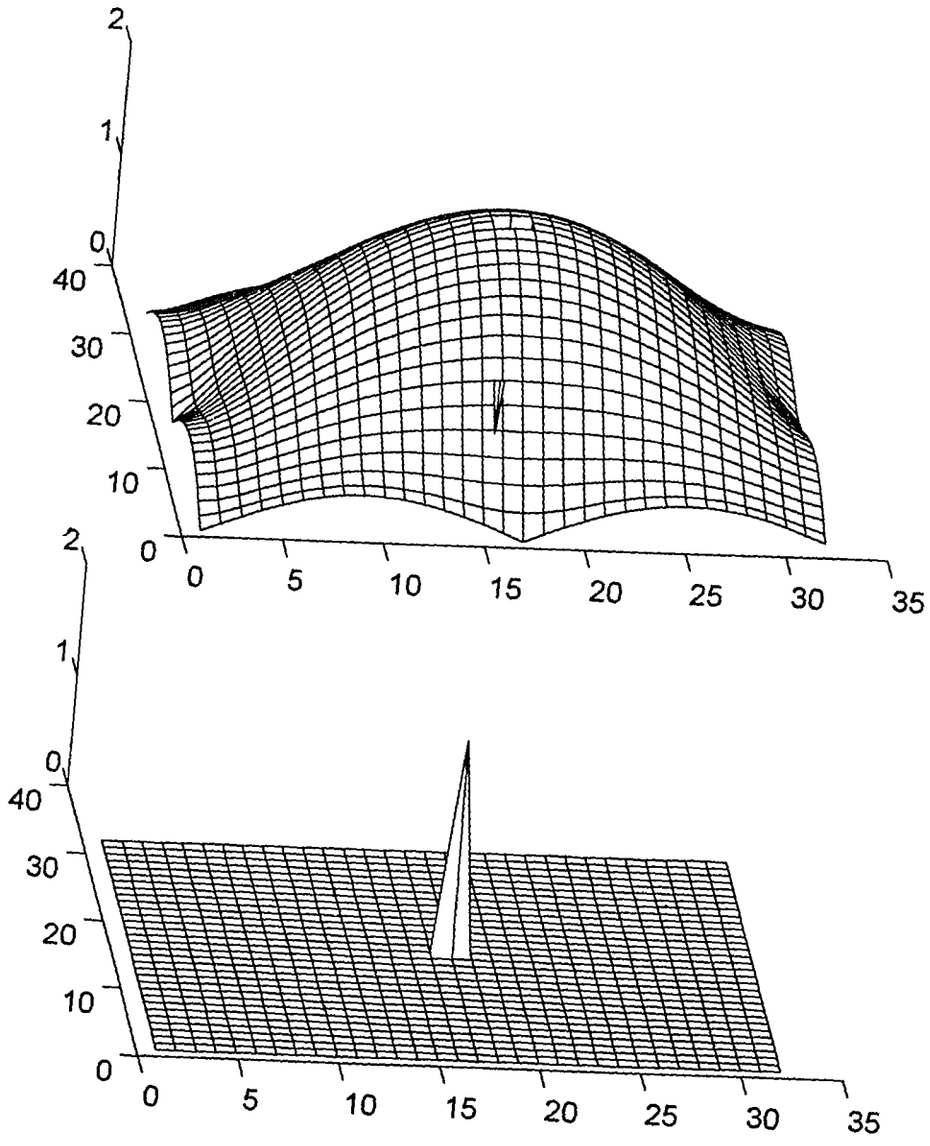

Figure 4.2: Factorization of F for Case 1.A.: F_0 (top), F_1 (bottom).

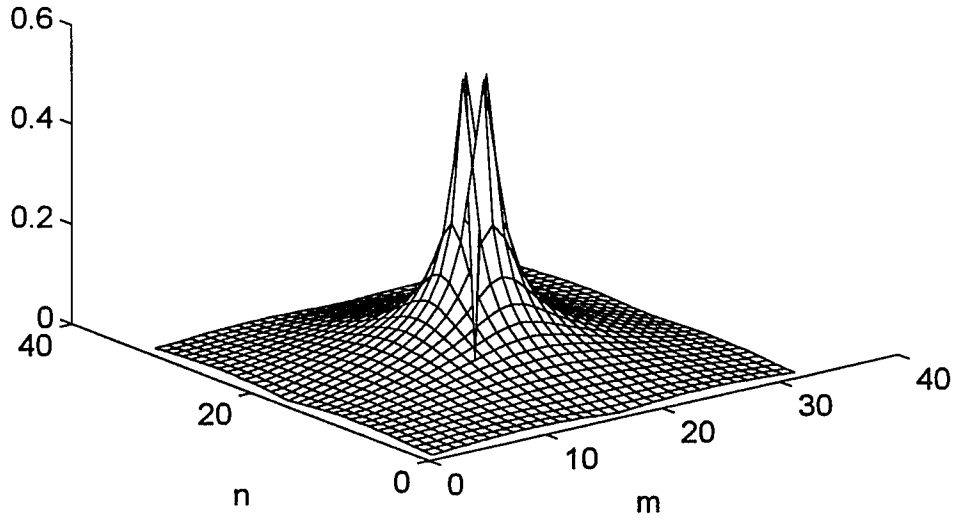

Figure 4.3: Gabor coefficients corresponding to the factor F_0 in Case 1.A.

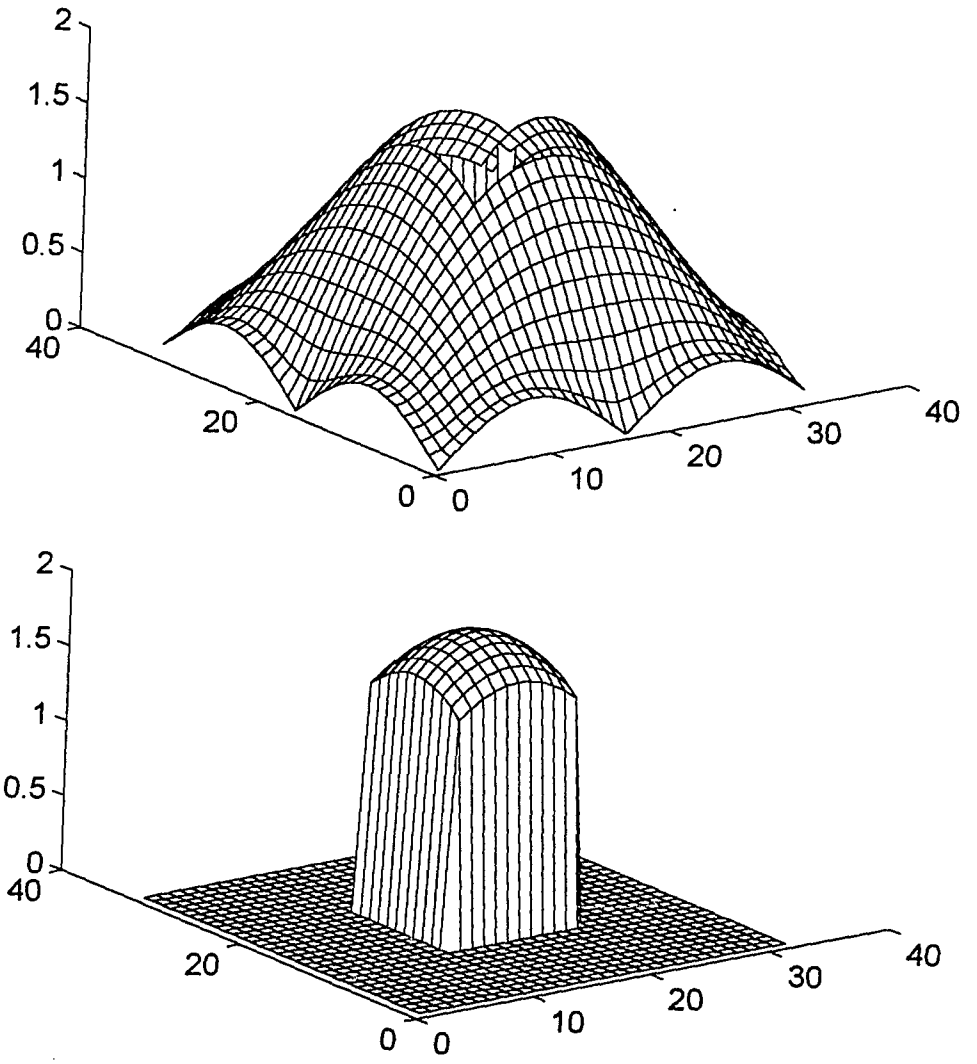

Figure 4.4: Factorization of F for Case 1.B.: F_0 (top), F_1 (bottom).

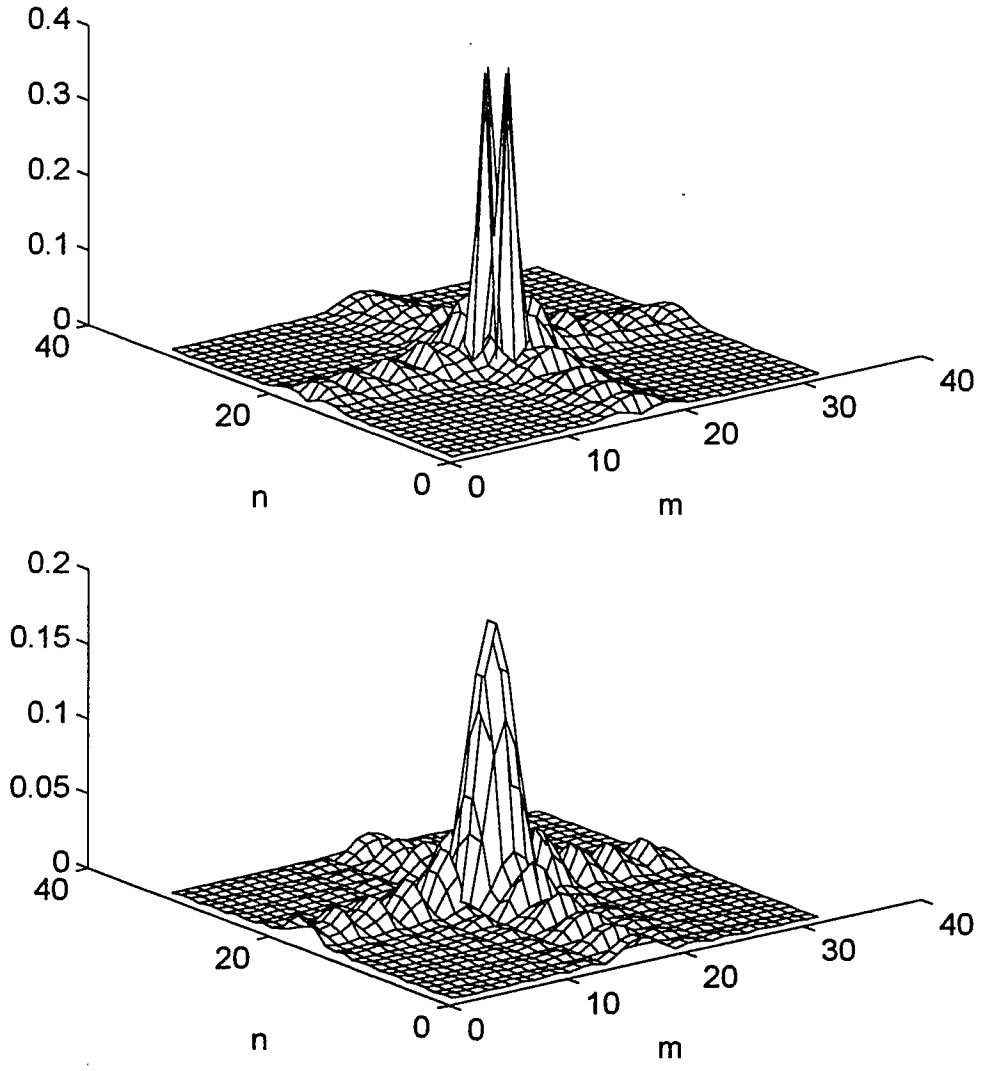

Figure 4.5: Gabor coefficients corresponding to factorization in Case 1.B.

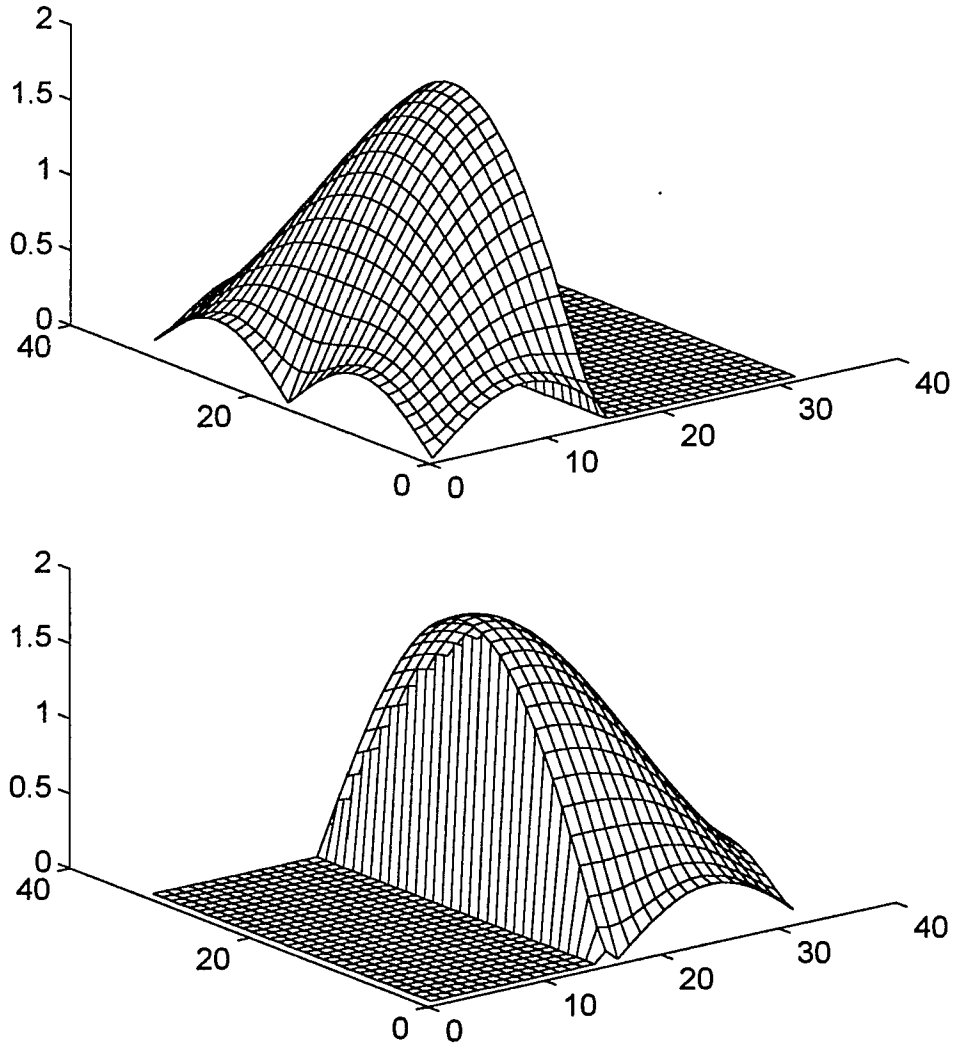

Figure 4.6: Factorization of F for Case 1.C.: F_0 (top), F_1 (bottom).

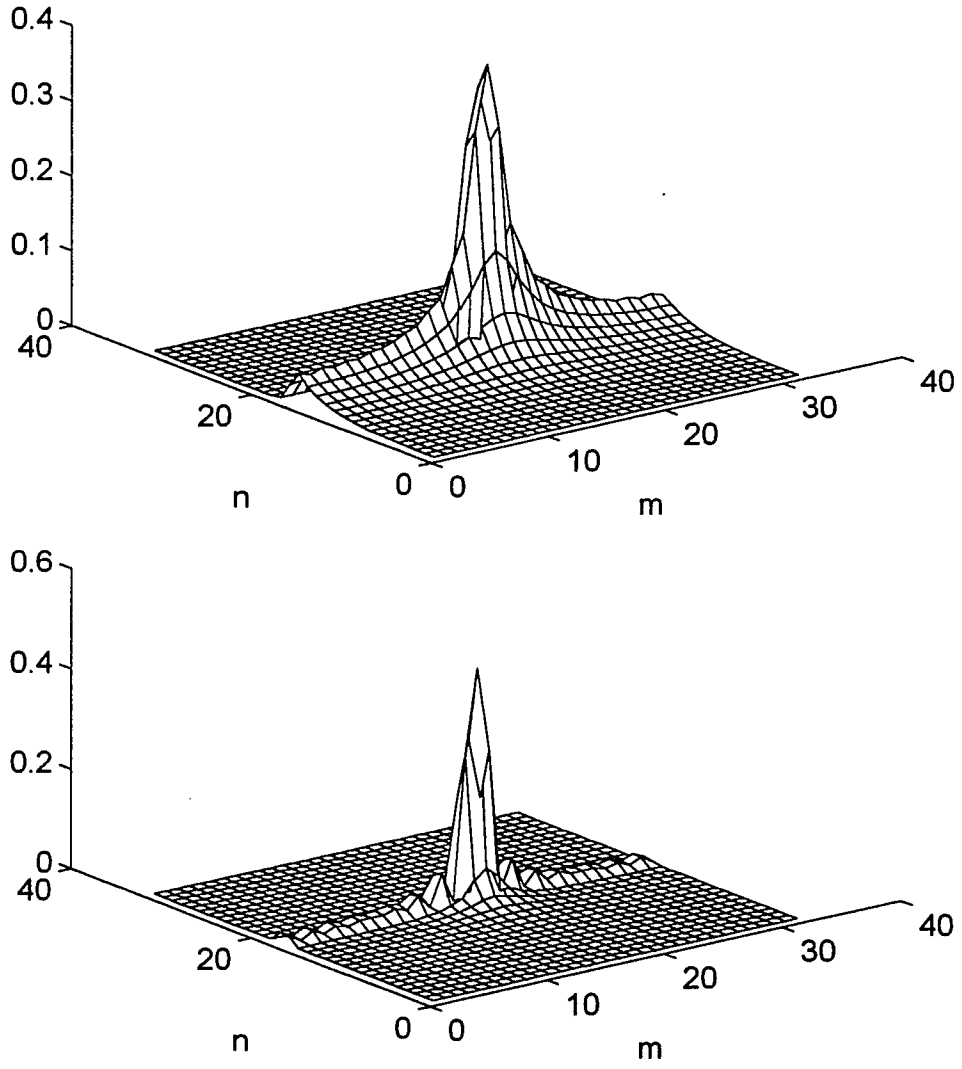

Figure 4.7: Gabor coefficients corresponding to factorization in Case 1.C.

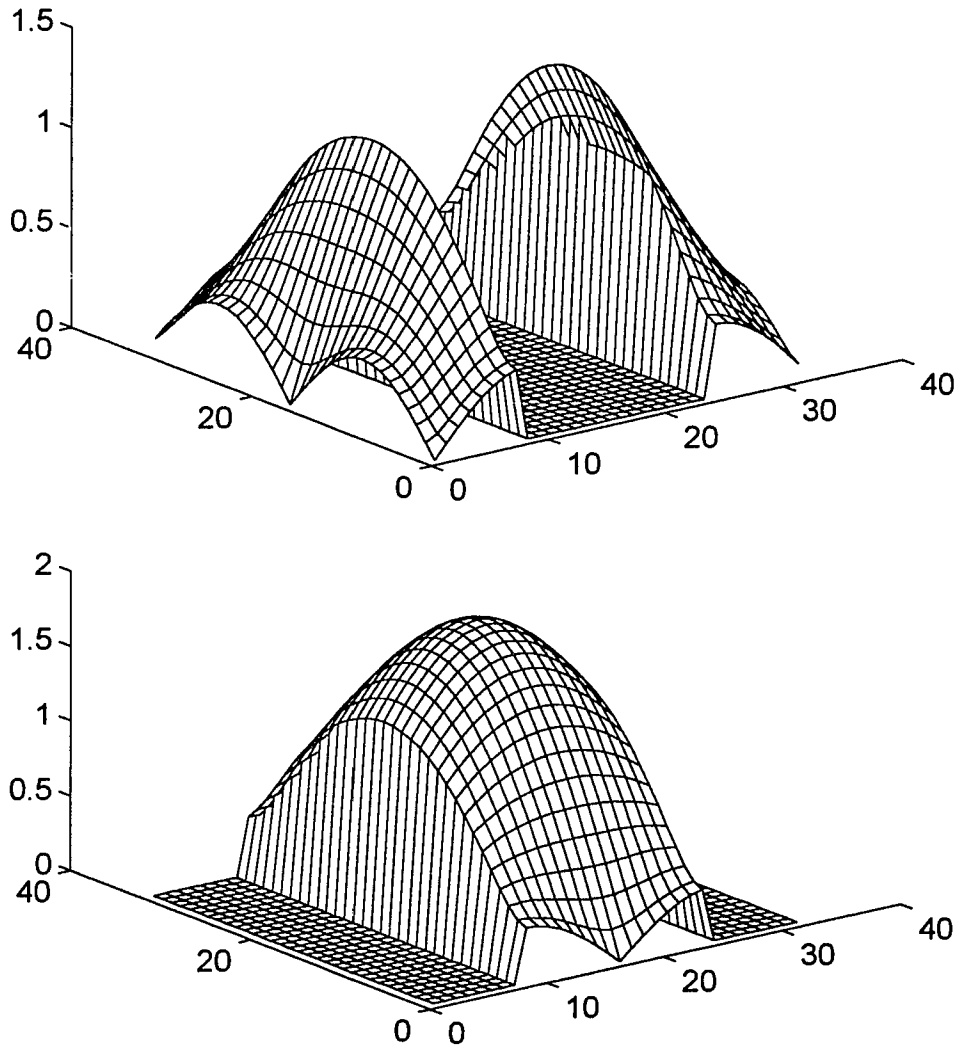

Figure 4.8: Factorization of F for Case 1.D.: F_0 (top), F_1 (bottom).

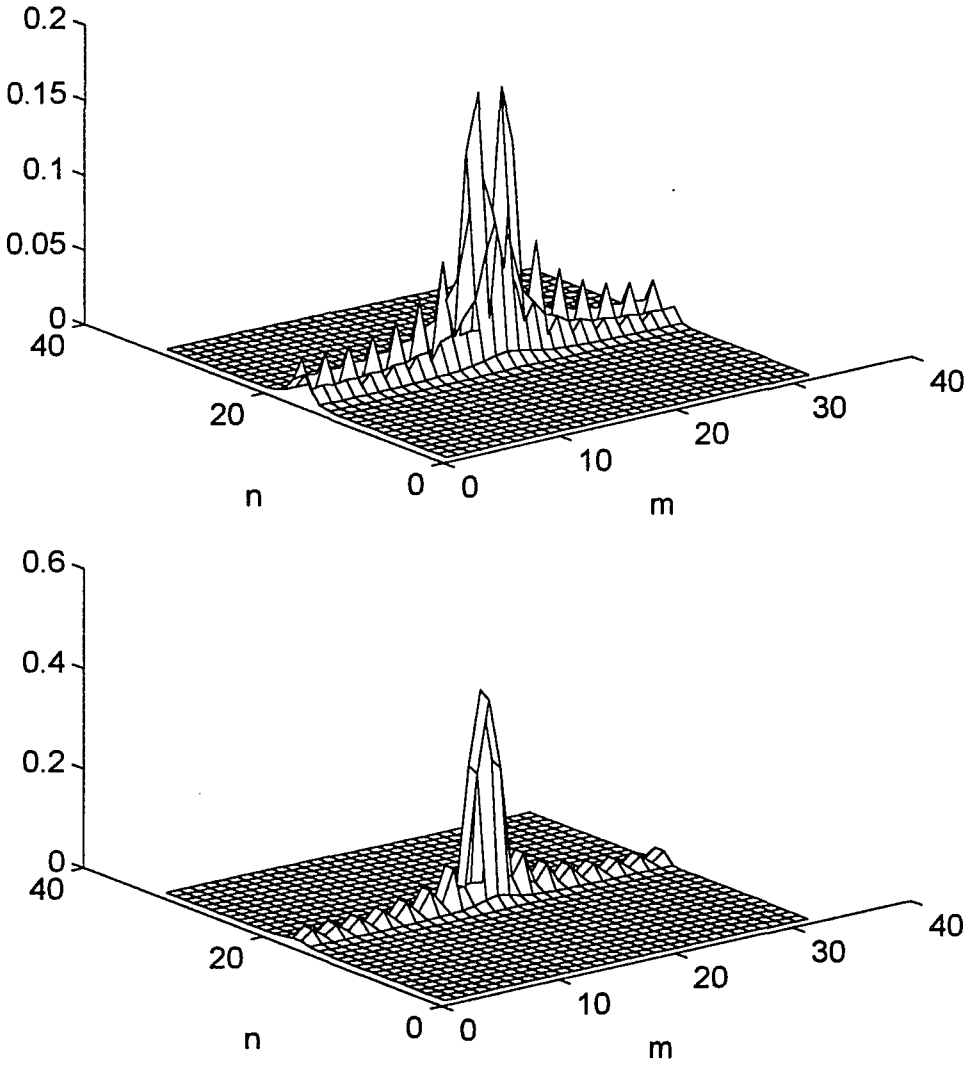

Figure 4.9: Gabor coefficients corresponding to factorization in Case 1.D.

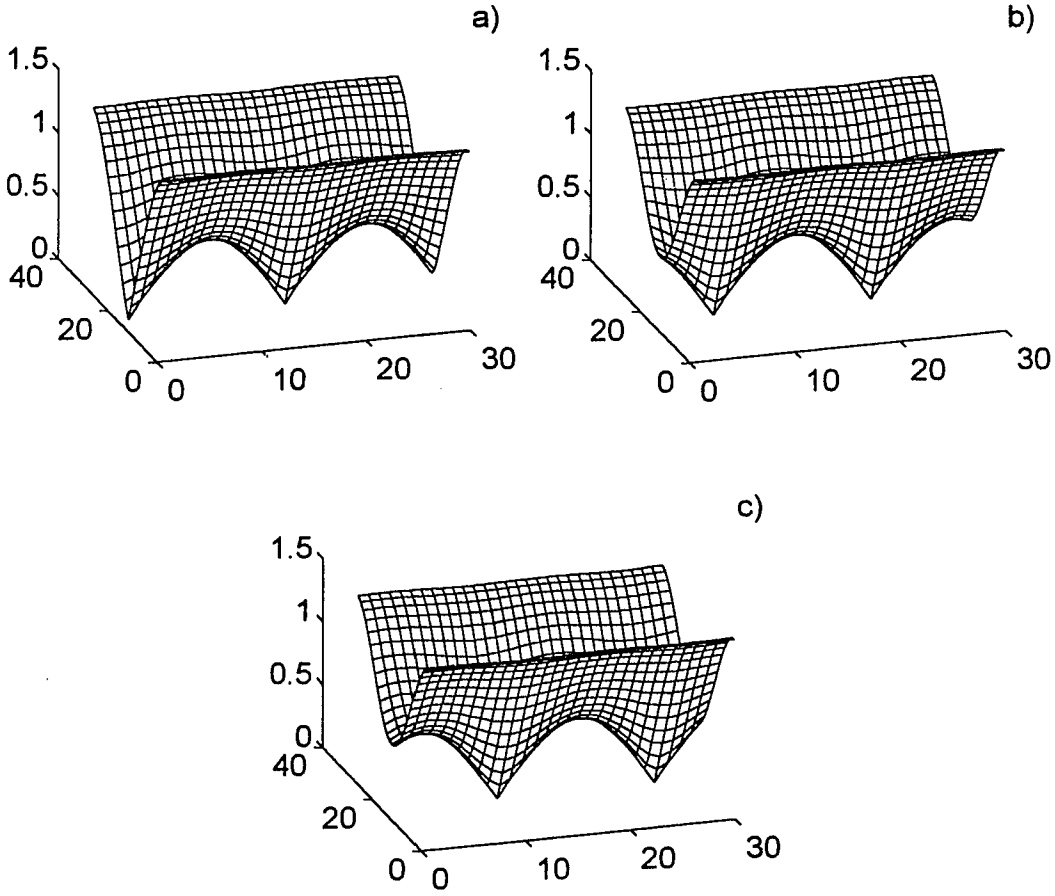

Figure 4.10: Zak transform partition of a composite window for $R = 3$ (Case 2.): (a) Z_{g_0}, (b) Z_{g_1}, (c) Z_{g_2}.

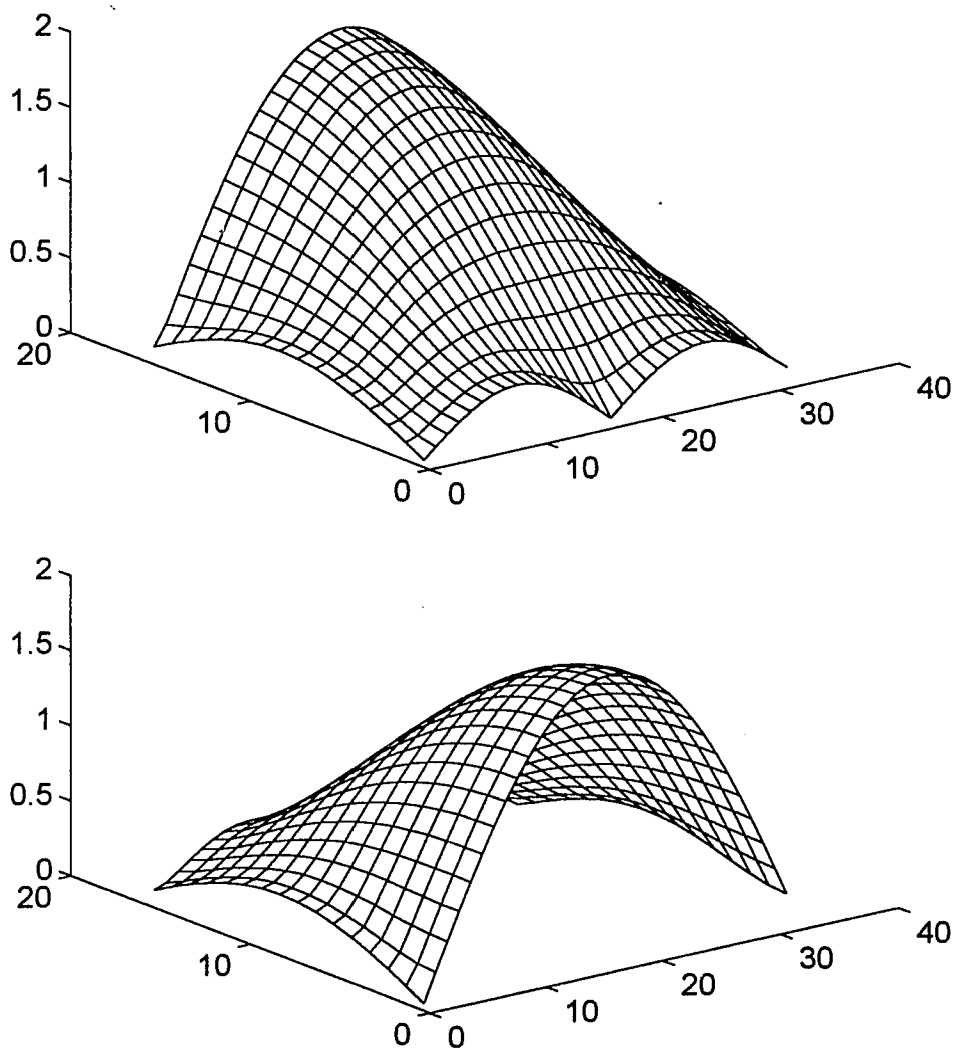

Figure 4.11: Partition of F for $S' = 3$, $S = 2$ (Case 3.): F_0 (top), F_1 (bottom).

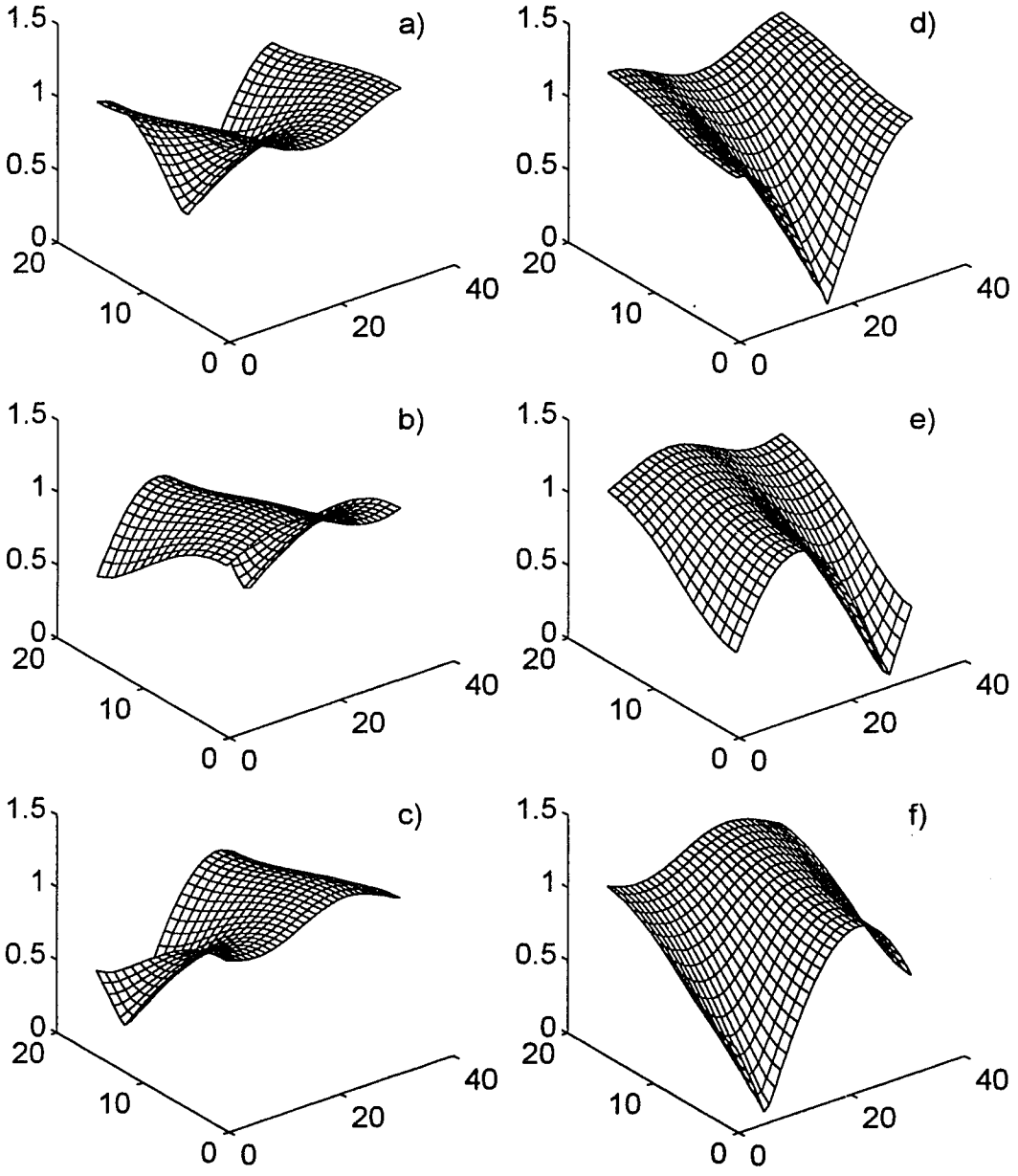

Figure 4.12: Partition of G for $S' = 3$, $S = 2$ (Case 3.): (a) $G_{1,1}$, (b) $G_{2,1}$, (c) $G_{3,1}$, (d) $G_{1,2}$, (e) $G_{2,2}$, (f) $G_{3,2}$.

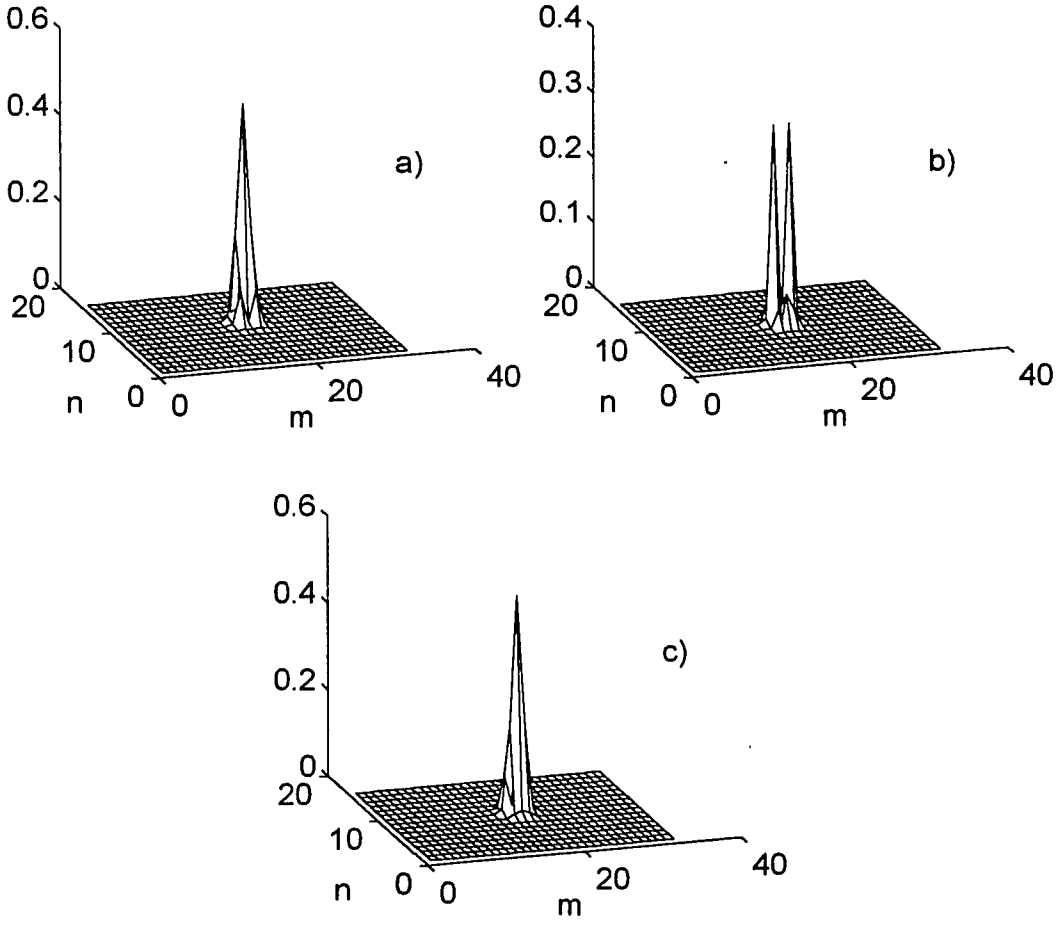

Figure 4.13: Gabor coefficients (Case 3.): (a) $s' = 0$, (b) $s' = 1$, (c) $s' = 2$

Chapter 5

Extrapolation of Band-Limited Signals and the Finite Zak Transform

The iterative procedure of Gerchberg-Papoulis for restoration of a band-limited signal from partial data involves transition between the time domain and the frequency domain at each iteration, rendering the algorithm computationally expensive, especially for problems requiring several hundred iterations. In this chapter a new approach is proposed for partial data signal restoration, in which the computations are exported to a joint time-frequency space. The finite Zak transform calculus serves as the main tool in algorithm design. The new approach accomplishes reduction in multiplicative complexity from $2Plog_2P$ to $2P$ per iteration, while preserving the structure of the Gerchberg-Papoulis method.

5.1 Introduction

Signal extrapolation from incomplete data is encountered in many different situations. Several examples are X-ray diffraction, optical astronomy, radar, computer-aided tomography (CAT) and geophysical modeling. Typically, some of the information is lost in the measurement (due e.g. to atmospheric turbulence in optical astronomy) or, as in medical CAT, incomplete view data is acquired when obstructions prevent 360 degree viewing.

Over the last twenty years a number of techniques have been developed, that attempt to solve the partial data problem. They fall into two major categories: series expansion methods and transform based methods [81]. The series expansion algorithms include the prolate spheroidal functions (PSF) method [50], the singular value decomposition (SVD) method [76,82], the conjugate gradient method, the algebraic reconstruction techniques (ART), the multiplicative algebraic reconstruction algorithms (MART) [81] and techniques that use stochastic model of the signal and data errors (the maximum a posteriori probability, maximum likelihood and minimum mean-squared error techniques). The second category includes the Fourier transform based Gerchberg-Papoulis algorithm [64], the Hartley transform method [19,81,83] and the Radon transform method [77], all three of them roughly equivalent in terms of computational efficiency. Another popular signal extrapolation technique, applied perhaps more frequently to the related problem of signal reconstruction from phase or magnitude of its Fourier transform, is the method of convex projections [74,75,90].

The focus of this work is on signal restoration from partial data, as formulated by Papoulis, in the transform domain. Since all the transform based techniques (and in fact most of the series expansion methods with the exception of SVD) are iterative and slow in convergence, reduction in computational complexity is at a premium. All three transform based techniques (Fourier, Hartley and Radon) involve translation between the time domain and the transform domain at each iteration, which is the main component in the computation. It is natural to pose a question, if a more efficient technique could not be constructed by employing a more general type of transform operating in a joint time-frequency space. In this chapter a time-frequency algorithm will be designed that retains simplicity of the Gerchberg-Papoulis method while improving its efficiency by $log_2 P$ per iteration. The technique used to bring the computations to the joint time-frequency space is the finite Zak transform.

5.2 Gerchberg-Papoulis Algorithm

Take an integer $P = MN > 0$. Consider an unknown P-periodic signal g

$$g = [g_0, g_1, ..., g_{P-1}], \tag{5.1}$$

with a Fourier transform G

$$G = [G_0, G_1, ..., G_{N-1}, 0, ..., 0] \tag{5.2}$$

vanishing outside the interval $[0, N)$. If an M-point segment f

$$f = [g_0, g_1, ..., g_{M-1}, 0, ..., 0] \tag{5.3}$$

of g is given, the signal g can be reconstructed from an iterative algorithm due to Gerchberg and Papoulis [64] (a discrete version was given by Jones [55]), which is guaranteed to converge to a unique solution for $M \geq N$. A single iteration of the algorithm proceeds as follows:

1. Compute the Fourier transform F of f.

2. Truncate F outside an interval $[0, N)$ to produce F_N.

3. Compute an inverse Fourier transform $\check{F}_N$.

4. Replace the first M samples of $\check{F}_N$ by f.

Define

$$p_N(l) = \begin{cases} 1, & 0 \leq l < N, \\ 0, & elsewhere. \end{cases}$$

Then the iteration is completely described by

$$f_{r+1} = f + (1 - p_M)\{p_N F_r\}^{\check{}}$$

A good estimate of g might require several hundred iterations, each of them performing $2Plog_2P$ multiplications, rendering the procedure computationally inefficient.

Take an example of a dilated third Hermite function

$$g(k) = (2\lambda)^{-1/4}(4\pi\lambda\frac{k^2}{M^2} - 1)e^{(4\pi\lambda\frac{k^2}{M^2}-1)}, \quad -\frac{P}{2} \leq k < \frac{P}{2} - 1,$$

with $M = N = 32$ and $\lambda = .125$ (g in this example is centered at zero for the purpose of greater clarity, but a simple time-frequency shift can force the signal to comply with conditions 5.1-5.3). A segment f of g is supported on the interval $[-M, M)$. G vanishes outside interval $[-N, N)$. Figures 5.1-5.2 illustrate steps 1-4 of the algorithm. As can be seen from Fig. 5.3, the convergence is extremely slow and the hundredth iteration still fails to yield an acceptable estimate of g.

Since each step of the Gerchberg-Papoulis algorithm involves transition between the time and frequency domains, it is natural to ask, if an improvement could not be made by formulating the problem in a joined time-frequency space. In this work we will translate the Gerchberg-Papoulis algorithm into the language of the Finite Zak Transform, however many other possibilities for such a formulation exist (e.g. Wigner Distribution, ambiguity function, Gabor expansion, etc), and will be explored in future work.

The Zak transform has long been recognized as a valuable tool in building efficient signal processing algorithms [7,8,9,23], it is intimately related to the Fourier transform, and its calculus have been shown to lead to simplifications in deriving proofs of several signal processing formulas [53]. It will be shown that the Finite Zak Transform formulation of the Gerchberg-Papoulis algorithm allows reduction of computational complexity by a factor $log_2 P$, replacing Fourier transform computation with pointwise multiplication.

5.3 The Finite Zak Transform

Choose a positive integer P. A discrete function $f(k)$, $k \in Z$ is called P-periodic if

$$f(k+P) = f(k), \quad k \in Z. \tag{5.4}$$

Denote by $L^2(P)$ the Hilbert space of all P-periodic functions with inner product

$$< f, g >= \sum_{k=0}^{P-1} f(k)g^*(k), \qquad f, g \in L^2(P).$$

Suppose $P = MN$. For $f \in L^2(P)$ define the *finite Zak Transform* (FZT) $Z_f(l,k)$, by

$$Z_f(l,k) = \sum_{r=0}^{N-1} f(k+rM)e^{2\pi irl/N}, \quad l,k \in Z. \tag{5.5}$$

$Z_f(l,k)$ satisfies the following periodicity relations

$$Z_f(l,k+M) = e^{-2\pi il/N} Z_f(l,k), \quad l,k \in Z, \tag{5.6}$$

$$Z_f(l+N,k) = Z_f(l,k), \quad l,k \in Z. \tag{5.7}$$

It follows that Z_f is P-periodic in each variable and is completely determined by its values

$$Z_f(l,k), \quad 0 \leq k < M, \quad 0 \leq l < N. \tag{5.8}$$

The finite Zak transform is a unitary transformation. The function f can be recovered from its Zak transform by the formula

$$f(k+rM) = N^{-1} \sum_{l=0}^{N-1} Z_f(l,k)e^{-2\pi ilr/N}, \quad 0 \leq k < M, \quad 0 \leq l < N. \tag{5.9}$$

If f is time-limited to $[0, M)$ the inversion formula takes form

$$f(k) = N^{-1} \sum_{l=0}^{N-1} Z_f(l, k), \quad 0 \leq k < M, \quad 0 \leq l < N. \tag{5.10}$$

Modulation

Suppose f and $g \in L^2(P)$ and denote by $f \cdot g$ the product function

$$(f \cdot g)(k) = f(k)g(k). \tag{5.11}$$

We then have [53]

$$Z(f \cdot g)(l, k) = \sum_{c=0}^{N-1} Z_f(c, k) Z_g(l - c, k). \tag{5.12}$$

Hence we see that the effect of multiplication in the time domain is reflected by convolution with respect to the frequency variable in the Zak space. We will make use of (5.12) later in the section.

Truncation

Let $f \in L^2(P)$ and f_M be its M-point segment, i.e.

$$f = [f_0, f_1, ..., f_{P-1}] \tag{5.13}$$

and

$$f_M = [f_0, f_1, ..., f_{M-1}, 0, ..., 0]. \tag{5.14}$$

We have the following relation

$$Z_{f_M}(l, k) = \sum_{c=0}^{N-1} Z_f(c, k). \tag{5.15}$$

Similarly, if F is the P-point Fourier transform of f

$$F = [F_0, F_1, ..., F_{P-1}] \tag{5.16}$$

and F_N is its N-point segment

$$F_N = [F_0, F_1, ..., F_{N-1}, 0, ..., 0], \tag{5.17}$$

then

$$Z_{F_N}(k, l) = \sum_{c=0}^{M-1} Z_F(c, l), \tag{5.18}$$

where the Zak transform of F is defined as

$$Z_F(k, l) = \sum_{s=0}^{M-1} F(l + sN)e^{2\pi iks/M}, \tag{5.19}$$

and F can be recovered from Z_F by

$$F(l + sN) = \sum_{k=0}^{M-1} Z_F(k, l)e^{-2\pi iks/M}. \tag{5.20}$$

Proof. Define

$$p_M(k) = \begin{cases} 1, & 0 \leq k < M, \\ 0, & elsewhere. \end{cases}$$

We can write f_M as

$$f_M = p_M \cdot f.$$

Using (5.12) and the fact that

$$Z\{p_M(k)\} = e^{2\pi i[\frac{k}{M}+r]\frac{l}{N}} = 1,$$

where $[\frac{k}{M}+r]$ denotes the largest integer $\leq \frac{k}{M}+r$, we have

$$\begin{aligned} Z_{f_M}(l,k) &= Z\{p_M \cdot f\}(l,k) \\ &= \sum_{c=0}^{N-1} Z_f(c,k) Z_{p_M}(l-c,k) \\ &= \sum_{c=0}^{N-1} Z_f(c,k) \end{aligned}$$

Similarly, we have

$$\begin{aligned} Z_{F_N}(k,l) &= Z\{p_N \cdot F\}(k,l) \\ &= \sum_{c=0}^{M-1} Z_F(c,l) Z_{p_N}(k-c,l) \\ &= \sum_{c=0}^{M-1} Z_F(c,l) \end{aligned}$$

where

$$p_N(l) = \begin{cases} 1, & 0 \leq l < N, \\ 0, & elsewhere, \end{cases}$$

and

$$Z\{p_N(l)\} = e^{2\pi i[\frac{l}{N}+s]\frac{k}{M}} = 1,$$

$[\frac{l}{N}+s]$ being the largest integer $\leq \frac{l}{N}+r$. □

Formulas (5.15) and (5.18) allow us to perform truncation of time and frequency signals in the Zak space by a simple addition of columns of Z_f and Z_F, respectively.

Fourier Transform

If $f \in L^2(P)$ and F is its P-point Fourier transform, we have the following relation

$$M^{-1} Z_F(k,l) = Z_f(l,-k) e^{-2\pi i k l/P} \tag{5.21}$$

Loosely speaking, formula (5.21) asserts that, up to the factor $e^{-2\pi i a b/N}$, 90 degrees rotation of the Zak transform $Z_f(l,k)$ produces the Zak transform $Z_F(k,l)$.

The main part of Cooley-Tukey FFT algorithm is also contained in formula (5.21). Neglecting permutations we can compute F by the following sequence of steps.

1. Compute $Z_f(l,k)$, $0 \le k < M$, $0 \le l < N$. This step requires M N-point Fourier transforms.

2. Twiddle by the factor $e^{-2\pi i k l/P}$. This step requires P multiplications as $0 \le k < M$, $0 \le l < N$.

3. Compute the inverse Zak transform Z_F by (5.20) with N and M interchanged. This step requires N M-point Fourier transforms.

5.4 Gerchberg-Papoulis-Zak Algorithm

In the previous section the Finite Zak Transform was introduced and it was shown that Fourier transformation and truncation in time/frequency corresponds to rotation+multiplication and summation in the Zak space, respectively. Now, we can reformulate the Gerchberg-Papoulis algorithm.

1. Compute the Zak transform $Z_f(l,k)$ of $f(k)$.
2. Rotate $Z_f(l,k)$ by 90 degrees and multiply by the phase factor $e^{-2\pi ikl/P}$, yielding $Z_F(k,l)$.
3. Add columns of Z_F according to (5.18). This step yields $Z_{F_N}(k,l)$.
4. Rotate $Z_{F_N}(k,l)$ by 90 degrees and multiply by a phase factor, yielding $Z_{\tilde{F}_N}(l,k)$.
5. Add columns of $Z_{\tilde{F}_N}(l,k)$ according to (5.15) to produce $Z_{(\tilde{F}_N)_M}(l,k)$.
6. Add $Z_{f_1} = Z_f + Z_{\tilde{F}_N} - Z_{(\tilde{F}_N)_M}$.
7. Compute the inverse Zak transform.

Computation of either the forward or the inverse Zak transform requires $Plog_2N$ multiplications, and needs to be performed only once. Since steps 3., 5. and 6. involve only additions, the multiplicative complexity of a single iteration is $2P$. Figures 5.4-5.7 illustrate steps 1-6 of the Gerchberg-Papoulis-Zak algorithm for the signal g from section 5.2 appropriately time-frequency shifted to meet conditions 5.1-5.3. A segment f is supported on the interval $[0, M)$.

The Gerchberg-Papoulis-Zak procedure can be easily extended to two-dimensional signals via generalization of the FZT to two dimensions. The 2-D FZT [91] retains all the useful properties of 1-D FZT, such as periodicity, convolution and relation with the Fourier transform.

Application of the Finite Zak transform to signal extrapolation from partial data is not the only way to bring the computations to the joint time-frequency space. Formulation of the problem in the language of the discrete Gabor expansion offers an alternative approach, which is extremely efficient if a Gaussian window is employed. An interesting direction to take in future research would be to investigate the effect the selection of the window has on efficiency and convergence of the algorithm. Applications of Wigner distribution and ambiguity function to the Gerchberg-Papoulis problem should also be investigated.

A problem related to the Gerchberg-Papoulis signal extrapolation is signal restoration from phase or magnitude of its Fourier transform [48,49]. Methods similar to the Gerchberg-Papoulis algorithm exist (e.g. Gerchberg-Saxton technique), however they are elaborate and computationally expensive. Again, reformulating the phase/magnitude problem in a joint time-frequency space (Zak, Gabor, Wigner, etc) might prove to be a rewarding enterprise.

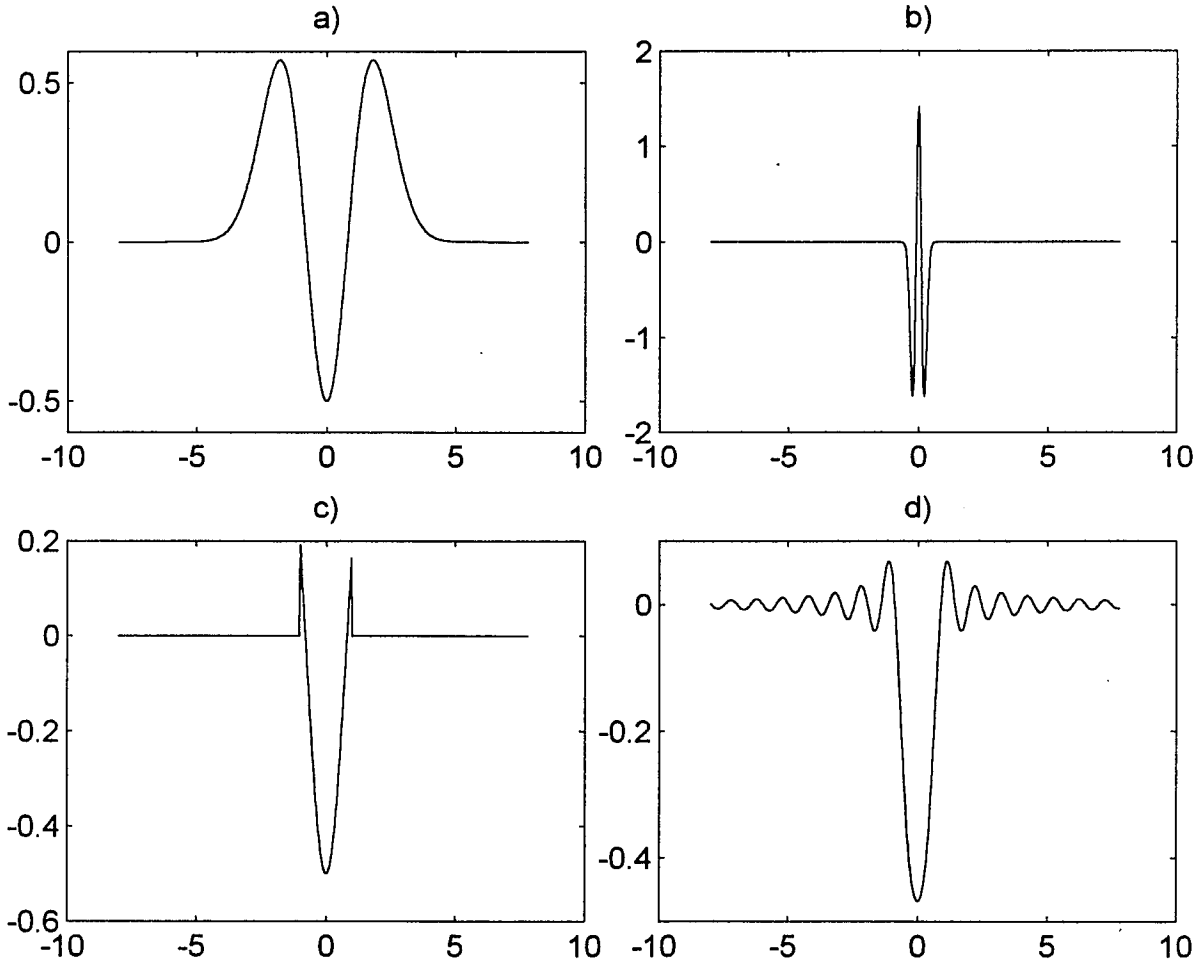

Figure 5.1: The signal g: a), its Fourier transform G: b), the segment f: c) and its Fourier transform F: d).

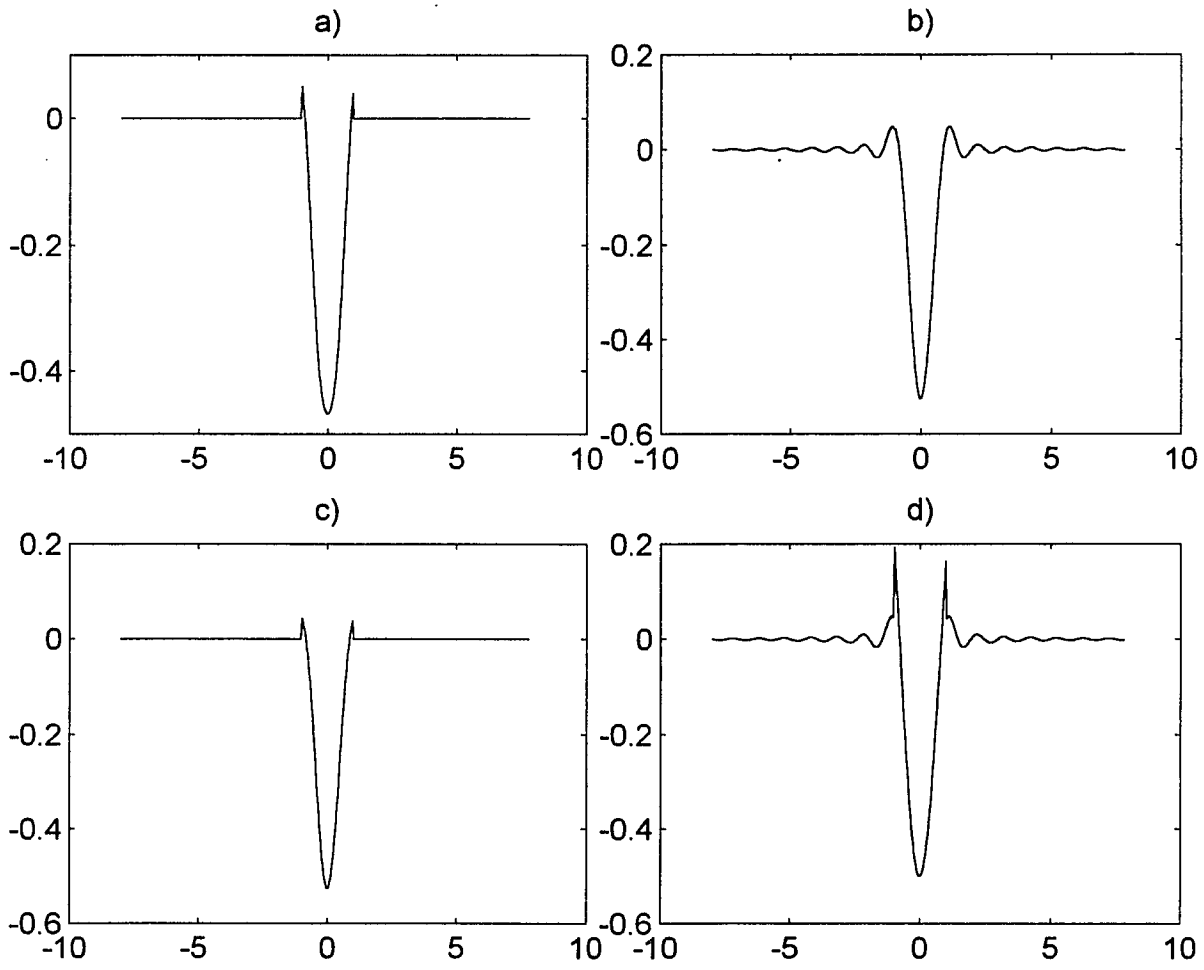

Figure 5.2: F_N, the truncation of F: a), its inverse Fourier transform $\tilde{F_N}$: b), truncation of $\tilde{F_N}$: c) and result of the last step of the iteration: d).

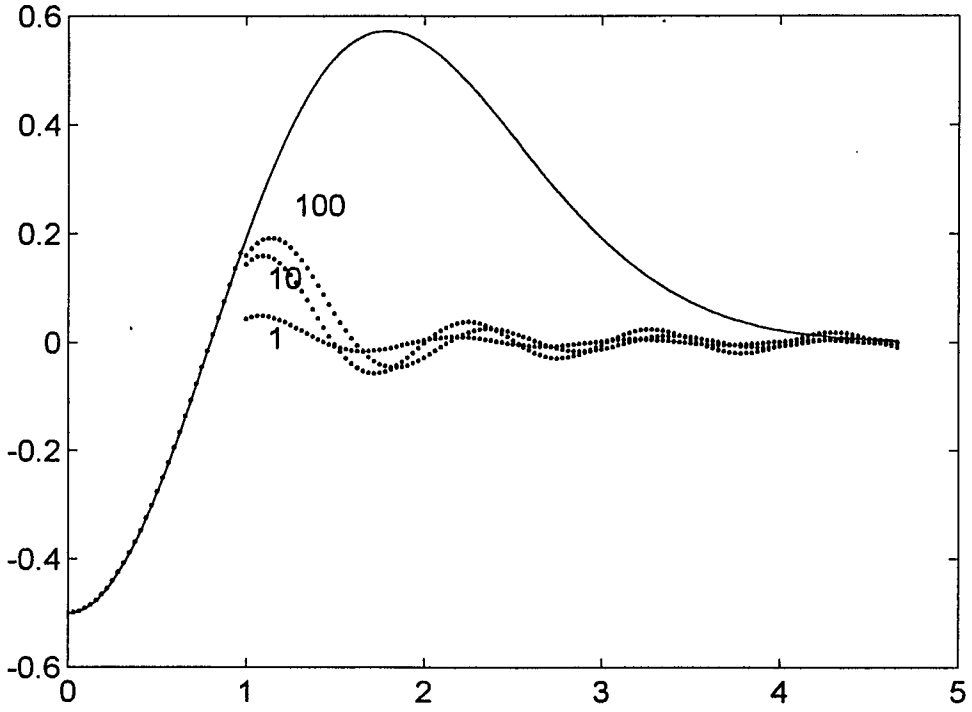

Figure 5.3: Restored signal f_r at r-th iteration: a) $r = 1$, b) $r = 10$, c) $r = 100$.

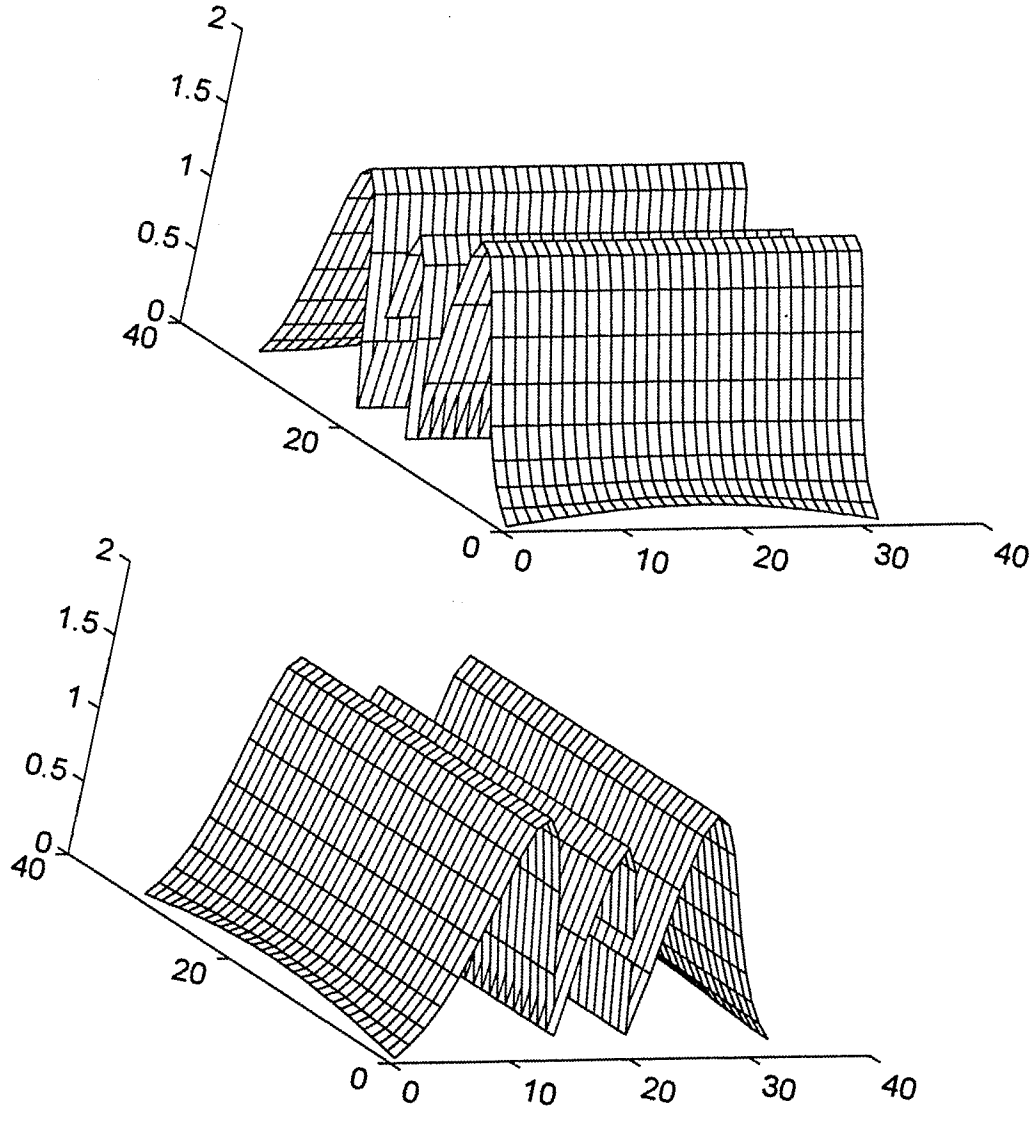

Figure 5.4: Zak transform magnitudes of g (top) and its Fourier transform G (bottom).

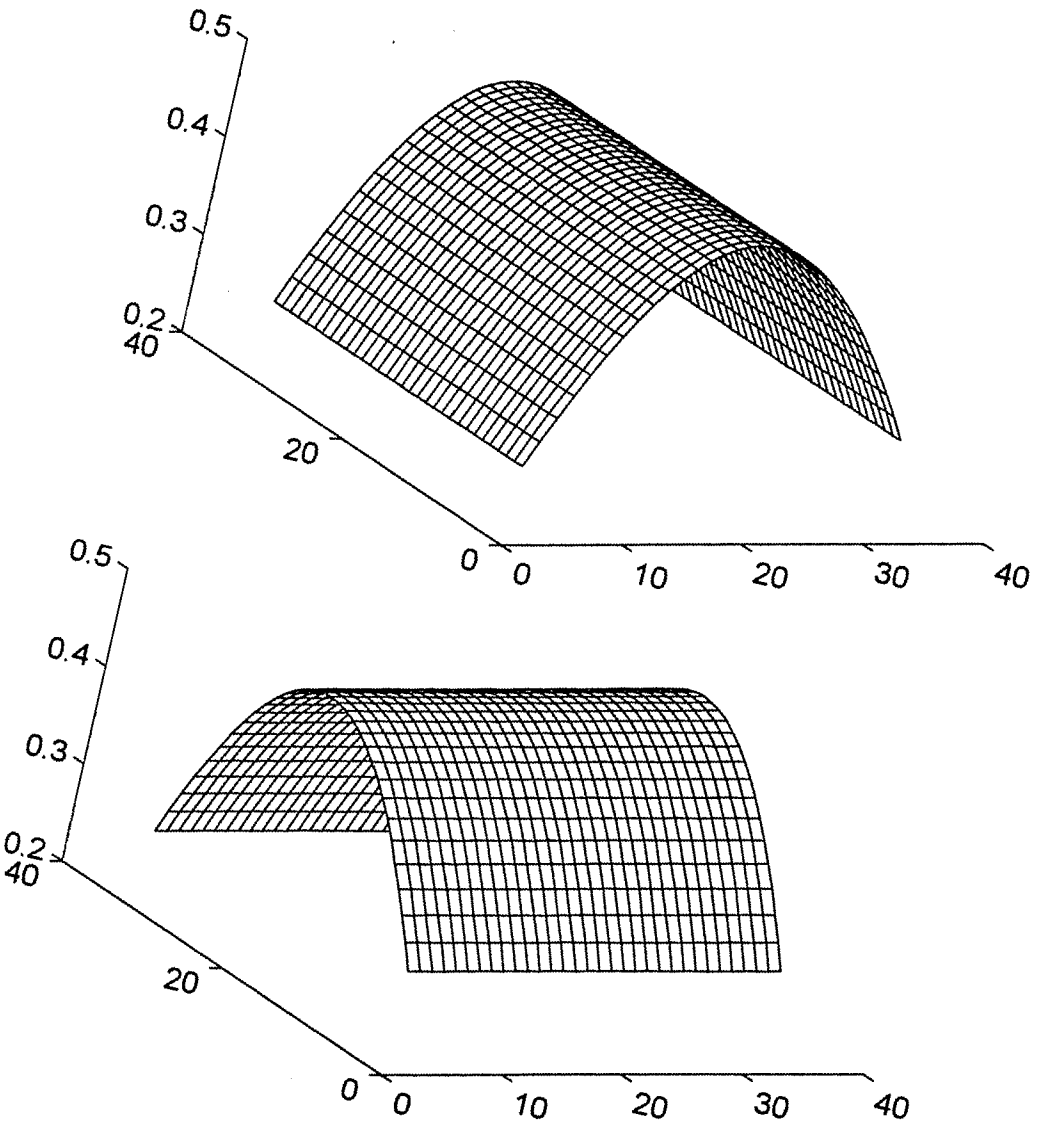

Figure 5.5: Zak transform magnitudes of segment f (top) and its Fourier transform F (bottom).

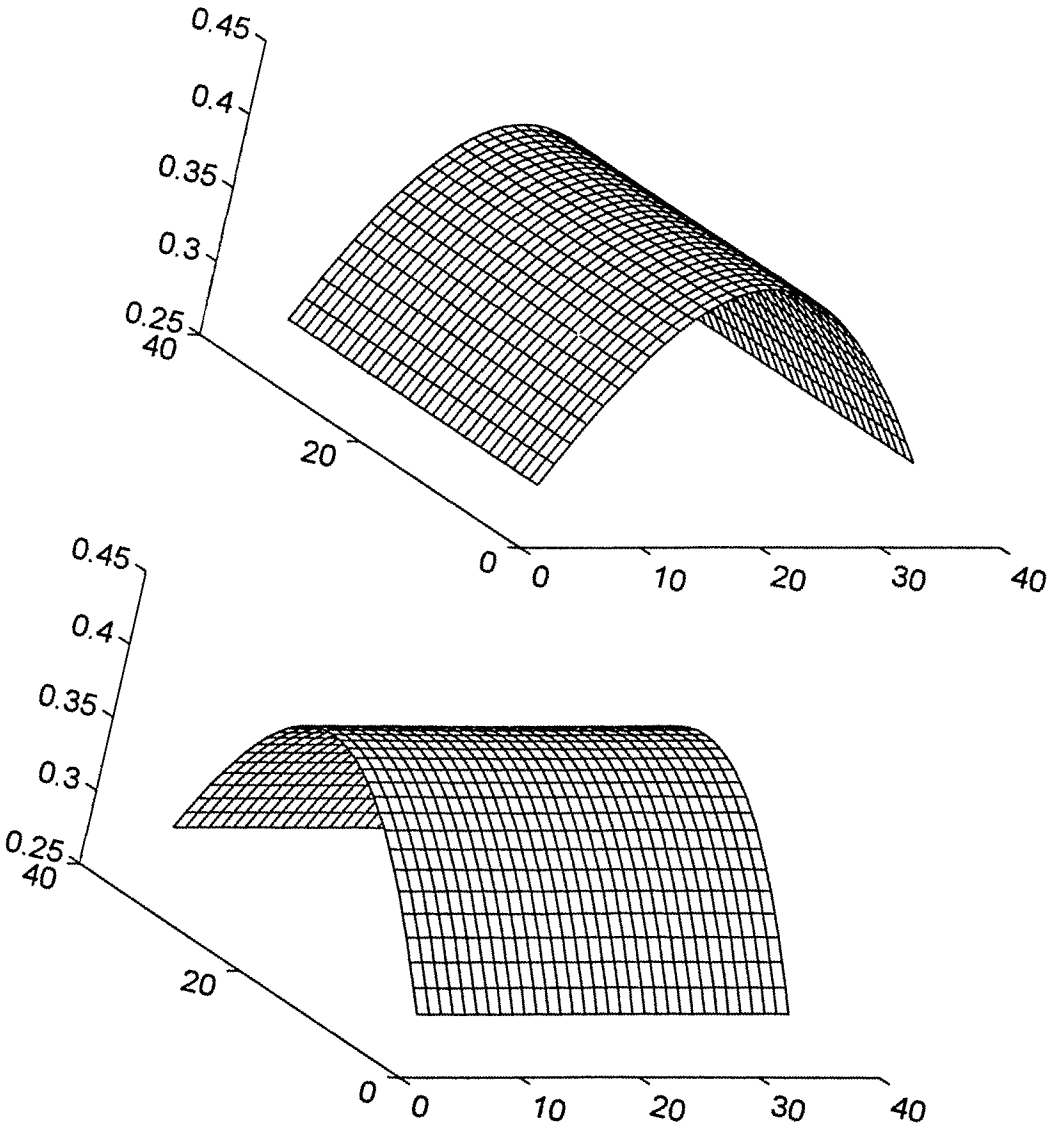

Figure 5.6: Truncation in the Zak space Z_{F_N} (top) and its inverse Fourier transform $\check{Z}_{F_N}$ (bottom).

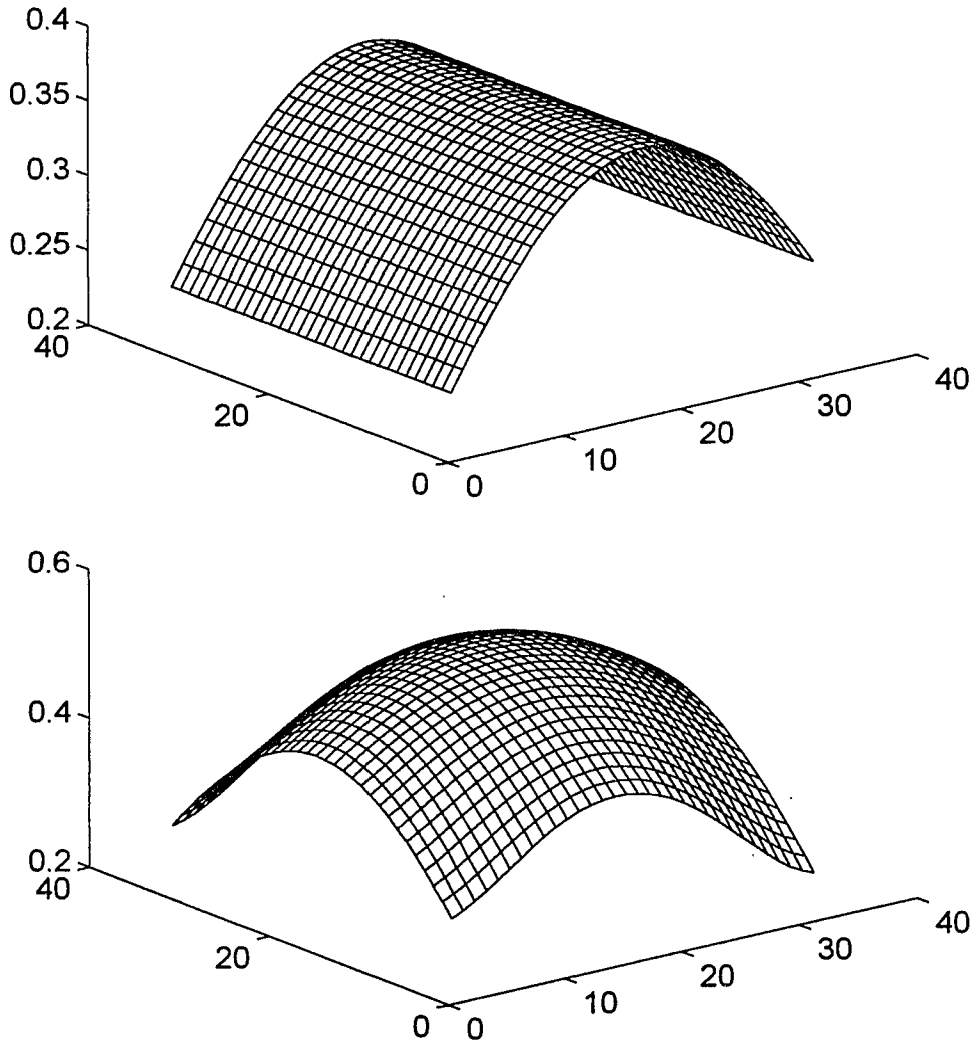

Figure 5.7: Truncation in the Zak space of $\check{Z_{F_N}}$ (top) and the result of addition (step 6 of the algorithm, bottom).

Chapter 6

Conclusions

6.1 Role of Time-Frequency Analysis

Time-frequency techniques has been known to the scientific and engineering community for about half a century. Indeed, Gabor expansion, Wigner distribution, Woodward's ambiguity function, even wavelet transform are hardly novelties - they have long been recognized as useful in radar signal processing, speech processing, communication and coding. Still, the applications were found mostly in a few selected fields, and the mutual relationship between the transforms has not been fully explored, which obstructed the time-frequency analysis from reaching its full potential.

This is probably going to change dramatically in the near future: computing power has become available to attack complex problems requiring a non-stationary approach. Recent interest in wavelets, which stimulated many signal processing discoveries, should spread to other joint-domain techniques, once researchers realize that 'one method does not fit all' and that despite its com-

plexity, time-frequency methods may lead to simple solutions of traditionally unaccessible problems. It is hoped that this work is a step in this direction. The two main contributions of this dissertation are:

- exposition of the intimate relationship between two time-frequency techniques (the discrete Gabor expansion and the finite Zak transform), which lead to design of simple, efficient and flexible algorithms and
- application of a time-frequency method (the finite Zak transform) towards a signal processing problem (which has been worked on for over twenty years) and producing a simple yet efficient solution.

The focus of this work was on the finite Zak transform. It was shown that the Zak transform is instrumental in establishing clear and easily computable conditions for existence of Gabor expansions and for stability of the computations. The applicability of the Zak transform approach was extended to integer and fractionally oversampled Gabor systems. The relationship between the Fourier transform and the Zak transform was exploited to formulate an efficient algorithm for extrapolating band-limited signals from partial data.
The ideas presented in this dissertation offer many avenues for farther research. A few of these are mentioned below.

- Although the fundamental properties of the Zak transform are fairly well known, the relationship between the Zak space and time space characteristics is not fully understood. The significance of Zak transform zeros, their number, location and sharpness as well as Zak surface curvature for

design of time-signals in the Zak space should be thoroughly investigated. Furthermore, the relevance of the Zak transform for feature extraction in image processing, texture discrimination and speech recognition should be fully explored.

- The nonuniqueness of discrete Gabor expansions in the general oversampling case can be used advantageously by imposing constrains on factorizations to yield solutions with desirable characteristics, such as maximum efficiency, minimum energy, localization, etc. Better understanding the impact signal factorization has on Gabor coefficients requires farther research.

- It has been demonstrated that application of the Zak transform to the Gerchberg-Papoulis problem produces a simple and efficient signal extrapolation algorithm. Formulation of the problem in the language of the discrete Gabor expansion offers an alternative approach, which is extremely efficient if a Gaussian window is employed. An interesting direction to take in future research would be to investigate the effect the selection of the window has on efficiency and convergence of the algorithm. Application of other time-frequency techniques should also be explored, especially ambiguity function and Wigner distribution.

- A problem that is related to the Gerchberg-Papoulis signal extrapolation is signal restoration from phase or magnitude of its Fourier trans-

form. Iterative methods similar to the Gerchberg-Papoulis algorithm exist, however they are elaborate and computationally expensive. Reformulating the phase/magnitude problem in a joint time-frequency space might prove to be a rewarding enterprise.

Bibliography

[1] J. B. Allen and L. R. Rabiner, "A Unified Approach to Short-Time Fourier Analysis and Synthesis", *Proc. IEEE*, Vol. 65, No. 11, pp 1558-1564, 1977.

[2] M. An, M. Conner, R. Orr and R. Tolimieri, "Computation and Meaning of Gabor Coefficients", *SPIE*, Vol. 1565, pp 383-401, 1991.

[3] M. P. Anderson, M. H. Loew and D. G. Brown, "Information Processing in Medical Images", *IPMI'93 Proc.*, pp 553-567, 1993.

[4] L. Auslander, M. An, M. Conner, I. Gertner and R. Tolimieri, "Fine Structure of the Classical Gabor Approximation", *IMA on Radar and Sonar*, Part II, 39, pp 11-20, Springer-Verlag, New York, 1991.

[5] L. Auslander, C. Buffalano, R. Orr and R. Tolimieri, "A Comparison of the Gabor and Short-Time Fourier Transforms for Signal Detection and Feature Extraction in Noisy Environments", *SPIE*, Vol. 1348, pp 230-247, 1990.

[6] L. Auslander and R. Tolimieri, "Abelian Harmonic Analysis, Theta Functions and Function Algebra on a Nilmanifold", Springer-Verlag, 1975.

[7] L. Auslander and R. Tolimieri, "On Finite Gabor Expansion of Signals", *IMA Proceedings on Signal Processing*, Minneapolis, 1988.

[8] L. Auslander, I. Gertner and R. Tolimieri, "Finite Zak Transforms and the Finite Fourier Transforms", *IMA on Radar and Sonar*, Part II, Vol. 39, pp 21-36, Springer-Verlag, New York, 1991.

[9] L. Auslander, I. Gertner and R. Tolimieri, "The Discrete Zak Transform Application to Time-Frequency Analysis and Synthesis of Nonstationary Signals", *IEEE Trans. Signal Processing*, Vol. 39, No. 4, pp 825-835, April 1991.

[10] L. Auslander and R. Tolimieri, "Radar Ambiguity Functions and Group Theory", *SIAM J.Math.Anal.*, Vol. 16, pp 577-601, 1985.

[11] L. Auslander and R. Tolimieri, "Computing Decimated Finite Cross-Ambiguity Functions", *IEEE Trans. ASSP*, Vol. 36, No. 3, pp 359-363, 1988.

[12] M. J. Bastiaans, "A Sampling Theorem for Complex Spectrogram and Gabor Expansion of a Signal into Gaussian Elementary Signals", *Opt. Eng.*, Vol. 20, No. 4, pp 594-598, 1981.

[13] M. J. Bastiaans, "Gabor Signal Expansion and Degrees of Freedom of a Signal", *Optica Acta*, Vol. 29, pp 1223-1229, 1982.

[14] M. J. Bastiaans, "Gabor's Expansion of a Signal into Gaussian Elementary Signals", *Proc. IEEE*, Vol. 68, No. 4, pp 538-539, 1984.

[15] M. J. Bastiaans, "On the Sliding-Window Representation in Digital Signal Processing", *IEEE Trans. ASSP*, Vol. 33, No. 4, pp 868-873, 1985.

[16] M. J. Bastiaans, "Gabor's Signal Expansion and its Relation to Sampling of the Sliding Window Spectrum", *Advanced Topics in Shannon Sampling and Interpolation Theory*, Springer-Verlag, pp 1-37, 1993.

[17] M. J. Bastiaans, "Gabor's Signal Expansion and the Zak Transform", *Opt. Eng.*, Vol. 33, No. 23, pp 5241-5255, 1994.

[18] J. Behar, M. Porat and Y. Zeevi, "Image Reconstruction form Localized Phase", *IEEE Trans. SP*, Vol. 40, No. 4, pp 736-743, 1992.

[19] R. N. Bracewell, "Assessing the Hartley Transform", *IEEE Trans. ASSP*, Vol. 38, No. 12, pp 2174-2176, 1990.

[20] A. Brodzik and M. Conner, "Generalized Biorthogonal Methods for Computing Gabor Expansions", *ISS*, 1992.

[21] A. Brodzik and M. Conner, "Time-Limited Signals and Gabor Expansion", *Proc. IEEE-SP Symposium on Time-Frequency and Time-Scale Analysis*, pp 268-271, 1994.

[22] A. Brodzik and R. Tolimieri, "The Computation of Weyl-Heisenberg Coefficients for Critically Sampled and Oversampled Signals", *Proc. IEEE-SP Symposium on Time-Frequency and Time-Scale Analysis*, pp 272-275, 1994.

[23] A. Brodzik and R. Tolimieri, "Weyl-Heisenberg Systems and the Finite Zak Transform", *submitted*, 1994.

[24] T.A.C.M. Classen and W.F.G. Mecklenbrauker, "The Wigner Distribution - A Tool for Time-Frequency Analysis: Part 1: Continuous-Time Signals", *Phillips J. Res.*, Vol. 35, No. 3, pp 217-250, 1980.

[25] T.A.C.M. Classen and W.F.G. Mecklenbrauker, "The Wigner Distribution - A Tool for Time-Frequency Analysis: Part 2: Discrete-Time Signals", *Phillips J. Res.*, Vol. 35, No. 3, pp 276-300, 1980.

[26] T.A.C.M. Classen and W.F.G. Mecklenbrauker, "The Wigner Distribution - A Tool for Time-Frequency Analysis: Part 2: Relations with Other Time-Frequency Signal Transformations", *Phillips J. Res.*, Vol. 35, No. 6, pp 372-389, 1980.

[27] L. Cohen, "Time-Frequency Distributions - a Review", *Proc. IEEE*, Vol. 77, No. 7, pp 941-981, 1989.

[28] I. Daubechies, "Orthonormal Basis of Compactly Supported Wavelets ", *Comm. Pure Appl. Math*, vol. 41, no , pp 909-996, 1988.

[29] I. Daubechies, "The Wavelet Transform, Time-Frequency Localization and Signal Analysis ", *IEEE Trans. IT*, vol. 36, no 5, pp 961-1005, 1990.

[30] I. Daubechies, "Ten Lectures on Wavelets ", *SIAM*, 1992.

[31] I. Daubechies, S. Jaffard and Jean-Lin Journes, "A Simple Wilson Orthonormal Basis with Exponential Decay ", *SIAM J. Math. Anal.*, vol. 22, no 2, pp 554-573, 1991.

[32] J. Daugman, "Two Dimensional Spectral Analysis of Cortical Receptive Field Profiles", *Vision Res.*, vol. 20, pp 847-856, 1980.

[33] J. Daugman, "Complete Discrete 2-D Gabor Transforms by Neural Networks for Image Analysis and Compression", *IEEE Trans. ASSP*, vol. 36, no 7, pp 1169-1179, 1988.

[34] J. Daugman, "Uncertainty Relation for Resolution in Space, Spatial Frequency, and Orientation Optimized by Two-Dimensional Visual Cortical Filters", *J. Opt. Soc. Am. A*, vol. 2, no 7, pp 1160-1169, 1985.

[35] T. Ebrahimi and M. Kunt, "Image Compression by Gabor Expansion", *Optical Engineering*, vol. 30, no 7, pp 873-880, 1991.

[36] S. Farkash, S. Raz and D. Malah, "Analog Speech Scrambling via the Gabor Representation ", *17th. Conv. IEEE Proc.*, pp 365-368, 1991.

[37] H. G. Feichtinger and K. Grochenig, "Gabor Wavelets and the Heisenberg Group: Gabor Expansions and Short-Time Fourier Transform from the Group Theoretical Point of View", *Wavelets and Their Applications*, ed. M. B. Ruskai, pp 359-397, 1991.

[38] P. Flandrin, "Some Aspects of Non-Stationary Signal Processing with Emphasis on Time-Frequency and Time-Scale Methods", *Wavelets, Time-Frequency Methods and Phase-Space*, Springer-Verlag, pp 68-98, 1989.

[39] G.E. Forsythe, "Computer Methods for Mathematical Computations", , Prentice-Hall, 1977.

[40] B. Friedlander and M. Porat, "Detection of Transient Signals by the Gabor Representation ", *IEEE Trans. ASSP*, vol. 37, No. 2, pp 169-180, 1989.

[41] D. Gabor, "Theory of Communications", *J. IEE*, Vol. 93, No. 3, pp 429-457, November 1946.

[42] I. Gertner and G. Geri, "Conjoined Image Representation with a Weighted Zak Transform", *J. Opt. Soc. Am. A*, Vol. 11, No. 8, pp 2215-2219, 1994.

[43] I. Gertner and G. Geri, "Image Representation Using Hermite Functions", *Biol. Cyber.*, Vol. 71, No. 2, pp 147-151, 1994.

[44] C. Heil and D. Walnut, "Continuous and Discrete Wavelet Transforms", *SIAM Review*, Vol. 31, No. 4, pp 628-666, 1989.

[45] J.R. Higgins, "Completeness and Basis Properties of Sets of Special Functions", , Cambridge University, 1977.

[46] F. Hlawatsch, "Interference Terms in the Wigner Distribution", *Proc. 1984 Internat. Conf. on DSP*, Florence, Italy, pp 363-367.

[47] F. Hlawatsch and G. F. Boudreaux-Bartels, "Linear and Quadratic Time-Frequency Signal Representations", *Signal Processing Magazine*, Vol. 9, No. 2, pp 21-67, 1992.

[48] M. H. Hayes, "The Reconstruction of a Multidimensional Sequence from the Phase or Magnitude of its Fourier Transform", *IEEE Trans. ASSP*, Vol. 30, No. 2, pp 140-154, 1982.

[49] P. L. Van Hove, M. H. Hayes, J. S. Lim and A. V. Oppenheim, "Signal Reconstruction from Signed Fourier Transform Magnitude", *IEEE Trans. ASSP*, Vol. 31, No. 5, pp 1286-1293, 1983.

[50] A. K. Jain and S. Ranganath, "Extrapolation Algorithms for Discrete Signals with Application in Spectral Estimation", *IEEE Trans. ASSP*, Vol. 29, No. 4, pp 830-845, 1981.

[51] A.J.E.M. Janssen, "Gabor Representation of Generalized Functions", *J. Math. Anal. Appl.*, Vol. 83, pp 377-394, 1981.

[52] A.J.E.M. Janssen, "Gabor Representation and Wigner Distribution of Signals", *Proc.Int.Conf.ASSP*, pp 41B.2.1-4, 1984.

[53] A.J.E.M. Janssen, "The Zak Transform: A Signal Transform for Sampled Time-Continuous Signals", *Phillips J. Res.*, No. 43, pp 23-69, 1988.

[54] D.L. Jones and T. W. Parks, "A Resolution Comparison of Several Time-Frequency Representations", *IEEE Trans. SP*, Vol. 40, No. 2, pp 413-420, 1992.

[55] M. C. Jones, "The Discrete Gerchberg Algorithm", *IEEE Trans. ASSP*, Vol. 34, No. 3, pp 624-626, 1986.

[56] S. Kadambe and G. F. Boudreaux-Bartels, "A Comparison of the Existence of 'Cross Terms' in the Wigner Distribution and the Squared Magnitude of the Wavelet Transform and the Short Time Fourier Transform", *IEEE Trans. SP*, Vol. 40, No. 10, pp 2498-2516, 1992.

[57] S. Kawata and O. Nalcioglu, "Constrained Iterative Reconstruction by the Conjugate Gradient Method", *IEEE Trans. MI*, Vol. 4, No. 2, pp 65-71, 1985.

[58] S. Mallat, "A Theory for Multiresolution Signal Decomposition: The Wavelet Representation", *IEEE Trans. PAMI*, Vol. 11, No. 7, pp 674-693, 1989.

[59] J. Morris and H. Xie, "Fast Algorithms for Generalized Discrete Gabor Expansion", *preprint.*

[60] A. V. Oppenheim, "Applications of Digital Signal Processing", Prentice Hall, 1978.

[61] R. Orr, "The Order of Computation for Finite Discrete Gabor Transforms", *IEEE Trans. SP*, Vol. 41, No. 1, pp 122-130, 1993.

[62] R. Orr, "Derivation of the Finite Discrete Gabor Transform by Periodization and Sampling", *Signal Processing*, Vol. 34, No. 1, pp 85-97, 1993.

[63] A. Papoulis, "Signal Analysis", McGraw-Hill, 1977.

[64] A. Papoulis, "A New Algorithm in Spectral Analysis and Band-Limited Extrapolation", *IEEE Trans. Circ. Sys.*, Vol. CAS-22, No. 9, pp 735-742, 1975.

[65] M. Porat and Y. Zeevi, "The Generalized Gabor Scheme of Image Representation in Biological and Machine Vision", *IEEE Trans. PAMI*, Vol. 10, No. 4, pp 452-468, 1988.

[66] M. Porat and Y. Zeevi, "Localized Texture Processing in Vision: Analysis and Synthesis in the Gaborian Space", *IEEE Trans. BE*, Vol. 36, No. 1, pp 115-129, 1989.

[67] M. Portnoff, "Time-Frequency Representation of Digital Signals and Systems Based on Short-Time Fourier Analysis", *IEEE Trans. ASSP*, Vol. 28, No. 1, pp 55-69, 1980.

[68] S. Qian and J.M. Morris, "Wigner Distribution Decomposition and Cross-Term Deleted Representation", *Signal Processing*, Vol. 27, No. 2, pp 125-144, Elsevier Publishers, 1992.

[69] S. Qian and K. Chen, "Optimal Biorthogonal Functions for Finite Discrete-Time Gabor Expansion", *Signal Processing*, Vol. 27, No. 2, pp 177-185, Elsevier Publishers, 1992.

[70] S. Qian and K. Chen, "Signal Representation Using Adaptive Normalized Gaussian Functions ", *Signal Processing*, Vol. 36, pp 1-11, Elsevier Publishers, 1994.

[71] S. Qian, D. Chen and K. Chen, "Signal Approximation via Data-Adaptive Normalized Gaussian Functions and its Applications for Speech Processing", *ICASSP'92*, Vol. 1, pp 141-144, 1992.

[72] S. Raz, "Synthesis of Signals from Wigner Distributions: Representation on Biorthogonal Basis", *Signal Processing*, Vol. 20, No. 4, pp 303-314, Elsevier Publishers, 1990.

[73] O. Rioul and M. Vetterli, "Wavelets and Signal Processing", *Signal Processing Magazine*, Vol. 8, No. 4, pp 14-38, 1991.

[74] M. I. Sezan and H. Stark, "Tomographic Image Reconstruction from Incomplete View Data by Convex Projections and Direct Fourier Inversion", *IEEE Trans. MI*, Vol. 3, No. 2, pp 91-98, 1984.

[75] M. I. Sezan and H. Stark, "Image Restoration by the Method of Convex Projections: Part 2 - Applications and Numerical Results", *IEEE Trans. MI*, Vol. 1, No. 2, pp 95-101, 1982.

[76] B. J. Sullivan and B. Liu, "On the Use of Singular Value Decomposition and Decimation in Discrete-Time Band-Limited Signal Extrapolation", *IEEE Trans. ASSP*, Vol. 32, No. 6, pp 1201-1212, 1984.

[77] K.-C. Tam and V. Perez-Mendez, "Limited-Angle Three-Dimensional Reconstruction Using Fourier Transform Iterations and Radon Transform Iterations", *Opt. Eng.*, Vol. 20, No. 4, pp 586-589, 1981.

[78] J. G. Teti and H. N. Kritikos, "SAR Ocean Image Decomposition Using the Gabor Expansion", *IEEE Trans. GRS*, Vol. 30, No. 1, pp 192-196, 1992.

[79] R. Tolimieri, "Analysis on the Heisenberg Manifold", *Trans. Am. Math. Soc.*, Vol. 228, pp 329-343, 1977.

[80] R. Tolimieri and S. Winograd, "Computing the Ambiguity Surface", *IEEE Trans. ASSP*, Vol. 33, No. 4, pp 1239-1245, 1985.

[81] D. Verhoeven, "Limited-Data Computed Tomography Algorithms for the Physical Sciences", *Applied Optics*, Vol. 32, No. 20, pp 3736-3754, 1993.

[82] D. O. Walsh and P. A. Nielsen-Delaney, "Direct Method for Superresolution", *J. Opt. Soc. Am. A*, Vol. 11, No. 2, pp 572-579, 1994.

[83] A. B. Watson and A. Poirson, "Separable Two-Dimensional Discrete Hartley Transform", *J. Opt. Soc. Am. A*, Vol. 3, No. 12, pp 2001-2004, 1986.

[84] D. W. Watt and C. M. Vest, "Consistent Iterative Convolution: a Coupled Approach to Tomographic Reconstruction", *J. Opt. Soc. Am. A*, Vol. 6, No. 1, pp 44-51, 1989.

[85] J. Wexler and S. Raz, "Discrete Gabor Expansions", *Signal Processing*, Vol. 21, No. 3, pp 207-220, Elsevier Publishers, 1990.

[86] J. Wexler and S. Raz, "Wigner-Space Synthesis of Discrete-Time Periodic Signals", *IEEE Trans. on Signal Processing*, Vol. 40, No. 8, pp 1997-2006, August 1990.

[87] J. Womack and J. R. Cruz, "Seismic Data Filtering Using a Gabor Representation", *IEEE Trans. GRS*, Vol. 32, No. 2, pp 467-472, 1994.

[88] Y. Zeevi and M. Porat, "Computer Image Generation Using Elementary Functions Matched to Human Vision", *NATO ASI Series*, Vol. F40, pp 1197-1241, 1988.

[89] P. M. Woodward, "Probability and Information Theory with Application to Radar", London: Pergamon, 1953.

[90] D. C. Youla and H. Webb, "Image Restoration by the Method of Convex Projections: Part 2 - Theory", *IEEE Trans. MI*, Vol. 1, No. 2, pp 81-94, 1982.

[91] Y. Zeevi and I. Gertner, "The Finite Zak Transform: An Efficient Tool for Image Representation and Analysis", *J. Visual Comm. Image Repres.*, Vol. 3, No. 1, pp 13-23, 1992.

[92] Y. Zeevi and M. Porat, "Image Representation by Localized Phase", *SPIE*, Vol. 1199, pp 1512-1517, 1989.

[93] Z.Y. Zhu and J. Barba, "A Fast Multi-Level Decomposition Algorithm for n-dimensional Discrete Gabor Transforms", *Microscopy*, pp 313-322, 1992.

[94] M. Zibulski and Y. Zeevi, "Oversampling in the Gabor Scheme", *IEEE Trans. SP*, Vol. 41, No. 8, pp 2679-2687, 1993.

[95] J. Zak, "Finite Translations in Solid State Physics", *Phys. Rev. Lett.*, Vol. 19, pp 1385-1397, 1967.